12-2009

Influence of Turning on Military Vehicle Induced Rut Formation

Kun Liu
University of Tennessee - Knoxville

To the Graduate Council:

I am submitting herewith a dissertation written by Kun Liu entitled "Influence of Turning on Military Vehicle Induced Rut Formation." I have examined the final electronic copy of this dissertation for form and content and recommend that it be accepted in partial fulfillment of the requirements for the degree of Doctor of Philosophy, with a major in Biosystems Engineering.

Paul D. Ayers, Major Professor

We have read this dissertation and recommend its acceptance:

Donald D. Tyler, Eric C. Drumm, Jeffrey S. Freeman

Accepted for the Council:
Carolyn R. Hodges

Vice Provost and Dean of the Graduate School

(Original signatures are on file with official student records.)

To the Graduate Council:

I am submitting herewith a dissertation written by Kun Liu entitled "Influence of Turning on Military Vehicle Induced Rut Formation." I have examined the final electronic copy of this dissertation for form and content and recommend that it be accepted in partial fulfillment of the requirements for the degree of Doctor of Philosophy, with a major in Biosystems Engineering.

Paul D. Ayers, Major Professor

We have read this dissertation
and recommend its acceptance:

Donald D. Tyler

Eric C. Drumm

Jeffrey S. Freeman

Accepted for the Council:

Carolyn R. Hodges Vice Provost and
Dean of the Graduate School

(Original signatures are on file with official student records.)

INFLUENCE OF TURNING ON MILITARY VEHICLE INDUCED RUT FORMATION

A Dissertation
Presented for the
Doctor of Philosophy
Degree
The University of Tennessee, Knoxville

Kun Liu

December 2009

ACKNOWLEDGEMENTS

I would like to sincerely thank my advisor, Dr. Paul D. Ayers, for his direction, support and effort on this work. Without his guidance, this dissertation would not have been possible. I feel lucky to have such a good advisor. Additionally, I would like to thank my committee members, Drs. Donald D. Tyler, Eric C. Drumm, and Jeffrey S. Freeman. Thanks also to Dr. William Hart, Craig Wagoner, JR Candlish and Bryan McConkey for their technical help on my experiments.

Special thanks to my wife Xin Lu for her patience and sacrifice. Without her support, this effort would not have been possible.

ABSTRACT

Rut formation can severely influence soil conditions and vegetation, and reduce vehicle mobility. Vehicle operations can affect rut formation. Ruts formed in straight vehicle paths are different than when the vehicle turns. This research is mainly to investigate the effects of vehicle turning maneuvers on soil rut formation, including field tests, lab tests, and model development.

Field tests were conducted at Yuma Training Center, Fort Riley and Fort Lewis on wheeled and tracked military vehicles. In field tests, rut depth, rut width and rut index were used as the main indicators to quantify a rut. A Vehicle Tracking System was mounted onto each vehicle to utilize the Global Positioning System. The vehicles were operated in spiral patterns to get constantly decreasing turning radius.

The Vehicle Terrain Interaction terrain mechanics model was chosen to modify to predict rut formation during vehicle turning operations on yielding soils. In the modified VTI model, the resultant force on a single wheel is a dynamic variable correlated with the vehicle's weight, velocity, and turning radius.

In addition, lab tests were conduced on a tire and a track shoe in sand. Lateral forces and lateral displacements were applied under constant normal forces. The tire was pulled laterally and the track shoe was pulled back and forth to represent actual movement during vehicle turning.

Results indicate that (1) rut depth, rut width and rut index increase with the decrease of TR, especially when TR is less than 20 meters; (2) vehicle parameters and soil parameters are statistically significant to affect rut formation; (3) the

modified VTI model is able to predict rut formation when turning, with an improved R square of 0.43; (4) in lab tests, the final sinkage caused by the lateral force or displacement is 3 to 5 times the static sinkage; (5) rut depths increase from 65% to 548% of the initial rut depths under the effects of the combination of the multi-pass and turning maneuvers after multiple passes.

This dissertation is a collection of five individual papers. More detailed description of test procedures and conclusions are found in these papers.

Part 1 Introduction to vehicle-terrain interaction

1. Overview

Off-road vehicles, such as tractors and tanks, are widely used in mining, construction, forestry, agriculture and military in the society (Wong, 2001). The operation of off-road vehicles will form ruts which have been correlated with the loss of vegetation, soil compaction and decrement of vehicle's mobility.

The military training is an intensive land use and can result in negative effects on vegetation and soil (Haugen, 2003). Military vehicle operations on soft terrain surfaces can result in rutting due to the interaction of vehicle traction elements with the terrain surfaces. Such residual effects may have long-term social, political, and economic consequences. The primary residual impact of vehicles interacting with soft terrain surfaces is after-traffic rutting (Jones et al., 2005). Meanwhile the army is a national leader in environmental and natural resources and is making effort on the environmental protection of the training land. There is an urgent request for the Army to monitor rut formation caused by military training.

2. Effects of rut formation on environment and vehicle

Ruts can concentrate the surface water flow, thereby increasing the potential of erosion (Voorhees et al., 1979). A rut is actually a water channel, like a rill, which influences the velocity and erosivity of water flowing in it (Elliot and Laflen, 1993). Ruts can increase the soil compaction which has negative effects on vegetation. Soil compaction may be the most devastating effect of vehicle traffic. Soil is composed of three components: air, water, and mineral. When the soil compaction occurs, the

volume available for air and water, which are necessary for the vegetation, is reduced as the mineral components are pressed closer together (Raper, 2005). As a consequence of soil compaction, the erodibility increases and the soil productivity decreases, thus affecting additional components of the surrounding ecosystems (Arvidsson and Hakkanson, 1991). Plants have difficulty in compacted soil because the mineral grains are pressed together so as to leave little space for air and water, which are essential for root growth. For a sustainable use of the training land, the amount of vehicular training maneuvers should be under the land carrying capacity, based on the rut formation. Therefore, it is necessary to monitor the rutting of vehicular training for the management and maintenance of the training land.

Rutting research is important for the trafficability and mobility performance of off-road vehicles. Trafficability is the ability of a given vehicle to traverse a specified terrain. Trafficability is determined by terrain and soil factors. Terrain can be described by the occurrence of the obstacles and the slope gradient or by the terrain profile. Soil factors are used to describe the soil reactions under the wheel or track load. Mobility of the vehicle depends on the vehicle dimensions, engine power, drive line and wheel/track characteristics (Saarilahti, 2002). Terrain and soil factors are highly correlated with rut formation for off-road vehicles especially in loose soils. Trafficability and mobility research originally began at the U.S. Army Engineer Waterways Experiment Station (WES) in 1945, following the poor performance of trafficability and mobility by military vehicles during World War II (Willoughby and Turnage, 1988). Studies showed that the excessive sinkage with poor traction can

cause military vehicles to be immobilized by increasing the rolling resistance, which is the resistance that occurs when a round object such as a ball or tire rolls on a surface. This resistance is caused by the deformation of the object, the deformation of the surface, or both. It depends very much on the material of the wheel or tire and the sort of ground (Hibbeler, 2007).

3. Vehicle rutting model

From World War II, vehicle mobility prediction affected by rut formation has become an important research focus both for military vehicles, agricultural machines and engineering vehicles. Recently, it is also an urgent requirement to predict rut formation to protect the environment. To achieve this goal, several models have been developed mostly based on field and lab tests and experiences.

3.1 Bekker type model

Bekker conducted much of the research for off-road locomotion in the 1950s. His theory deals with computing the mobility and locomotion performance parameters of terrestrial vehicles on a variety of terrain. Bekker proposed pressure/sinkage relationship of soils and set a landmark in understanding non-linear soil deformation under the vehicular traffic (Park et al., 2004). Bekker assumed that a track could be represented by a rigid rectangular plate and the relationship between pressure and sinkage (rut depth) is characterized as (Wong, 2001):

$$p = (\frac{k_c}{b} + k_\varphi) z^n \tag{1}$$

where p is the vertical pressure, b is the smaller dimension of the contact patch, that is, the width of a rectangular contact area, or the radius of a circular contact area, z is the sinkage, and n, k_c and k_φ are pressure-sinkage parameters. It has been shown that k_c and k_φ are related to the width of rectangular plates with large aspect ratios (Length/Width) which exceed five to seven.

Based on Bekker's classic model, the pressure-sinkage relationship for an organic terrain is proposed as (Wong, 2001):

$$p = k_p z + 4 m_m z^2 / D_h \tag{2}$$

where p is the vertical pressure, z is the sinkage, k_p is a stiffness parameter for peat, m_m is a strength parameter for the surface mat, and D_h is the hydraulic diameter of the contact area (or sinkage plate), which is equal to $4A/L$. A and L are the area and the perimeter of the contact patch, respectively.

3.2 Soil compaction model

Soil compaction occurs when weight of heavy machinery compresses soil, causing it to lose pore space. Soil compaction can be defined as the movement of soil particles together (Ayers et al., 1990). When fragile soils become compacted, losing aeration by heavy machinery, it will become more resistant to absorb rainfall, thus increase runoff and gully erosion.

Boussinesq developed equations for the state of stress within homogeneous and linearly elastic material, assuming that the weight was applied at a single point on the soil surface. The value of the vertical stress is proposed as (Holtz and Kovacs,

1981):

$$\sigma_z = \frac{Q(3z^3)}{2\pi(r^2+z^2)^{5/2}} \tag{3}$$

where σ_z is the vertical stress, Q is the vertical point load, z is the depth from the ground to the place where σ_z is desired, and r is the horizontal distance from the point load to where σ_z is desired.

Assuming that a line load (force per unit) is applied on the soil surface, the value of the vertical stress is:

$$\sigma_z = \frac{2P}{\pi}\frac{z^3}{(z^2+r^2)^2} \tag{4}$$

where σ_z is the vertical stress, P is the line load, z is the depth from the ground to the place where σ_z is desired, and r is the horizontal distance from the line load to where σ_z is desired.

Assuming that an area load (force per area) is uniformly applied on the soil surface, the value of the vertical stress is:

$$\sigma_z = q_0 \frac{1}{4\pi}\left[\frac{2mn(m^2+n^2+1)^{1/2}}{m^2+n^2+1-m^2n^2}\times\frac{(m^2+n^2+2)}{(m^2+n^2+1)}+\arctan\frac{2mn(m^2+n^2+1)^{1/2}}{m^2+n^2+1-m^2n^2}\right] \tag{5}$$

where σ_z is the vertical stress, q_o is the surface load, z is the depth from the ground to the place where σ_z is desired, m is equal to x/z, n is equal to y/z, x and y are the length and width of the uniformly loaded area, respectively.

Jakobsen et al. (1989) predicted the soil compaction under pneumatic tires by computer simulation, using Newmark's model, as the following:

$$p(z) = p(0)(1.0-(1.0+(r/z)^2)^{-\nu/2}) \tag{6}$$

where $p(z)$ is the vertical pressure, z is the depth from the ground to the place where σ_z is desired, $p(0)$ is the uniform contact pressure between the soil and a circular plate with radius, r, and ν is a concentration factor, often in the range of 4 to 16.

Obviously, soil stress is related to soil displacement to determine sinkage, the higher stress, the bigger displacement, and the deeper sinkage.

3.3 Waterways Experiment Station (WES) rut depth model

Original research on off-road vehicle performance began during World War II at the U.S. Army Waterways Experiment Station to assess vehicle mobility on a "go/no go" basis in fine- and coarse-grained soil. Later, models to predict the sinkage were developed by them.

To compare the one-pass and multipass rut depths, Willoughby conducted experiments on vehicle performance in clay soils. The equation for predicting wheeled vehicle sinkage is as follows (Willoughby and Turnage, 1988):

$$z = dN^{1/2} \frac{5}{\left[\frac{RCI \cdot b \cdot d}{W \cdot (1-\delta/h)^{3/2} \cdot s^{1/5}}\right]^{5/3}} \tag{7}$$

where RCI is the rating cone index, b is the tire unloaded width, d is the tire unloaded diameter, W is the vertical wheel load, δ is the tire loaded deflection, h is the tire unloaded section height, s is the slip in decimal form, z is the sinkage of powered wheel after Nth wheel pass, and N is the number of wheel passes.

The equation for predicting tracked vehicle sinkage is as follows (Willoughby

and Turnage, 1988):

$$z = 0.00443 e^{\frac{5.887W}{RCI \cdot b \cdot l}} N^{1/2} \tag{8}$$

where RCI is the rating cone index, b is the track width, l is the track contact length measured on a flat, hard surface, W is the vertical load on each track, z is the sinkage of powered track after Nth pass, and N is the number of passes. For turning vehicles, Willoughby's analysis indicated that RCI values should be 5% less than actual values used in the straight-line relationships for wheeled vehicles, 25% less for tracked.

Two dimensionless prediction terms were developed by WES to predict the fundamental traction forces of drawbar, soil motion resistance, drive torque, slip and sinkage of single traction element. The clay-tire numeric Πc is for tires operating in purely cohesive soil (near-saturated clay). The sand-tire numeric Πs is for tires operating in purely frictional soil (dry sand). These two numerics are as follows (Reid et al., 2007):

$$\Pi_c = \frac{RCI(bd)}{w(1-\delta/h)^{3/2}(1+b/d)^{3/4}} \tag{9}$$

and

$$\Pi_s = \frac{G(bd)^{3/2}}{w(1-\delta/h)^3} \tag{10}$$

where,

RCI = the rating cone index

G = the cone index gradient

b = the tire section width

d = the nominal wheel diameter

h = the tire section height

δ = the tire deflection

w = the weight beneath a single tire (tire ground reaction force).

4. Effects of turning maneuvers on rut formation of off-road vehicles

Current reports show large variations in rut formation for turning vehicles. Rut formation on turns is different from on straight paths. Durham (1976) conducted laboratory testing of powered wheels in the turned mode operating on yielding soils. He found that the turn angle was of secondary importance to determine the sinkage coefficient and the sinkage coefficient increased with increasing wheel turn angle for a given sand mobility number. Braunack (1986) used an armored personnel carrier (M113) to impose various impacts on a fine sandy loam to investigate the changes in physical properties of two dry soils. He found that the degree of change depended on soil type, the number of vehicle passes and whether the vehicle was traveling in a straight line or turning. Braunack and Williams (1993) found that rut depth increased as the number of passes and turns increased, but especially after turning maneuvers, by testing a M113 armored personnel carrier and a Leopard tank at different soil strength and moisture conditions. Ayers (1994) used a M113 armored personnel carrier to perform three kinds of turning radii: Straight, Smooth turn and Sharp turn. He found that decreased turning radius (sharp turn) could increase soil disturbance and track ruts, and the width and depth of track and height of soil piled

also increased during the sharp turn. Halvorson et al. (2001) investigated the soil compaction and over-winter changes of a tracked vehicle, the M1A2 Abrams tank. They found that turning ruts had a greater amount of initial disturbance than straight-path ruts and smoothed more than straight-path ruts after the winter.

Affleck et al. (2005) revealed that soil disturbance was significantly different when the vehicle was turning rather than when moving straight ahead. A Stryker vehicle was used to conduct their impact tests, consisting of spiral and multi-pass tests. Althoff and Thien (2005) used a randomized complete-block design to investigate the impact of M1A1 tank disturbance on soil quality, invertebrates and vegetation characteristics. The treatments consisted of five passes (crossing, within, straight-a-way, and curve) and two soil conditions (dry and wet). They found that rut formation on a curve was significantly greater for the outside track than for the inside track. Jones et al. (2007) and Reid et al. (2007) introduced the Vehicle Terrain Interface (VTI) model developed by US Army Engineer Research and Development Center (ERDC) in their paper, which was used to predict the interactions of the vehicles with the terrain surfaces. The steering angle was considered as a factor affecting the interaction in VTI.

5. Summary

Vehicle ruts can cause severe environmental damages and reduce the vehicle's mobility. The degree of rut formation depends on vehicle dynamics and soil mechanics. The rut of a turning vehicle is greatly different from the rut of a static

vehicle or a going straight vehicle. Studies on rut formation were reviewed. Previous studies show that turning factor does have an important influence on rut formation. Field tests show that a turning vehicle can produce deeper ruts, which will limit the vehicle's mobility and damage the environment more severely. Models to predict rut formation were also reviewed. Currently there is little knowledge about turning influence. Some engineers and scientists have conducted wide researches on rut formation, but their vehicles went straight or were static during the testing. Military vehicles perform lots of turning maneuvers during training. It is necessary to investigate the rut formation caused by a turning military vehicle.

Reference

[1] Affleck RT. Disturbance measurements from off-road vehicles on seasonal terrain. U.S. Army Cold Regions Research and Engineering Laboratory, Technical Report: TR-05-12; 2005.

[2] Althoff PS, Thien SJ. Impact of M1A1 main battle tank disturbance on soil quality, invertebrates, and vegetation characteristics. J Terramechanics 2005; 42(3-4): 159-176.

[3] Arvidsson J, Hakkansson I. A model for estimating crop yield losses caused by soil compaction. Soil and Tillage Research 1991; 20(2-4): 319-332.

[4] Ayers PD, Shaw RB, Diersing VE, Riper JV. Soil compaction from military vehicles. Technical Report ASAE Meeting Paper No. 901096. St. Joseph, Michigan; 1990.

[5] Ayers PD. Environmental damage from tracked vehicle operation. J Terramechanics 1994; 31(3): 173-183.

[6] Braunack MV, Williams BG. The effect of initial soil water content and vegetative cover on surface disturbance by tracked vehicles. J Terramechanics 1993; 30(4): 299-311.

[7] Braunack MV. Changes in physical properties of two dry soils during tracked vehicle passage. J Terramechanics 1986; 23(3-4): 141-151.

[8] Durham GN. Powered wheels in the turned mode operating on yielding soils. U.S. Army Engineer Waterways Experiment Station, M-76-9; 1976.

[9] Elliot WJ, Laflen JM. A process-based rill erosion model. Transactions of ASAE 1993; 36: 65-72.

[10] Halvorson JJ, McCool DK, King LG, Gatto LW. Soil compaction and over-winter changes to tracked-vehicle ruts, Yakima Training Center, Washington. J Terramechanics 2001; 38(3): 133-151.

[11] Haugen LB, Ayers PD, Anderson AB. Vehicle movement patterns and vegetative impacts during military training exercises. J Terramechanics 2003; 40(2): 83-95.

[12] Hibbeler RC. Engineering Mechanics: Statics & Dynamics. NJ, Prentice Hall; 2007.

[13] Holtz RD, Kovacs WD. An introduction to geotechnical engineering. Englewood Cliffs. NJ, Prentice Hall; 1981.

[14] Jakobsen BF, Dexter AR. Prediction of soil compaction under pneumatic tyres. J Terramechanics 1989; 26(2): 107-119.

[15] Jones A, McKinley G, Richmond P, Creighton D. A vehicle terrain interface. In: ISTVS conference. Fairbanks, Alaska; 2007.

[16] Jones R, Horner D, Sullivan P, Ahlvin R. A methodology for quantitatively assessing vehicular rutting on terrains. J Terramechanics 2005; 42(3-4): 245-257.

[17] Park S, Popov AA, Cole DJ. Influence of soil deformation on off-road heavy vehicle suspension vibration. J Terramechanics 2004; 41(1): 41-68.

[18] Raper RL. Agricultural traffic impacts on soil. J Terramechanics 2005; 42(3-4): 259-280.

[19] Reid AA, Shoop S, Jones R, Nunez P. High-fidelity ground platform and terrain mechanics modeling for military applications involving vehicle dynamics and mobility analysis. In: ISTVS conference. Fairbanks, Alaska; 2007.

[20] Saarilahti M. Soil interaction model. Quality of Life and Management of Living Resources Contract, No. QLK5-1999-00991; 2002.

[21] Voorhees WB, Young RA, Lyles L. Wheel traffic considerations in erosion research. Transactions of ASAE 1979; 22: 786-790.

[22] Willoughby WE, Turnage GW. Review of a procedure for predicting rut depth. Unpublished memo; 1988.

[23] Wong JY. Theory of ground vehicles. New York, Wiley – Interscience; 2001.

Part 2 Influence of Soil and Vehicle Parameters on Soil Rut Formation

This chapter is a reformatted version of a paper, by the same name, submitted to Journal of Terramechanics by Kun Liu, Paul Ayers，Heidi Howard，and Alan Anderson.

Liu K, Ayers P, Howard H, Anderson A. Influence of turning radius on wheeled military vehicle induced rut formation. Journal of Terramechanics 2009; 46(2): 49-55.

Abstract

Soil and vehicle parameters have significant effects on soil rut formation. A randomized design was used to investigate the effects of five treatments: soil texture, soil moisture, vehicle type, turning radius and velocity, on rut depth, rut width and rut index, what measure the degree of soil disturbance. This vehicle rutting study was conducted on four off-road military vehicles under two soil moisture conditions and two soil texture conditions at Fort Riley, Kansas. A GPS-based vehicle tracking system was used to track the vehicle dynamics, and rut measurements were taken manually. SAS 9.1 was used to investigate the effects of soil and vehicle parameters on rut formation. Results show that all the vehicle parameters (vehicle type, weight, velocity and turning radius) and soil parameters (soil texture and moisture) are statistically significant to affect rut formation.

1. Introduction

Off-road military vehicles, including wheeled and tracked, can cause soil disturbance, which will damage the environment by decreasing plant development, concentrating runoff and increasing erosion. Also, soil disturbance, especially deep ruts, can reduce the mobility of military vehicles [1-6].

Many environment scientists and military engineers have conducted research on the interaction between military vehicles and soil. From the aspect of soil, moisture is a determinative factor on rut formation. Water content in soil is highly correlated with soil strength. The bearing capacity of soil with low moisture is higher than its

capacity with high moisture. Rajaram and Erbach [7] found that soil strength indicated by cone penetration resistance, cohesion, and soil aggregate size, increased with the degree of drying stress. Ibarra et al. [8] found that densification always increased soil strength independent of the compaction path, and drying the soil after densification could improve soil strength. Raper [9] reported that wet soil reduced soil strength and the increased moisture would decrease the density of the soil. The swelling of clay particles would increase sliding action between soil particles, reducing compaction for wet soil. Carter et al. [10] found that soil strength varied by soil disturbance class, and low soil strength and high moisture level appeared in high soil disturbance areas.

Texture can affect mechanical properties of soil, thereby affecting rut formation. Sánchez-Girón et al. [11] found that soil with higher clay content had higher capacity to bear normal stresses. Horn and Fleige [12] found that soil strength varied by soil suction, texture and structure. They also developed a function to predict the stress based on these terms. Peng et al. [13] reported that soil strength was affected by soil texture and initial soil bulk density. The coarser the soil texture, the lower the soil strength.

In addition, vehicle maneuver is an important factor to rut formation. Braunack and Williams [14] found that rut depth increased after turning maneuvers in different soil strength and moisture conditions. Ayers [2] found that decreased turning radius (sharp turn) would increase soil disturbance and track ruts, and the width and depth of track. The height of soil pile also increased during the sharp turn. Affleck et al.

[15] revealed that soil disturbance was significantly different when the vehicle was turning rather than going straight. Affleck [16] found that the volume of soil displacement was much higher when the vehicle was turning than on a straight path, both on wheeled and tracked vehicles.

The various factors mentioned above are actually correlated with each other in field tests. In order to evaluate the influence of these factors on rut formation, a comprehensive study is needed.

2. Objectives

The objective of this study was to investigate the effects of vehicle and soil parameters on rut formation. The vehicle parameters include vehicle type, weight, velocity and turning radius. The soil parameters include soil texture and moisture.

3. Methods and materials

A vehicle rutting study was conducted at Fort Riley, a United States Army Installation located in Northeast Kansas. There are three vegetation communities at Fort Riley: grasslands, shrublands and woodlands [1]. The test sites of this study are mainly covered by grass. The soil textures are clay upland soil and loamy upland soil. These tests were conducted on October 19, 2004 (dry conditions) and April 12, 2005 (wet conditions). The averaged gravimeter water contents were 11.3 % by weight dry basis for the clay upland soil (Irwin silty clay loam) and 11.6 % for the loamy upland soil (Wymore silty clay loam) in October, 2004. In dry conditions the soil

strength was very high. It was too hard to use the cone penetrometer to penetrate the soil, so drop cone was used instead of cone index. The drop cones were 4.9 cm for the clay upland soil, and 4.8 cm for the loamy upland soil. In April, 2005, the water contents were 26.8 % for the clay upland soil, and 30.2 % for the loamy upland soil. The drop cones were 7.6 cm for the clay upland soil, and 8.2 cm for the loamy upland soil. The cone index was 553 kPa for the clay upland soil, and 558 kPa for the upper 15 cm loamy upland soil.

Four vehicles were used for this study: the combat tank M1A1 (Fig. 2-1), the Armored Personnel Carrier (APC) M113 (Fig. 2-2), the Heavy Expanded Mobility Tactical Truck (HEMTT) M978 (Fig. 2-3), and the High Mobility Multi-purpose Wheeled Vehicle (HMMWV) M998 (Fig. 2-4). Table 2-1 shows the parameters of these vehicles.

A Vehicle Tracking System (VTS) was mounted onto each vehicle to utilize the Global Positioning System (GPS) in tracking the vehicle. The VTS consisted of a Trimble AgGPS 132, 12-channel receiver with Omnistar Satellite differential correction; differential GPS data for the vehicle were collected every second. The vehicles were operated in spiral patterns (constantly decreasing turning radius by turning to the right) at two different speeds, high and low (high 4-7 m/s and low 2-4 m/s). Travel speed can affect soil compaction, which decreases with the increase of speed [17]. Thus speed may affect the rut formation.

Vehicle rutting measurements were taken every 4 to 7 meters along each spiral track (inside and outside track), and GPS positions were taken at each measurement

point using the same VTS that was used to collect the vehicle tracking data. There were 1654 rut measurements along 32 spirals.

Measurements of soil rut depth and width were taken in the inside and outside track at each impact point. Rut width is a measurement across the vehicle track of the width of the rut. Rut depth is the vertical distance from the bottom of the track to the surface, taken at the middle of the rut width.

Rut index was also determined. Rut index is a composite indicator of soil profile disturbance, which is the product of rut depth and rut width, but has no units. As the shape of the rut cross section is not a rectangle and its area cannot be calculated by rut depth times rut width, providing a unit of area may incorrectly indicate this index as a cross-sectional area [18]. Note though rut index does not have units, its value depends on the units of rut depth and rut width. Vehicle velocity and turning radius were derived from the GPS tracking data [19]. Turning radius was calculated using a three-point method [20].

Soil rutting measurements were divided into three turning radius (TR) classes: 1. Sharp turns: TR<30 meters; 2. Intermediate turns: TR=30-80 meters; and 3. Straight: TR>80 meters. Rut depth and rut width were measured at points along the spiral and then related to the vehicle turning radius.

This experiment is a randomized design, in order to test if the treatments have effects on the dependent variables. In this paper, the dependent variables are rut depth, rut width and rut index. The treatments are soil texture (Clay and Loamy), soil moisture (Dry and Wet), vehicle type (M1A1, APC, HEMTT and HMMWV),

turning radius (Sharp turns, Intermediate turns and Straight), and rut placement (Inside and Outside of turns).

4. Results and discussion

4.1 Treatment effects on rut depth, rut width and rut index

All the 1654 observations were analyzed together. The dataset included all the four vehicles in different soil conditions. The impacts of the treatments on vehicles and soil were investigated using the Statistics Analysis System (SAS) 9.1.

Table 2-2 shows the results of tests of fixed effects on rut depth. Vehicle type has significant effects on rut depth (P value<0.0001). In this table, DenDF represents Density of Degree of Freedom, which is equal to the total number of observations minus 1. NumDF represents Number of Degree of Freedom, which is equal to total number of levels minus 1. Fig. 2-5 shows the inside rut depths of four vehicles in wet conditions. These four vehicles can form various rut depths. The heaviest one, M1A1 tank, can form the deepest ruts. The lightest one, HMMWV, has the shallowest ruts.

Moisture has significant effects on rut depth (P value<0.0001) (Table 2-2). Vehicles easily form ruts in wet soil. When the soil was dry, its bearing capacity was high enough to support the vehicles. For the M1A1, APC, HEMTT and HMMWV, there was no rut depth observed, or the ruts were very shallow and they were difficult to measure and considered zero. All the rut depths were measured in wet conditions. For the HMMWV, its rut depth was not observable even in wet conditions.

Speed has significant effects on rut depth (P value=0.0339) (Table 2-2). However, the effects are different on these four vehicles (Fig. 2-6), because the difference between the fast speed and the slow speed is small. For the M1A1 tank and HEMTT, fast speed can form deeper ruts than slow speed. For the APC, the ruts at slow speed are deeper.

Turning radius has significant effects on rut depth (Table 2-2). Though the P value is 0.1014, a little higher than 0.1000, it is significant near the 90% level of confidence, considering the complexity of the soil model. In addition, all the rut depths were measured in wet conditions and there were no observable rut depth data in dry conditions. If the interactions between treatments are considered, the effects of turning radius are significant (P value<0.0001). Soil texture does not have significant effects on rut depth (P value=0.6485). As observed in field tests, the strengths of clay and loamy soil determining the bearing capacity were very close to each other.

Table 2-3 shows the results of tests of fixed effects on rut width. Fig. 2-7 shows the inside rut widths of four vehicles in wet conditions. As on rut depth, vehicle type has significant effects on rut width (P value<0.0001). M1A1 can form the widest ruts and ruts of HMMWV are the narrowest. Rut width is highly correlated with the tread width or tire width of the vehicle. The tread of M1A1 tank is widest of these four vehicles, 63 cm, while the tire of HMMWV is the narrowest, 29.5 cm. Moisture has significant effects on rut width (P value<0.0001). In wet conditions, vehicles can form wider ruts than in dry conditions, as vehicles easily slide to form wider ruts

in wet conditions because of the reduced frictional resistance. An increase in water content thus results in a decrease in friction [21]. Speed does not have significant effects on rut width (P value=0.3389). As observed in field tests, rut widths at high speed are almost the same as rut widths at low speed. Turning radius has significant effects on rut width (P value<0.0001). During turning, vehicles will form wider ruts than when going straight. Soil texture has significant effects on rut width (P value<0.0001). Vehicles can form wider ruts on clay soil than on loamy soil. With the increase of water content the angle of internal friction for clayey sand decreases quickly [22]. Hence, it is easier for these vehicles to slide on wet clay soil and form wider ruts.

Table 2-4 shows the results of tests of fixed effects on rut index. Fig. 2-8 shows the inside rut indexes of four vehicles in wet conditions. Since rut index is equal to rut depth times rut width, it is influenced by both rut depth and rut width. Any treatment influencing rut depth or rut width may influence rut index. Table 2-4 shows that all the P values are < 5% and all the treatments have significant effects on rut index.

4.2 Treatment effects on individual vehicles

For an individual vehicle, only two treatments were included. One was to investigate the effects of turning radius of this vehicle on rut formation. The other was to investigate the effects of placement of rut on rut formation. The inside ruts are formed by wheels or treads on the inside of the turn and the outside ruts are formed by wheels or treads on the outside of the turn. Since there was no observable

rut depth data in dry conditions, all the data used in this part were collected in wet conditions.

4.2.1 M1A1 tank

Table 2-5 shows that turning radius has significant effects on rut depth (P value=0.0128) and the placement of rut has significant effects on rut depth (P value=0.0145). Fig. 2-9 shows the averages of rut depth in three classes of turning radius. For the M1A1 tank, the averages of rut depth are very close in these three classes, but it is still found that turning maneuvers can form deeper ruts than going straight. The inside ruts are deeper than the outside ruts. Though the inside rut depths are statistically different from the outside rut depths, the differences are very small.

Table 2-6 shows that turning radius has significant effects on rut width (P value<0.0001) and the placement of rut (inside or outside track) does not have significant effects on rut width (P value=0.7894). Fig. 2-10 shows the averages of rut width in three classes of turning radius. A turning M1A1 tank can form wider ruts than an M1A1 tank going straight. From the video of the field test it is found that the tread slides back and forth laterally during the turn, which can increase the depth and width of the rut.

Table 2-7 shows that turning radius has significant effects on rut index (P value<0.0001) and the placement of rut has significant effects on rut index (P value=0.0211). Fig. 2-11 shows the averages of rut index in three classes of turning radius. A turning M1A1 tank has higher rut index than a M1A1 tank going straight.

The inside rut indexes are higher than the outside rut indexes.

4.2.2 HEMTT

As mentioned above, P values close to 0.1000 are still considered to be significant enough, in view of the complexity of soil models. Thus Table 2-8 shows that turning radius has significant effects on rut depth (P value=0.1124) but the placement of rut does not have significant effects on rut depth (P value=0.3307). Fig. 2-12 shows the averages of rut depth in three classes of turning radius. The inside rut depths are the same as the outside rut depths. For the HEMTT, the effects of turning radius are special, because going straight can form deeper ruts than turning. When the HEMTT is going straight, all four wheels on each side are in the same rut, which is a multi-pass rut and deeper. However, when the vehicle is turning, the four wheels separate and every wheel will form a new rut, which is a single-pass rut and shallower.

Table 2-9 shows that turning radius has significant effects on rut width (P value<0.0001) and the placement of rut does not have significant effects on rut width (P value=0.7128). Fig. 2-13 shows the averages of rut width in three classes of turning radius. A turning HEMTT can form wider ruts than a HEMTT going straight. The inside rut widths are the same as the outside rut widths.

Table 2-10 shows that turning radius has significant effects on rut index (P value=0.0058) and the placement of rut does not have significant effects on rut index (P value=0.3805). Fig. 2-14 shows the averages of rut index in three classes of turning radius. A turning HEMTT have higher rut index that a HEMTT going

straight. The inside rut indexes are the same as the outside rut indexes.

4.2.3 APC

Table 2-11 shows that turning radius has significant effects on rut depth (P value<0.0001) and the placement of rut does not have significant effects on rut depth (P value=0.9919). Fig. 2-15 shows the averages of rut depth in three classes of turning radius. A turning APC can form deeper ruts than an APC going straight. The inside rut depths are the same as the outside rut depths.

Table 2-12 shows that turning radius has significant effects on rut width (P value<0.0001) and the placement of rut has significant effects on rut width (P value=0.0910). Fig. 2-16 shows the averages of rut width in three classes of turning radius. A turning APC can form wider ruts than an APC going straight. For the APC, the outside ruts are wider than the inside ruts.

Table 2-13 shows that turning radius has significant effects on rut index (P value<0.0001) and the placement of rut does not have significant effects on rut index (P value=0.5563). Fig. 2-17 shows the averages of rut index in three classes of turning radius. A turning APC has a higher rut index than an APC going straight. The inside rut indexes are the same as the outside rut indexes.

4.2.4 HMWWV

For the HMWWV, there was no observable rut depth measured in both wet and dry conditions. Even in wet conditions the soil could support the vehicle. What can be measured was the impact width on vegetation. Rut index cannot be calculated. Table 2-14 shows that turning radius has significant effects on impact

width on vegetation (P value<0.0001) and the placement of rut does not have significant effects on impact width on vegetation (P value=0.7345). Fig. 2-18 shows the averages of impact width on vegetation in three classes of turning radius. A turning HMWWV can have wider track on vegetation than a HMWWV going straight. The inside impact widths on vegetation are similar to the outside impact widths.

4.2.5 Influence of the placement of rut

It is apparent that the placement of rut has no effect on rut widths and rut indexes of vehicles except the M1A1 tank and the APC from the statistical analysis. For the APC, the placement of rut has no effect on rut depth, significant effects on rut width, and no effect on rut index. However, for the M1A1 tank, the placement of rut has significant effects on rut depth, no effect on rut width, and significant effects on rut index. Since rut index is the product of rut depth and rut width, it is affected by both. It can be seen that even after multiplying rut depth and rut width together to get rut index, the placement of rut for the M1A1 tank is still able to generate a big enough difference of two sample means, thus producing significant effects on the product, rut index. Conversely, the placement of rut can not produce a big enough difference to generate significant effects on rut index for the APC. One possible reason is that the M1A1 tank is heavier than the APC, and consequently generates higher rut depth, rut width and rut index, overcoming the variability due to field measurement error.

5. Conclusions

Based on a comprehensive study, field tests were conducted to investigate the

effects of many vehicle and soil factors on rut formation. The treatments were vehicle parameters, including vehicle type, weight, velocity and turning radius, and soil parameters, including soil texture and moisture.

Field data were analyzed using the Statistics Analysis System (SAS) 9.1 to make statistical conclusions. Results show that vehicle parameters (vehicle type, weight, velocity and turning radius) and soil parameters (soil texture and moisture) are statistically significant to affect rut formation. These four vehicles can produce various soil disturbances. The M1A1 tank will cause the most serious environmental damage, the widest and deepest rut and highest rut index. When the soil is dry, vehicles do not easily produce ruts, but vehicles can produce deep ruts on wet soil. Soil texture did not have significant effects on rut depth. However, vehicles can form wider ruts on clay soil. At high speed vehicles can form deeper ruts, but speed does not have effects on rut width. Turning maneuvers have significant effects on rut formation. For the M1A1 tank, APC and HMMWV, turning maneuvers can increase rut depth, rut width and rut index. For the HEMTT, turning maneuvers can increase rut width and rut index, but its rut depth decreases when it is turning, from a multi-pass rut to four single-pass ruts. For some vehicles, the inside ruts are different from the outside ruts. The M1A1 tank has deeper inside ruts, while the APC has wider outside ruts.

Acknowledgements

The authors thank Phil Woodford and Chris Otto of Fort Riley Military Installation for helping with coordination efforts and field assistance and expertise. The authors also thank the

U.S. Army Corps of Engineers, Construction Engineering Research Laboratory for project support. The authors are also grateful to the Environmental Security Technology Certification Program (ESTCP) project SI-0815 for providing support for this study.

References

[1] Althoff PS, Thien SJ. Impact of M1A1 main battle tank disturbance on soil quality, invertebrates, and vegetation characteristics. J Terramechanics 2005; 42(3): 159-176.

[2] Ayers PD. Environmental damage from tracked vehicle operation. J Terramechanics 1994; 31(3):173–183.

[3] Evans I. The sinkage of tracked vehicles on soft ground. J Terramechanics 1964; 1(2): 33-43.

[4] Gatto LW. Overwinter changes to vehicle ruts and natural rills and effects on soil erosion potential. In: 10th International Soil Conservation Organization Meeting, Purdue University, 2001.

[5] Shoop S, Affleck R, Collins C, Larsen G, Barna L, Sullivan P. Maneuver analysis methodology to predict vehicle impacts on training lands. J Terramechanics 2005; 42(3): 281-303.

[6] Sullivan PM, Anderson AB. A methodology for estimating army training and testing area carrying capacity (ATTACC) vehicle severity factors and local condition

factors. US Army Engineer Waterways Experiment Station, Technical Report: ERDC-TR-00-2; 2000.

[7] Rajaram G, Erbach DC. Effect of wetting and drying on soil physical properties. J Terramechanics 1999; 36(1):39-49.

[8] Ibarra SY, McKyes E, Broughton RS. A model of stress distribution and cracking in cohesive soils produced by simple tillage implements. J Terramechanics 2005; 42(2):115-139.

[9] Raper RL. Agricultural traffic impacts on soil. J Terramechanics 2005; 42(3):259-280.

[10] Carter EA, Aust WM, Burger JA. Soil strength response of select soil disturbance classes on a wet pine flat in South Carolina. Forest Ecology and Management 2007; 247(1):131-139.

[11] Sánchez-Girón V, Andreu E, Hernanz JL. Response of five types of soil to simulated compaction in the form of confined uniaxial compression tests. Soil and Tillage Research 1998; 48(2):37-50.

[12] Horn R, Fleige H. A method for assessing the impact of load on mechanical stability and on physical properties of soils. Soil and Tillage Research 2003; 73(1):89-99.

[13] Peng XH, Horn R, Zhang B, Zhao QG. Mechanisms of soil vulnerability to compaction of homogenized and recompacted Ultisols. Soil and Tillage Research 2004; 76(2):125-137.

[14] Braunack MV, Williams BG. The effect of initial soil water content and vegetative cover on surface disturbance by tracked vehicles. J Terramechanics 1993; 30(4): 299-311.

[15] Affleck RT, Shoop S, Simmons K, Ayers PD. Disturbance from off-road vehicle during spring thaw. In: 12th ASCE conference, Edmonton, Canada; 2004.

[16] Affleck RT. Disturbance measurements from off-road vehicles on seasonal terrain. US Army Cold Regions Research and Engineering Laboratory, Technical Report: TR-05-12; 2005.

[17] Aboaba FO. Effects of time on the compaction of soil by rollers. Trans. ASAE 1969; 12(3): 302–304.

[18] Liu K, Ayers P, Howard H, Anderson A. Influence of turning radius on wheeled military vehicle induced rut formation. Journal of Terramechanics 2009; 46(2): 49-55.

[19] Li Q, Ayers PD, Anderson AB. Prediction of impacts of wheeled vehicles on terrain. J Terramechanics 2007; 44(2): 205-215.

[20] Haugen LB. Design and testing of a vehicle tracking system for monitoring environmental impact at U.S. army training installations. Master thesis, Colorado State University, Fort Collins, U.S.; 2002.

[21] Ampoorter E, Goris R, Cornelis WM, Verheyen K. Impact of mechanized logging on compaction status of sandy forest soils. Forest Ecology and Management 2007; 241(1): 162-174.

[22] Al-Shayea NA. The combined effect of clay and moisture content on the behavior of remolded unsaturated soils. Engineering Geology 2001; 62(4): 319-342.

Appendix

Fig. 2-1 Combat tank M1A1.

Fig. 2-2 Armored Personnel Carrier (M113).

Fig. 2-3 Heavy Expanded Mobility Tactical Truck (M978).

Fig. 2-4 High Mobility Multi-purpose Wheeled Vehicle (M998).

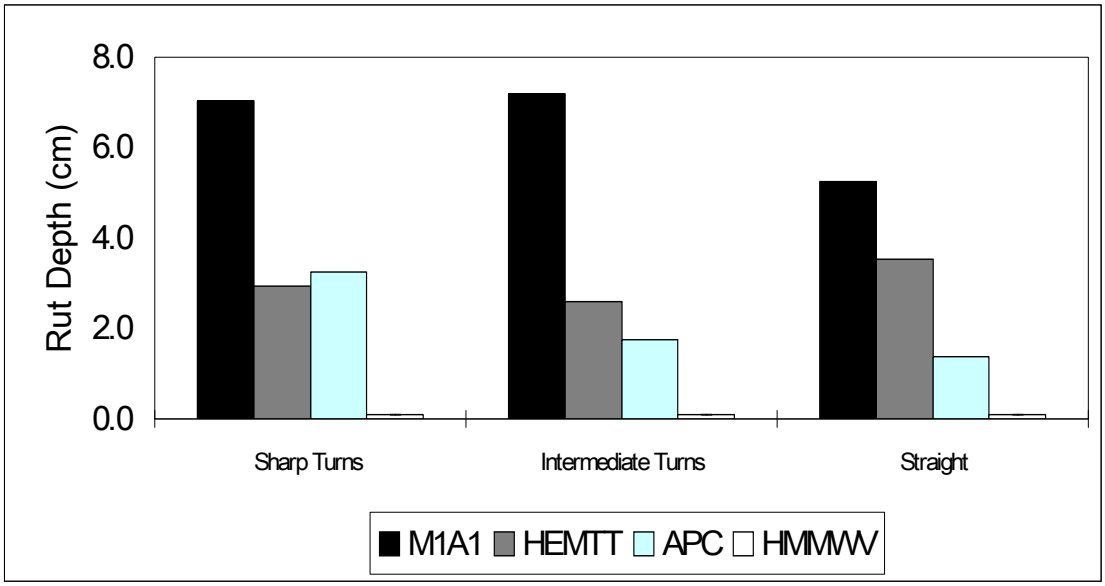

Fig. 2-5 Rut depth in wet conditions (Inside).

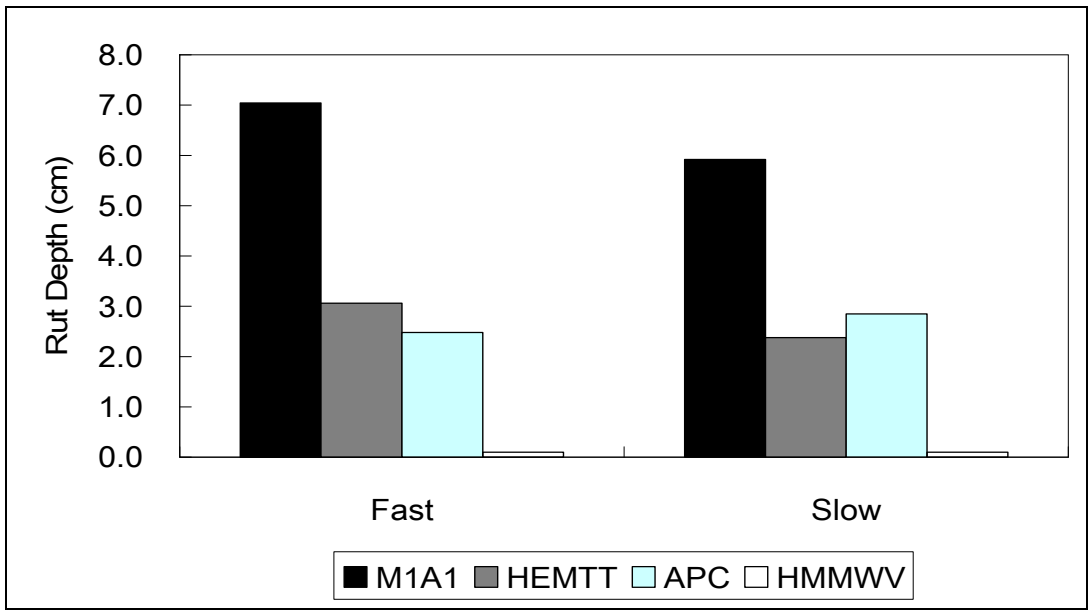

Fig. 2-6 Rut depth at fast and slow speeds.

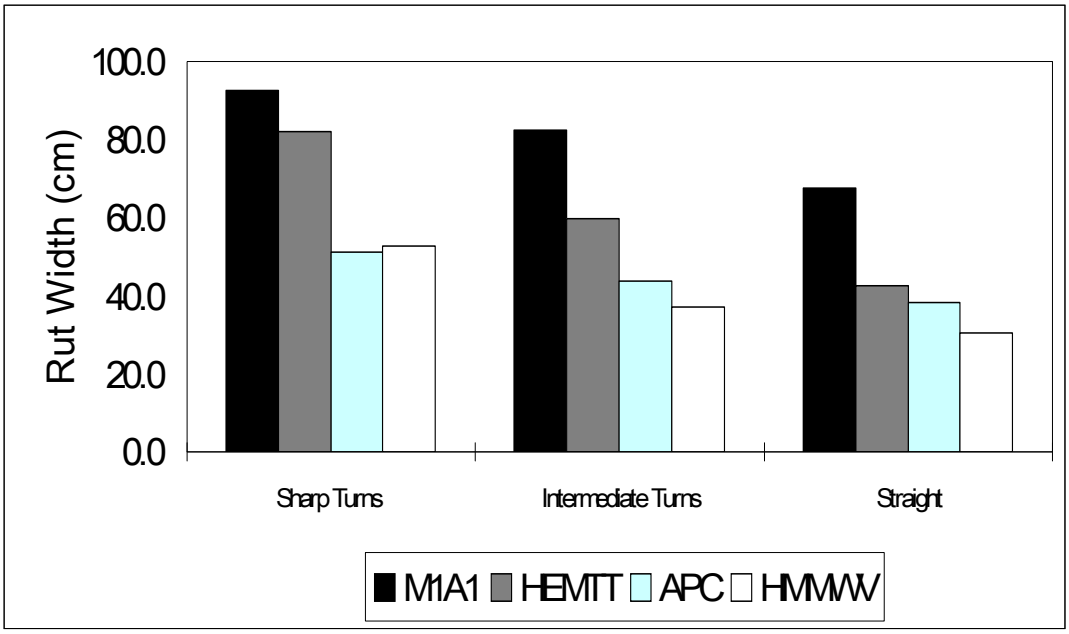

Fig. 2-7 Rut width in wet conditions (Inside).

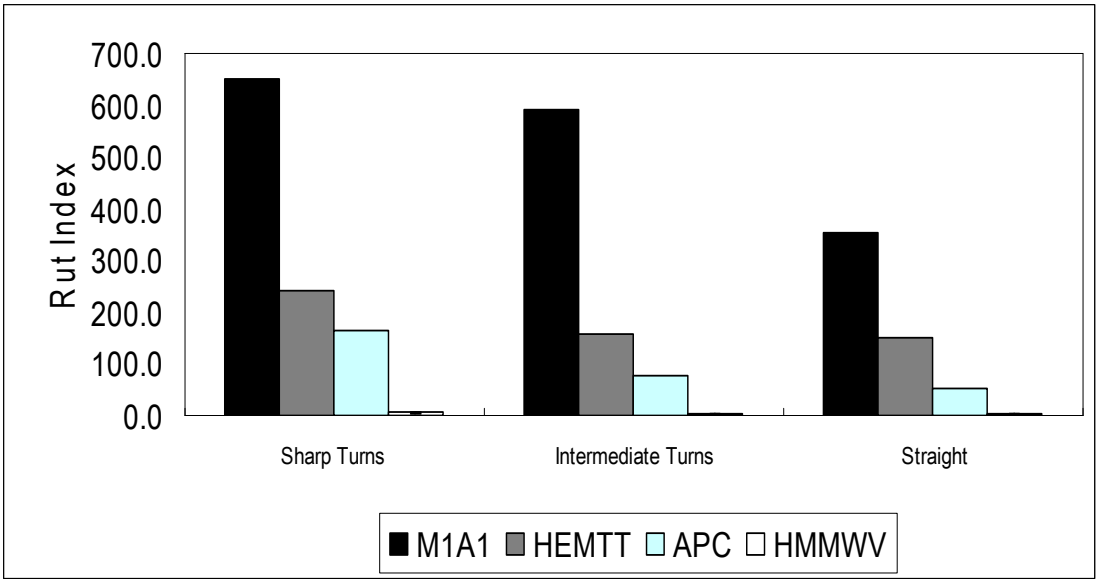

Fig. 2-8 Rut index in wet conditions (Inside).

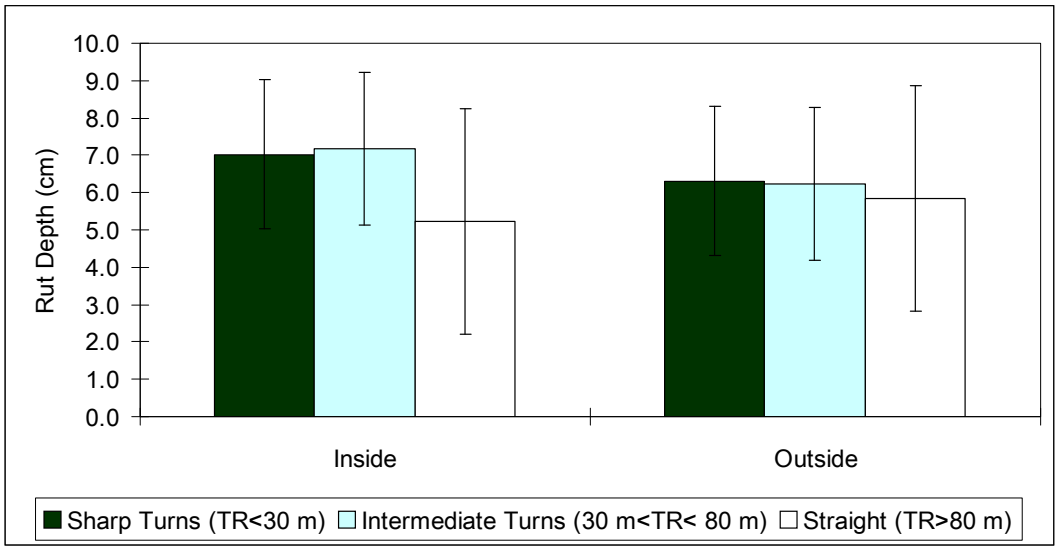

Fig. 2-9 Rut depth of the M1A1 tank.

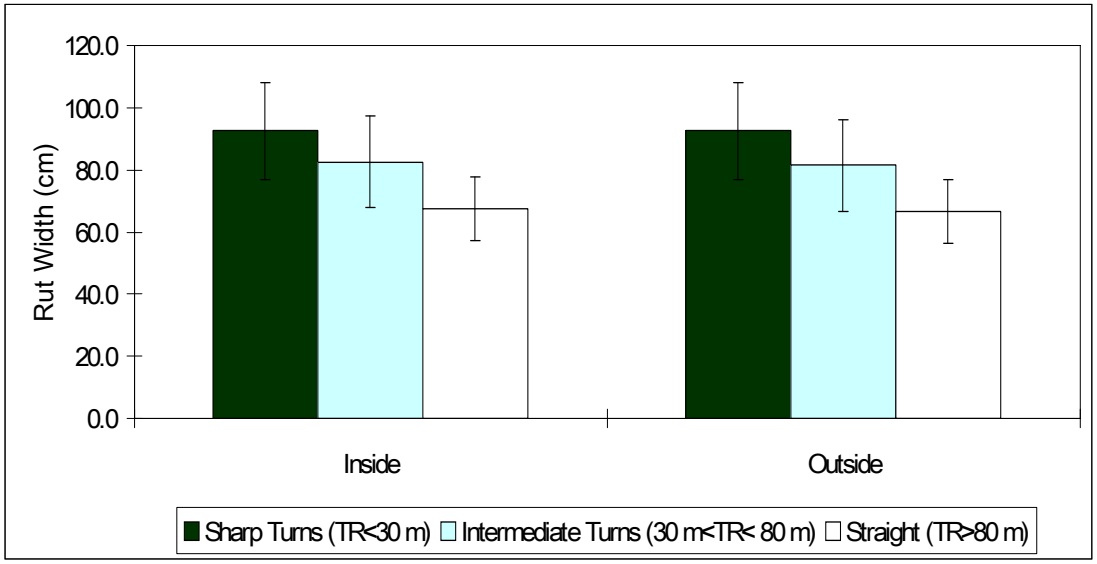

Fig. 2-10 Rut width of the M1A1 tank.

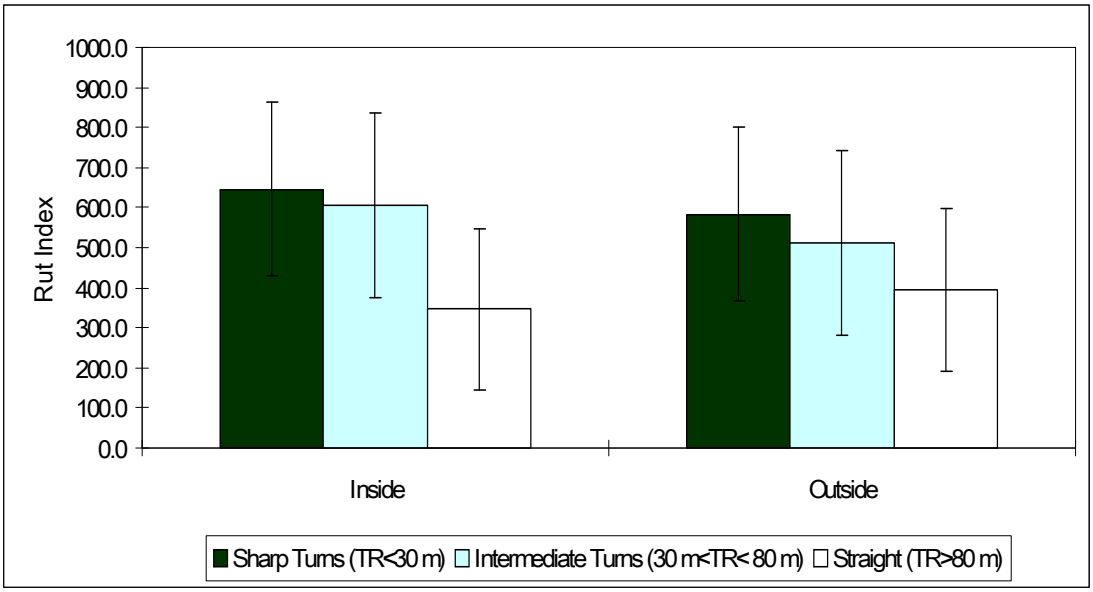

Fig. 2-11 Rut index of the M1A1 tank.

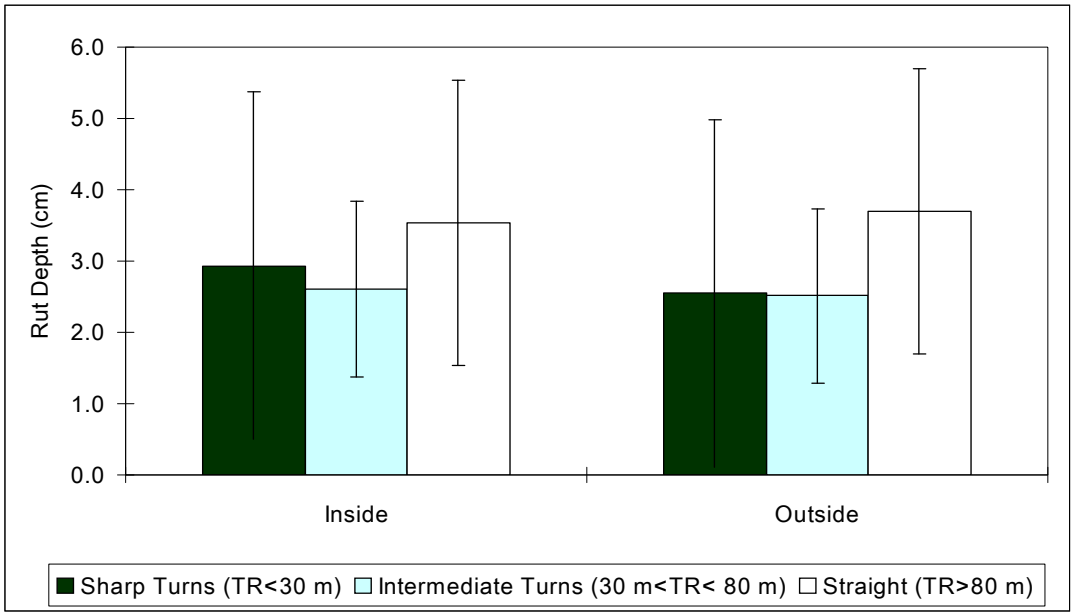

Fig. 2-12 Rut depth of the HEMTT.

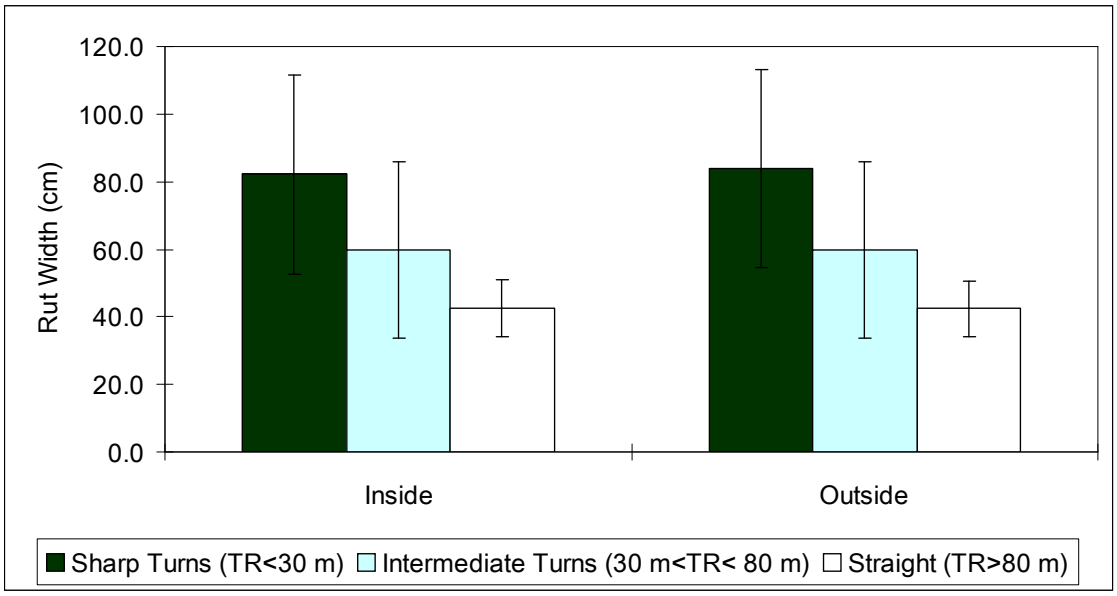

Fig. 2-13 Rut width of the HEMTT.

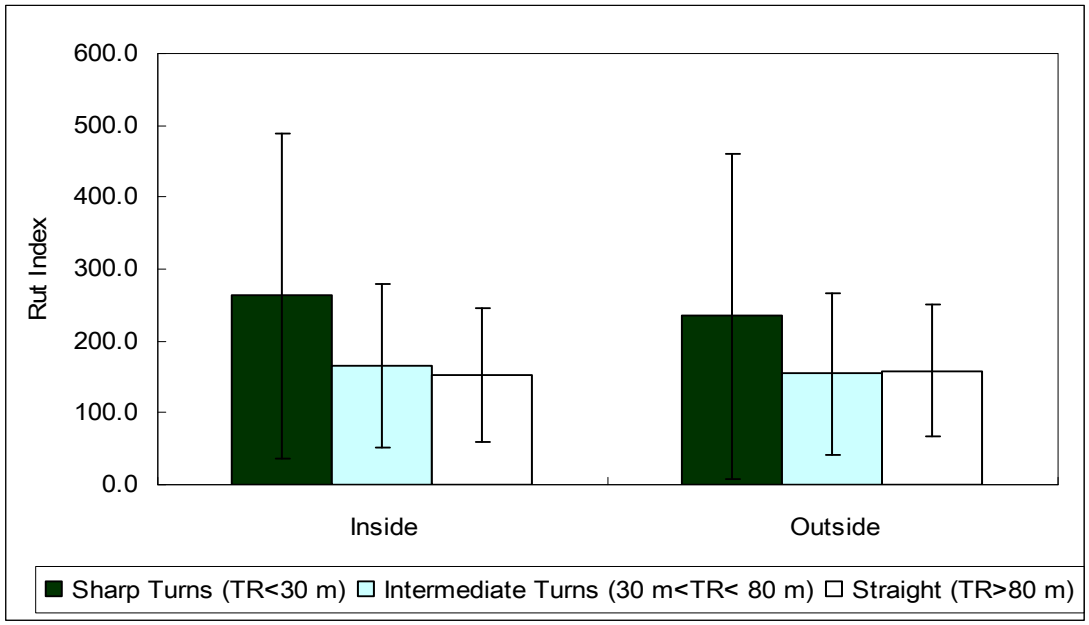

Fig. 2-14 Rut index of the HEMTT.

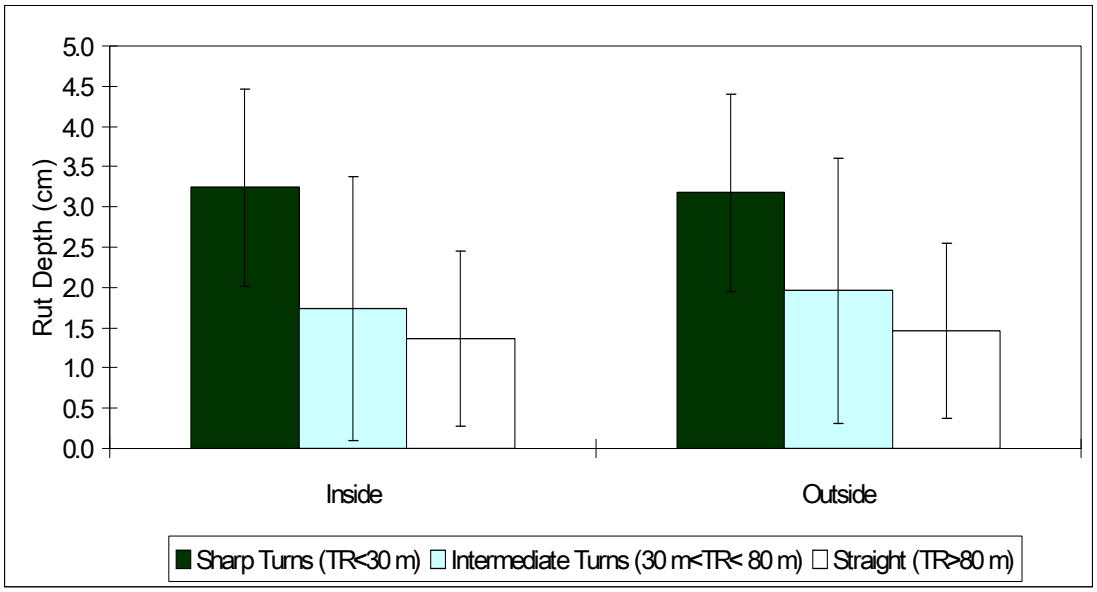

Fig. 2-15 Rut depth of the APC.

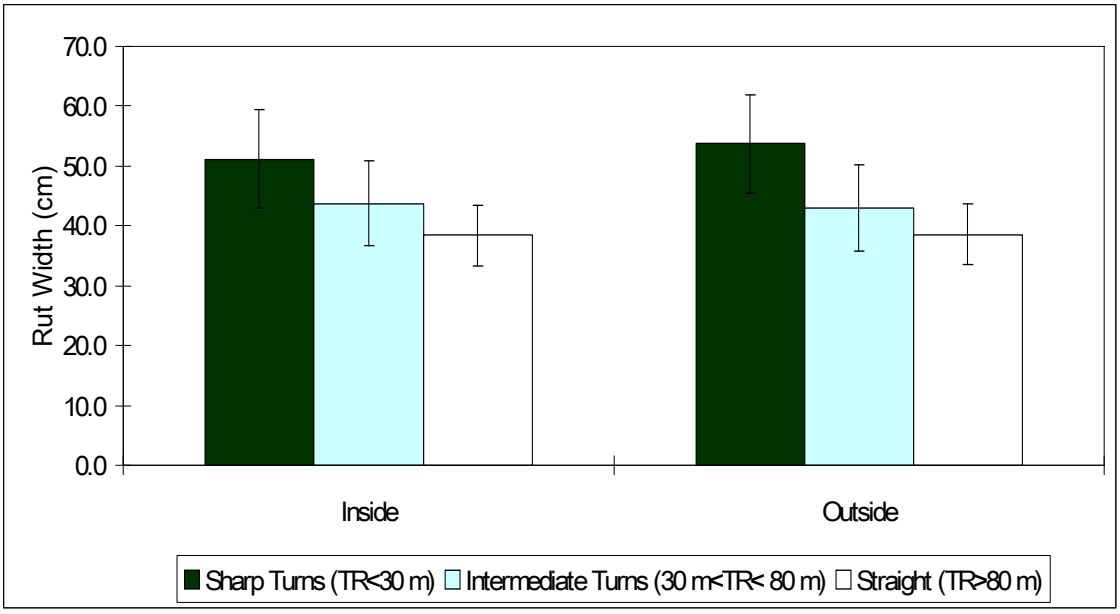

Fig. 2-16 Rut width of the APC.

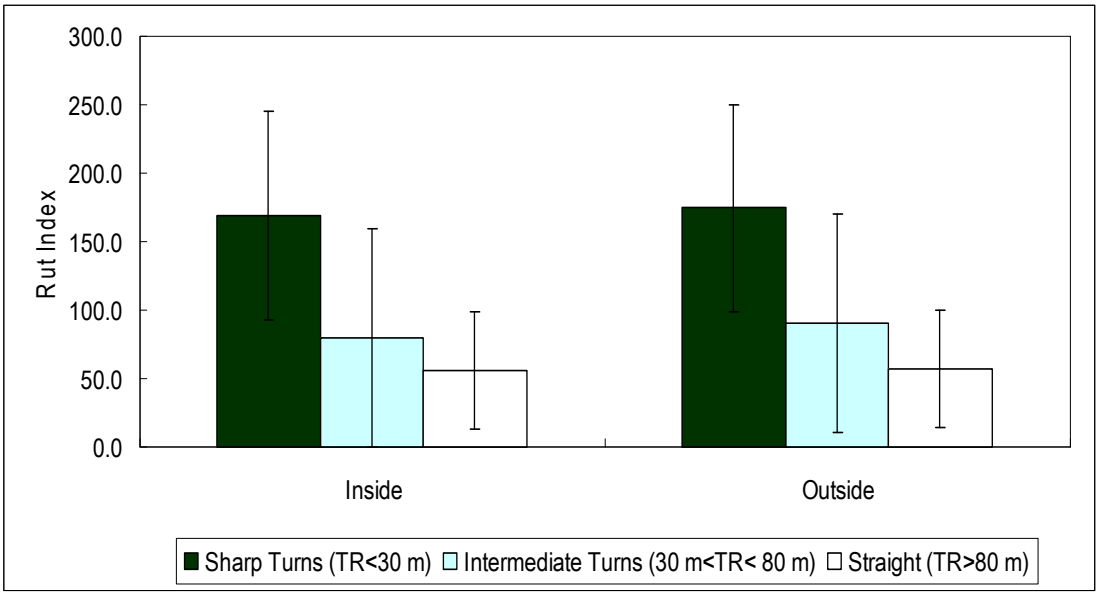

Fig. 2-17 Rut index of the APC.

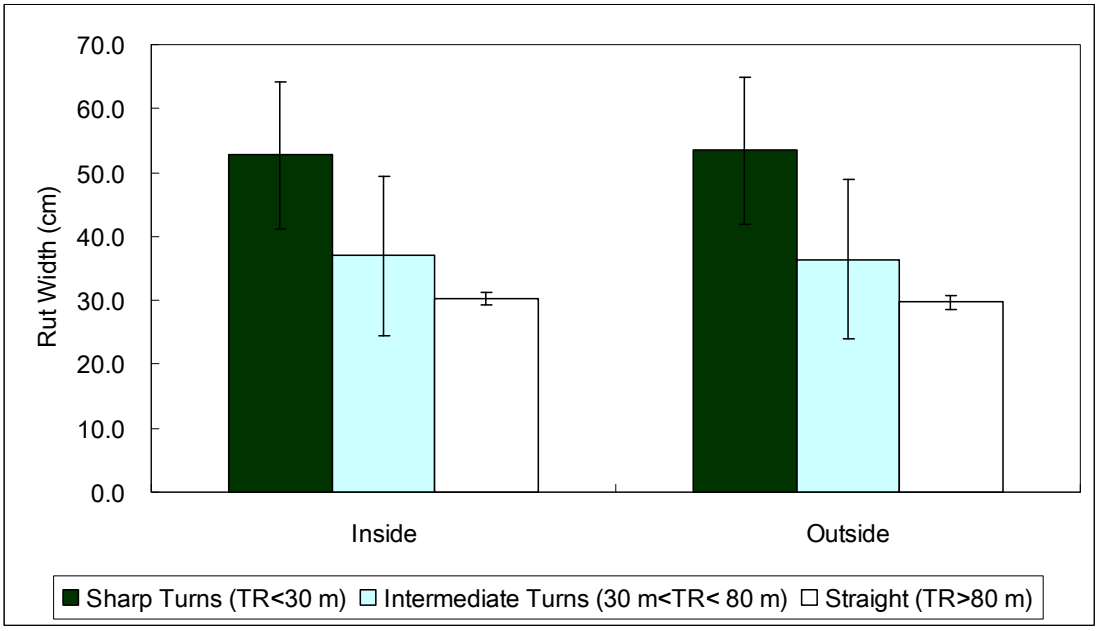

Fig. 2-18 Impact width of the HMMWV.

Table 2-1 Parameters of vehicles.

	Vehicle Weight (kg)	Vehicle Length (m)	Vehicle Width (m)	Track/Tire Width (cm)
M1A1	57153	9.03	3.66	63.0
APC	11709	4.85	2.44	38.0
HEMTT	24948	10.16	2.44	31.0
HMMWV	3493	4.57	2.16	29.5

Table 2-2 Treatment effects on rut depth.

Type 3 Tests of Fixed Effects

Effect	Num DF	Den DF	F Value	Pr > F
Vehicle	3	1653	242.91	<.0001
Moisture	1	1653	1387.92	<.0001
Speed	1	1653	4.51	0.0339
TR	2	1653	2.29	0.1014
Texture	1	1653	0.21	0.6485

Table 2-3 Treatment effects on rut width.

Type 3 Tests of Fixed Effects

Effect	Num DF	Den DF	F Value	Pr > F
Vehicle	3	1653	519.39	<.0001
Moisture	1	1653	38.44	<.0001
Speed	1	1653	0.92	0.3389
TR	2	1653	329.81	<.0001
Texture	1	1653	37.96	<.0001

Table 2-4 Treatment effects on rut index.

Type 3 Tests of Fixed Effects

Effect	Num DF	Den DF	F Value	Pr > F
Vehicle	3	1653	260.21	<.0001
Moisture	1	1653	1049.89	<.0001
Speed	1	1653	5.88	0.0155
TR	2	1653	9.05	0.0001
Texture	1	1653	5.68	0.0172

Table 2-5 Treatment effects on rut depth of the M1A1 tank.

Type 3 Tests of Fixed Effects

Effect	Num DF	Den DF	F Value	Pr > F
TR	2	288	4.43	0.0128
OI	1	288	6.04	0.0145

Table 2-6 Treatment effects on rut width of the M1A1 tank.

Type 3 Tests of Fixed Effects

Effect	Num DF	Den DF	F Value	Pr > F
TR	2	288	46.52	<.0001
OI	1	288	0.07	0.7894

Table 2-7 Treatment effects on rut index of the M1A1 tank.

Type 3 Tests of Fixed Effects

Effect	Num DF	Den DF	F Value	Pr > F
TR	2	288	17.87	<.0001
OI	1	288	5.38	0.0211

Table 2-8 Treatment effects on rut depth of the HEMTT.

Type 3 Tests of Fixed Effects

Effect	Num DF	Den DF	F Value	Pr > F
TR	2	250	2.20	0.1124
OI	1	250	0.95	0.3307

Table 2-9 Treatment effects on rut width of the HEMTT.

Type 3 Tests of Fixed Effects

Effect	Num DF	Den DF	F Value	Pr > F
TR	2	250	34.10	<.0001
OI	1	250	0.14	0.7128

Table 2-10 Treatment effects on rut index of the HEMTT.

Type 3 Tests of Fixed Effects

Effect	Num DF	Den DF	F Value	Pr > F
TR	2	250	5.26	0.0058
OI	1	250	0.77	0.3805

Table 2-11 Treatment effects on rut depth of the APC.

Type 3 Tests of Fixed Effects

Effect	Num DF	Den DF	F Value	Pr > F
TR	2	234	38.09	<.0001
OI	1	234	0.00	0.9919

Table 2-12 Treatment effects on rut width of the APC.

Type 3 Tests of Fixed Effects

Effect	Num DF	Den DF	F Value	Pr > F
TR	2	234	58.57	<.0001
OI	1	234	2.88	0.0910

Table 2-13 Treatment effects on rut index of the APC.

Type 3 Tests of Fixed Effects

Effect	Num DF	Den DF	F Value	Pr > F
TR	2	234	48.06	<.0001
OI	1	234	0.35	0.5563

Table 2-14 Treatment effects on impact width for the HMMWV.

Type 3 Tests of Fixed Effects

Effect	Num DF	Den DF	F Value	Pr > F
TR	2	164	35.34	<.0001
OI	1	164	0.12	0.7345

Part 3 Influence of Turning Radius on Wheeled Military Vehicle Induced Rut Formation

This chapter is a reformatted version of a paper, by the same name, submitted to Journal of Terramechanics by Kun Liu, Paul Ayers，Heidi Howard，and Alan Anderson. Paper is in press.

Abstract

A rut is a depression or groove formed into the ground by the travel of wheels and tracks. Ruts can cause severe influences on soil and vegetation, and reduce vehicle mobility. In this paper, rut depth and rut width were used as the main indicators to quantify a rut. A new indicator, rut index, was proposed, combining rut depth and rut width. A Light Armored Vehicle (LAV) and a High Mobility Multi-purpose Wheeled Vehicle (HMMWV) were used for testing the influence of turning radius on rut depth, rut width and rut index. The LAV and the HMMWV were operated in spiral patterns at different speeds. Differential GPS data for the vehicles were collected every second during the spiral. Rut measurements were manually taken every 4 to 7 meters along each of the spiral tracks. The results of field tests indicate that rut depth, rut width and rut index increase with the decrease of turning radius, especially when turning radius is less than 20 meters. Velocity influences rut formation for the LAV but not HMMWV.

1. Introduction

Off-road vehicles can form ruts. A rut is a depression or groove formed into the ground by the travel of wheels and tracks. Ruts are formed when the soil compacts or is displaced. Soil compaction results from the vertical stress on the soil. Soil displacement can also be produced from vertical forces when the bearing capacity is reached. Soil lateral and longitudinal forces can displace soil and form a rut. Longitudinal forces, producing wheel slip, can displace the soil. Turning vehicles

can add a lateral force to the soil, displacing the soil out of the wheel track and towards the outside of the turn.

Ruts can cause severe influences on soil and vegetation [1, 2]. Ruts can decrease plant development by damaging the root system of native plants [3, 4]. Ruts can cause environmental damage by concentrating runoff and increasing erosion [5]. Rut formation can also decrease vehicle mobility [6].

The impact of a vehicle can be measured as the rut width, which is a measurement across the vehicle track of the width of the soil and vegetation impacted by the vehicle, and the rut depth, which is the vertical distance between the bottom of the track and the adjacent undisturbed soil surface. Durham [7] tested the powered wheels in the turned mode operating on yielding soils. He found that the turn angle was of secondary importance to determine the sinkage coefficient, which increased with the increasing wheel turn angle for a given sand mobility number, an empirical parameter based on soil strength, vehicle's weight, tire size and tire deformation. Braunack and Williams [8] found that rut depth increased as the number of passes and turns increased, but especially after turning maneuvers, by testing a M113 armored personnel carrier and a Leopard tank at different soil strength and moisture conditions. Ayers [4] used a M113 armored personnel carrier to perform three kinds of turning radii: Straight, Smooth turn and Sharp turn. He found that the decreased turning radius (sharp turn) could increase soil disturbance and track ruts, and the width and depth of track and height of soil piled also increased during the sharp turn (Fig. 3-1). Halvorson et al. [9] investigated the soil compaction and over-winter changes of a

tracked vehicle, the M1A2 Abrams tank. They found that turning ruts had a greater amount of initial disturbance than straight-path ruts and smoothed more than straight-path ruts after the winter. Affleck et al. [10] revealed that soil disturbance was significantly different when the vehicle was turning rather than when moving straight ahead. A Stryker vehicle was used to conduct their impact tests, consisting of spiral and multi-pass tests. Affleck [11] conducted rut depth measurements on both wheeled and tracked vehicles. Investigating the relationships between rut depth and soil prosperities and vehicle maneuvers, she found that the volume of soil displacement was much higher when the vehicle was turning than on a straight path. Althoff and Thien [3] used a randomized complete-block design to investigate the impact of M1A1 tank disturbance on soil quality, invertebrates and vegetation characteristics. The treatments consisted of five passes (crossing, within, straight-a-way, and curve) and two soil conditions (dry and wet). They found that rut formation on a curve was significantly greater for the outside track than for the inside track.

Shoop et al. [1] used the NATO (North Atlantic Treaty Organization) Reference Mobility Model (NRMM II) to predict vehicle impacts on training lands. In this model, rut formation was highly correlated with the traction and the motion resistance for vehicles operating on deformable terrain. The traction and the motion resistance of turning were different from going straight. Jones et al. [12] introduced the Vehicle Terrain Interface (VTI) model developed by the U.S. Army Engineer Research and Development Center (ERDC), which was used to predict the

interactions of the vehicles with the terrain surfaces. The steering angle was considered as a factor affecting the interaction in the VTI.

The studies mentioned above introduced a general influence of turning on rut formation and vegetation damage, but did not focus on the special effect of turning maneuver. In this paper, the turning factors, including turning radius and velocity, will be discussed specifically.

2. Objectives

This study was conducted to investigate the relationship between rut depth, rut width, rut index, and vehicle dynamic properties (turning radius and velocity) for a Light Armored Vehicle (LAV) (Fig. 3-2) at Fort Lewis, Washington, and a High Mobility Multi-purpose Wheeled Vehicle (HMMWV) (Fig. 3-3) at Yuma, Arizona.

3. Vehicle and soil description

Vehicle tests were performed for the Light Armored Vehicle (LAV) at Fort Lewis Military Installation on June 11, 2002, and the High Mobility Multi-purpose Wheeled Vehicle (HMMWV) at Yuma Proving Ground on March 11, 2003.

The LAV was an eight-wheeled vehicle with a mass of 13,930 kg. The vehicle length was 6.98 m, and the tread width was 2.30 m. The tires were Michelin X 12.00-R20, with a width of 27.9 cm and diameter of 111.8 cm. The vehicle was capable of varying tire pressure which, for the study, was 483 kPa, and the vehicle was operated in four wheel drive mode. The soil texture was 67% sand, 29% silt and

4% clay and was characterized as a sandy loam. The average moisture content was 37.1% by dry weight basis. Drop cone measurements were taken to classify the soil strength, as the soil strength was too high, higher than 1000 kPa, to use a manual penetrometer. The average drop cone was 5.0 cm. The common type of grass was Colonial bentgrass.

The HMMWV had a mass of 2,608 kg. The vehicle length was 4.57 m and the tread width was 1.79 m. The tires were Goodyear Wrangler MT, with a width of 31.8 cm and diameter of 92.7 cm. The front tire pressure was measured at 123 kPa and the rear tire pressure was at 146 kPa. The texture of field was sand, which composed more than 95% of the soil. The average moisture content was 8.9% by dry weight basis. The average soil cone index was 921 kPa for the upper 15 cm. The average drop cone was 10.8 cm. This field was comprised of bare soil without vegetation cover.

4. Field testing method

The Light Armored Vehicle (LAV) was operated in spiral patterns (constantly decreasing turning radius by turning to the right) at two speeds. Five high speed and 5 low speed spirals were conducted. A Trimble AgGPS 132 12 channel DGPS (differential global positioning system) receiver was mounted on the LAV with Omnistar Satellite differential correction. Differential GPS data for the vehicle were collected every second. Rut depth and rut width measurements were manually taken every 4 to 7 meters along each of the spiral tracks. Rut depth was measured (Fig.

3-4) as the vertical distance between the bottom of the track that has been caused by vehicle traffic and the adjacent undisturbed soil surface. Rut width was measured as the total width of soil depression. The GPS location was taken at each measurement point using the same GPS receiver so the vehicle velocity and turning radius could be related to the rut measurement.

The High Mobility Multi-purpose Wheeled Vehicle (HMMWV) was operated in 4 spirals, 2 at high speed, and 2 at low speed. The GPS receiver was the same Trimble. Rut and location data were also collected in the same way as for the LAV (Fig. 3-5).

The vehicle turning radius was calculated by a three-point turning radius calculation method [13]. To compress the data range, any turning radius greater than 150 meters was classified as 150 meters. Using the distance between two GPS points and the time interval, vehicle velocity was determined.

5. Results

5.1. Rut depth and turning radius

The low speed of the Light Armored Vehicle (LAV) was approximately 4 m/s and the high speed was 8 m/s at the maximum safe operating speed (driver determined for field conditions). Fig. 3-6 shows that there is a good relationship between turning radius and rut depth of the outside track (wheels on the outside of the turn). To show the general difference between the outside ruts and the inside ruts, simple power equations are used to describe the data. Rut depth is found to increase with the

decrease of turning radius. The rut depth increases sharply at smaller turning radii (less than 30 meters). However, the relationship between turning radius and rut depth of the inside track (wheels on the inside of the turn) is less obvious. Nearly all the rut depths are less than 4 cm at different turning radii for the inside wheel. The reason was that the outside weight on the ground increased when the vehicle turned, while the inside weight on the ground decreased because of the dynamic weight shift to the outside wheels. Higher loading was able to form deeper ruts.

All the rut depth data of the LAV used here were from the high speed tracks. Low speed tracks showed no ruts. The reason could be that the lateral force was not big enough to form ruts as the velocity was low. When the lateral force overcame the resistive strength of vegetation and soil, ruts and piles were formed. Also, the penetration resistance was high enough to support the weight of this vehicle.

The low speed of the High Mobility Multi-purpose Wheeled Vehicle (HMMWV) was approximately 3 m/s and the high speed was 8 m/s. Fig. 3-7 shows the relationship between the HMMWV turning radius and rut depth. The relationships are weak for this lighter vehicle. Compared to the heavy LAV, the lateral force for the HMMWV is low, which could be an important reason for the shallow ruts. Also, as the HMMWV turns its wheels no longer fall in the same path, and rut changes from double pass to single pass. Though the relationships are weak, it is still found that rut depth increases slightly with the decrease of turning radius. Fig. 3-8 and Fig. 3-9 show that velocity has effects on rut depth. The higher the velocity, the deeper the rut.

5.2. Rut width and turning radius

Rut width was investigated. Fig. 3-10 shows that the smaller the turning radius the larger the rut width for the LAV. Rut width dramatically decreases at smaller turning radii less than 20 meters. The influence of turning radius to soil disturbance diminishes as the turning radius increases. When the turning radius is greater than 150 meters, meaning that the vehicle is moving in a straight line, the rut width is nearly the same as the width of the tire. There is little difference found between the outside rut width and the inside rut width. Fig. 3-11 shows the relationships between turning radius and rut width for the HMMWV. Fig. 3-12 and Fig. 3-13 show that velocity has little effect on rut width for the HMMWV. Note that soil pile was formed in the procedure as well. During sharp and high-velocity turns, most or all of the disturbed width was scraped free of surface vegetation and soil, which was piled to the outside of each tire track [14]. If the formation of soil pile is consistent, the width and height of soil pile can be used as indicators of rut formation.

5.3. Rut index and turning radius

Rut index is a composite indicator of a rut, which is the product of rut depth and rut width, but with no unit. Providing a unit of area may incorrectly indicate this index as a cross-sectional area. In reality, the shape of the rut cross section is not a rectangular and its area cannot be calculated by rut depth times rut width. Fig. 3-14 shows that rut index increases with the decrease of turning radius for the LAV. Rut index of the outside track is higher than the inside track, which is mainly caused by

the different effects of the outside wheel and the inside wheel on rut depth when the rut widths are almost the same. Fig. 3-15 also shows a similar relationship for the HMMWV: the smaller the turning radius, the larger the rut index, but the rut index of the outside track is the same as that of the inside track. Fig. 3-16 and Fig. 3-17 show that velocity has little effect on rut index.

6. Conclusions

In this paper, a Light Armored Vehicle (LAV) with a weight of 13,930 kg and a High Mobility Multi-purpose Wheeled Vehicle (HMMWV) with a weight of 2,608 kg were used to investigate the relationships between rut depth, rut width and rut index, and vehicle dynamic properties (turning radius and velocity). The conclusions are the following.

The heavy LAV produces deeper ruts than the light HMMWV. Turning maneuvers also produce deeper ruts. Rut depth increases with the decrease of turning radius. Rut width increases with the decrease of turning radius for both vehicles. Rut index also increases with the decrease of turning radius.

The outside rut depth is deeper than the inside rut depth for the same vehicle when the vehicle turns, while, the outside rut width and the inside rut width are almost the same. The outside rut index is higher than the inside rut index for the LAV, but for the HMMWV they are the same.

Velocity has effects on rut formation for the LAV when soil strength is high: the higher the speed, the deeper the rut, but has little effect for the HMMWV. Because

of the small weight, the lateral force of the HMMWV is not enough to overcome the soil resistance to form deeper ruts even at high speed.

Considering that military vehicles do lots of turning maneuvers during training, turning radius is an important factor affecting the rut formation that can cause negative effects on the environment. This study examines the influence of turning radius and velocity on rut formation and should be useful in further investigations of the influence of turning maneuvers on vehicular mobility and soil damage.

References

[1] Shoop S, Affleck R, Collins C, Larsen G, Barna L, Sullivan P. Maneuver analysis methodology to predict vehicle impacts on training lands. J Terramechanics 2005; 42(3): 281-303.

[2] Sullivan PM, Anderson AB. A methodology for estimating army training and testing area carrying capacity (ATTACC) vehicle severity factors and local condition factors. U.S. Army Engineer Waterways Experiment Station, Technical Report: ERDC-TR-00-2; 2000.

[3] Althoff PS, Thien SJ. Impact of M1A1 main battle tank disturbance on soil quality, invertebrates, and vegetation characteristics. J Terramechanics 2005; 42(3): 159-176.

[4] Ayers PD. Environmental damage from tracked vehicle operation. J Terramechanics 1994; 31(3):173–183.

[5] Gatto LW. Overwinter changes to vehicle ruts and natural rills and effects on soil erosion potential. In: 10th International Soil Conservation Organization Meeting, Purdue University, 2001.

[6] Evans I. The sinkage of tracked vehicles on soft ground. J Terramechanics 1964; 1(2): 33-43.

[7] Durham GN. Powered wheels in the turned mode operating on yielding soils. U.S. Army Engineer Waterways Experiment Station, Technical Report: M-76-9; 1976.

[8] Braunack MV, Williams BG. The effect of initial soil water content and vegetative cover on surface disturbance by tracked vehicles. J Terramechanics 1993; 30(4): 299-311.

[9] Halvorson JJ, McGool DK, King LG, Gatto LW. Soil compaction and over-winter changes to tracked-vehicle ruts, Yakima Training Center, Washington. J Terramechanics 2001; 38(2): 133-151.

[10] Affleck RT, Shoop S, Simmons K, Ayers PD. Disturbance from off-road vehicle during spring thaw. In: 12th ASCE conference, Edmonton, Canada; 2004.

[11] Affleck RT. Disturbance measurements from off-road vehicles on seasonal terrain. U.S. Army Cold Regions Research and Engineering Laboratory, Technical Report: TR-05-12; 2005.

[12] Jones AR, McKinley GB, Richmond PW, Creighton DC. A vehicle terrain interface. In: ISTVS Conference, Fairbanks, U.S.; 2007

[13]Haugen LB. Design and testing of a vehicle tracking system for monitoring environmental impact at U.S. army training installations. Master thesis, Colorado State University, Fort Collins, U.S.; 2002.

[14]Foster JR, Ayers PD, Lombardi-Przybylowicz AM, Simmons K. Initial effects of light armored vehicle use on grassland vegetation at Fort Lewis, Washington. Journal of Environmental Management 2006; 81(4): 315-322.

Appendix

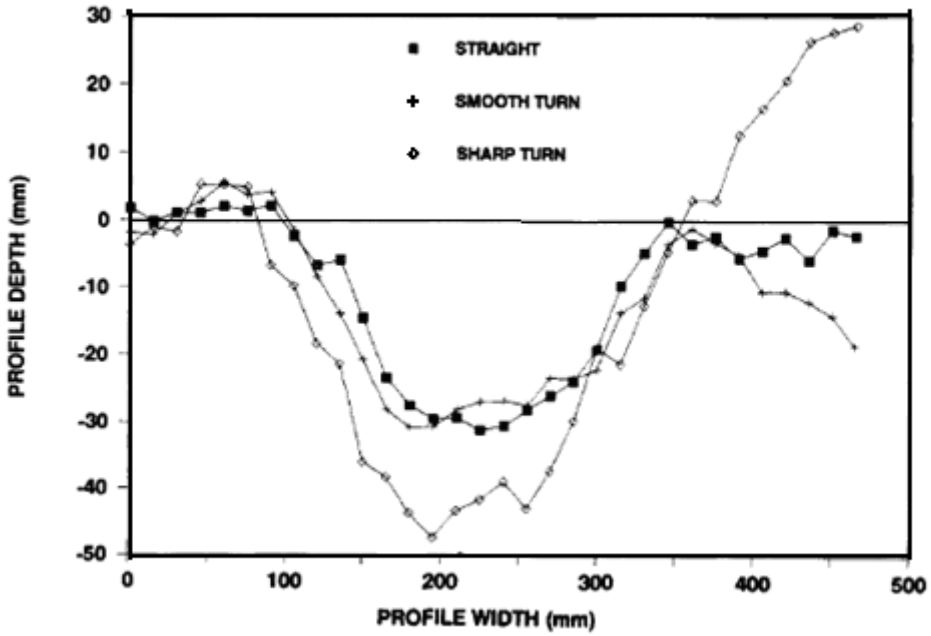

Fig. 3-1 Comparison of soil disturbance resulting from three different operating modes.

Fig. 3-2 Light Armored Vehicle (LAV).

Fig. 3-3 High Mobility Multi-purpose Wheeled Vehicle (HMMWV).

Fig. 3-4 Measurement method for the LAV.

Fig. 3-5 Measurement method for the HMMWV.

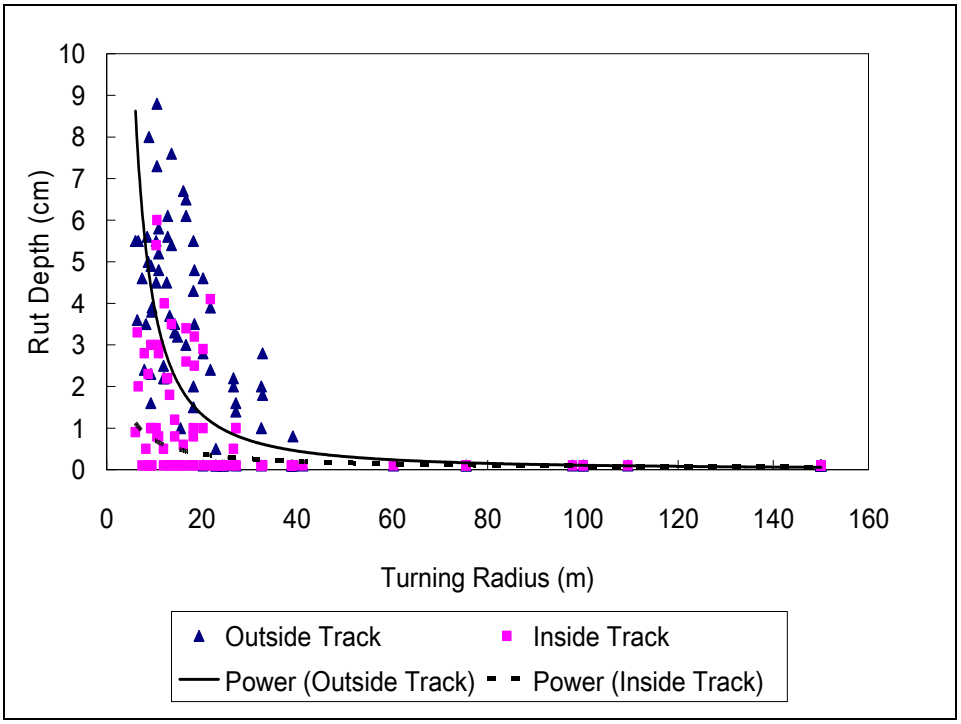

Fig. 3-6 Relationship between LAV turning radius and rut depth influenced by track locations.

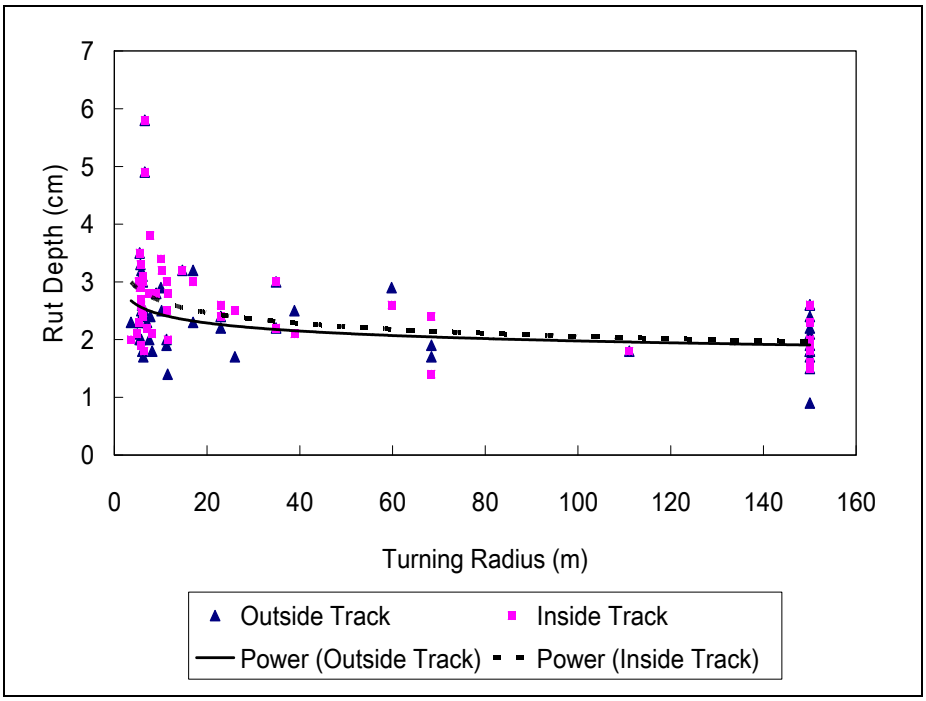

Fig. 3-7 Relationship between HMMWV turning radius and rut depth influenced by wheel locations.

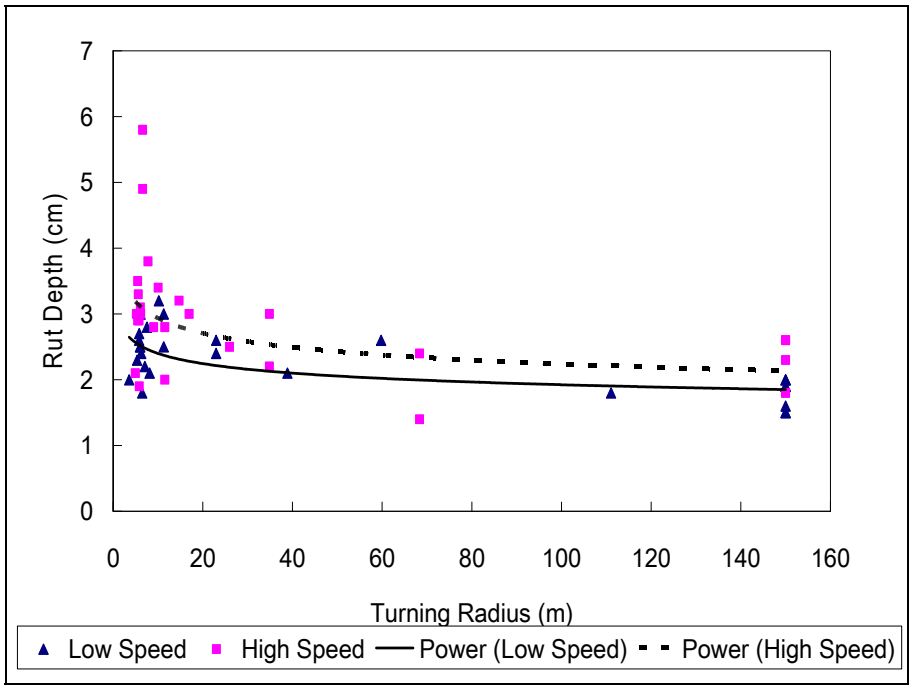

Fig. 3-8 Relationship between HMMWV turning radius and inside rut depth influenced by vehicle speeds.

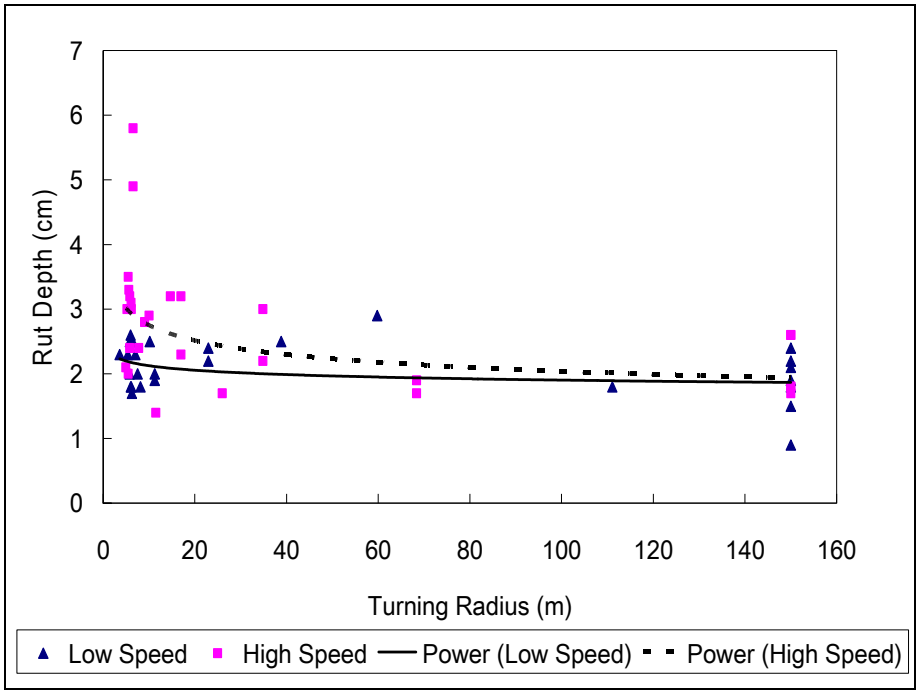

Fig. 3-9 Relationship between HMMWV turning radius and outside rut depth influenced by vehicle speeds.

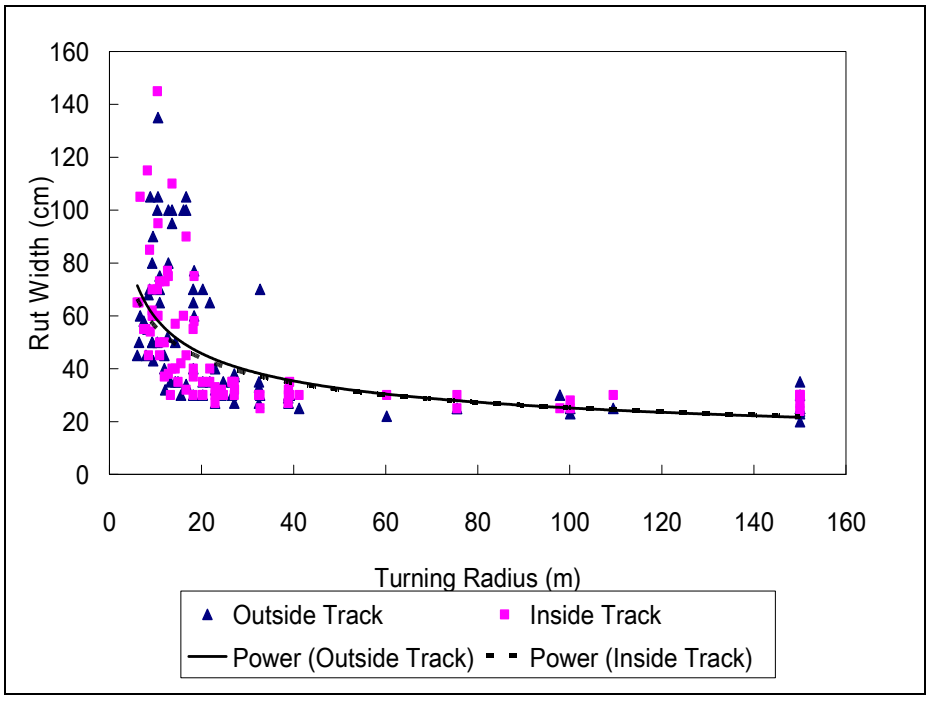

Fig. 3-10 Relationship between LAV turning radius and rut width influenced by track locations.

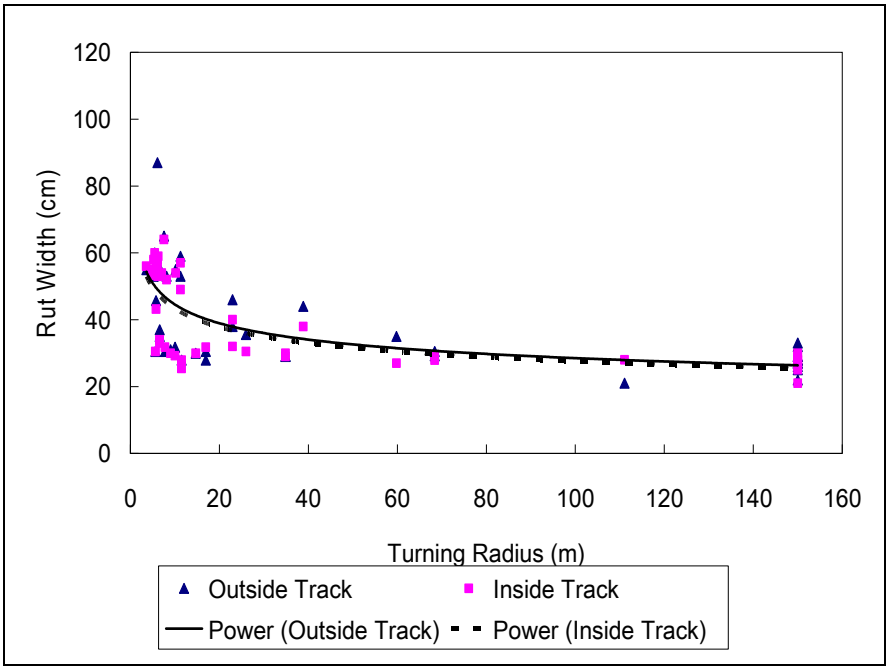

Fig. 3-11 Relationship between HMMWV turning radius and rut width influenced by wheel locations.

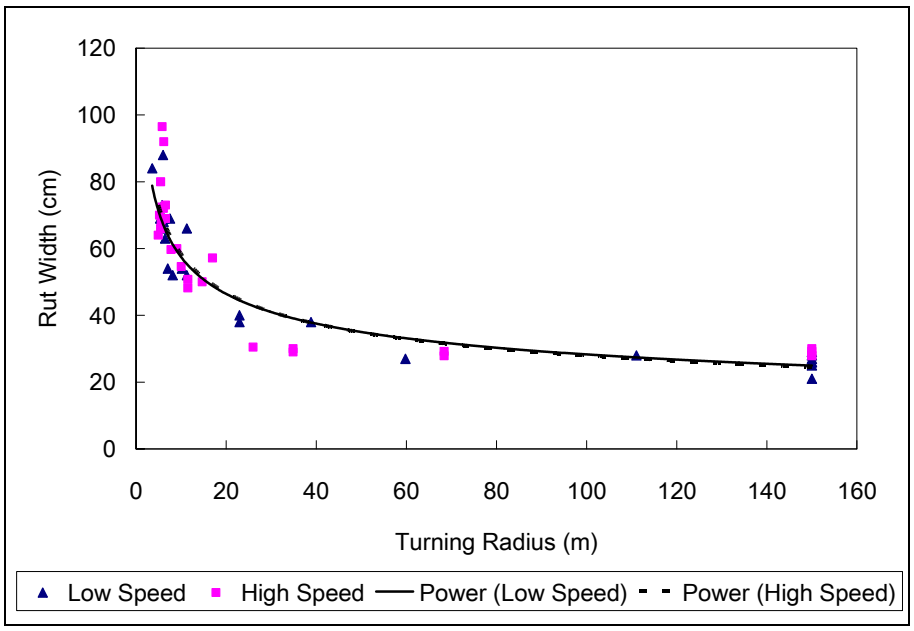

Fig. 3-12 Relationship between HMMWV turning radius and inside rut width influenced by vehicle speeds.

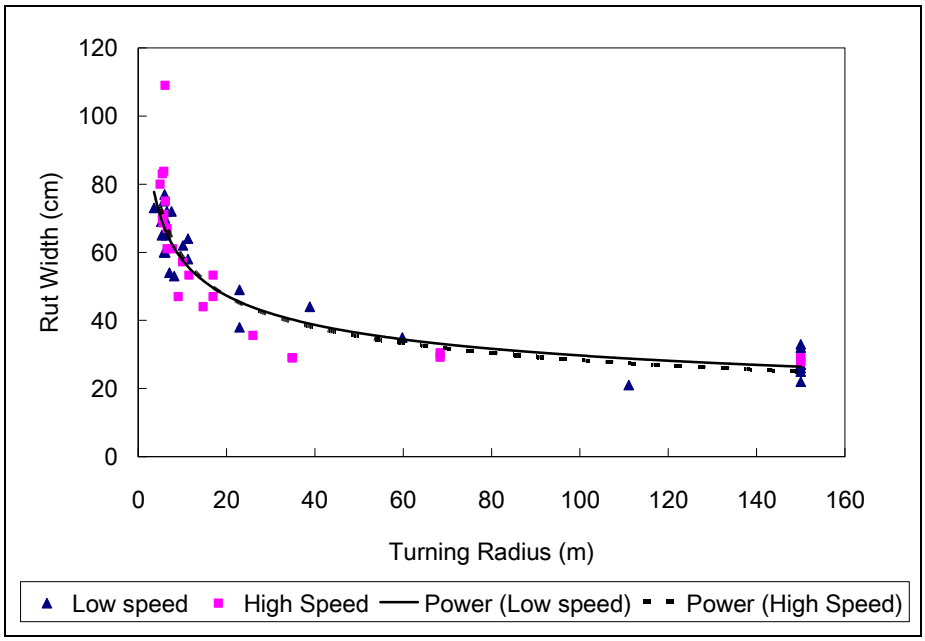

Fig. 3-13 Relationship between HMMWV turning radius and outside rut width influenced by vehicle speeds.

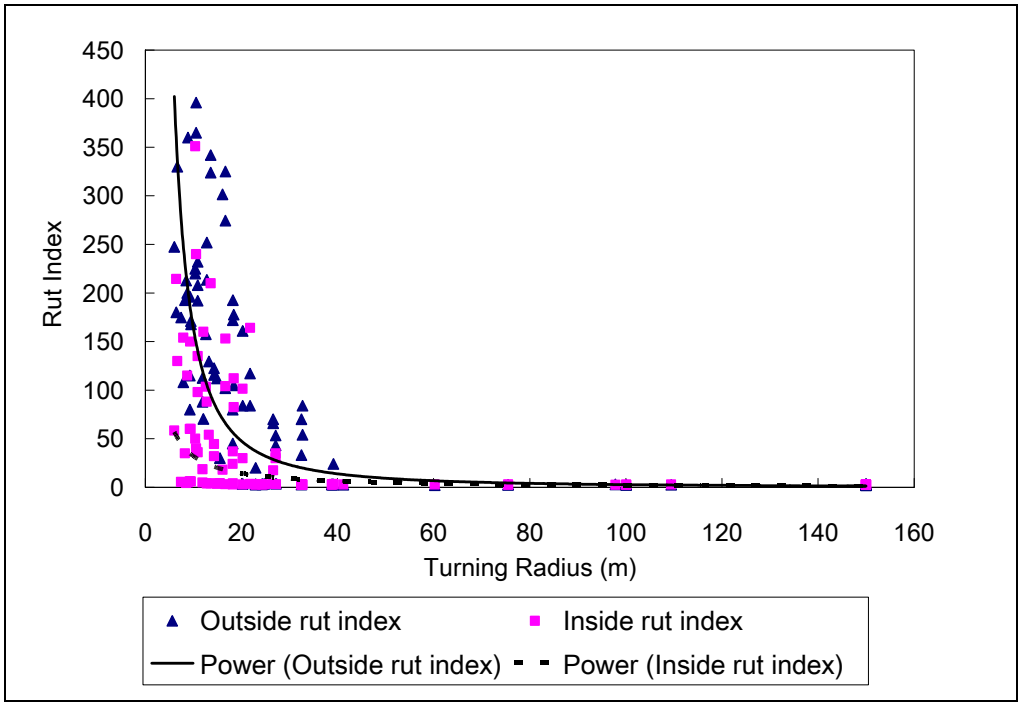

Fig. 3-14 Relationship between LAV turning radius and rut index influenced by track locations.

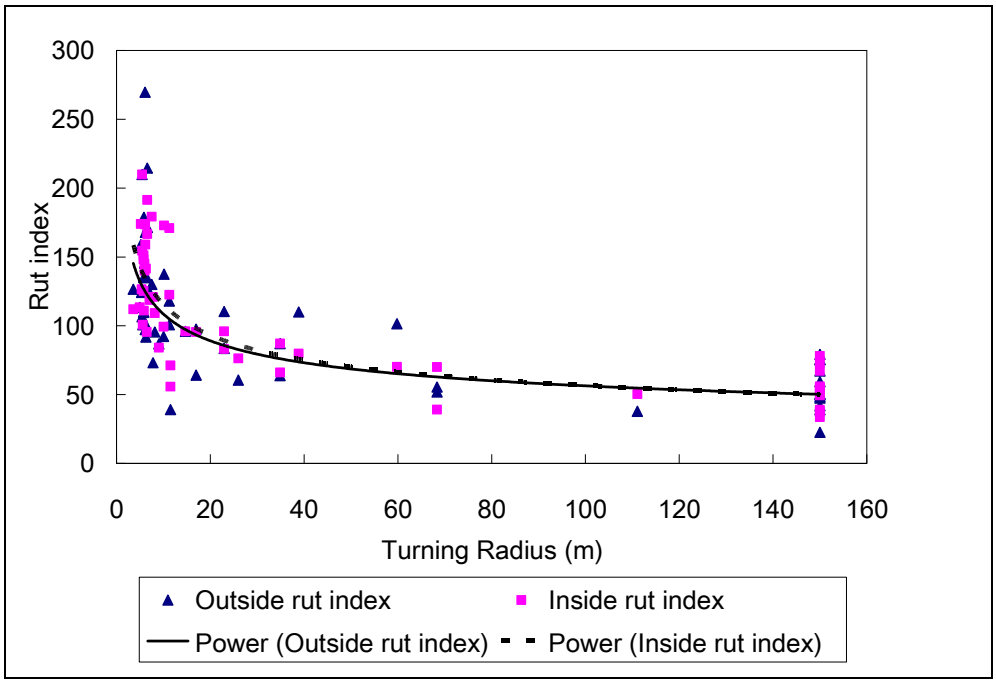

Fig. 3-15 Relationship between HMMWV turning radius and rut index influenced by track locations.

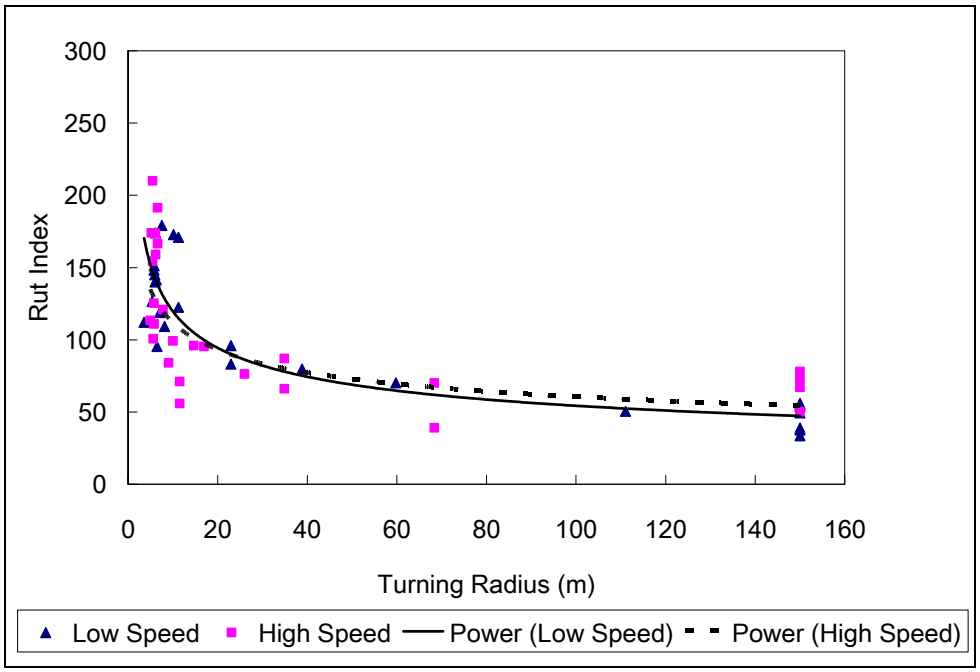

Fig. 3-16 Relationship between HMMWV turning radius and inside rut index influenced by vehicle speeds.

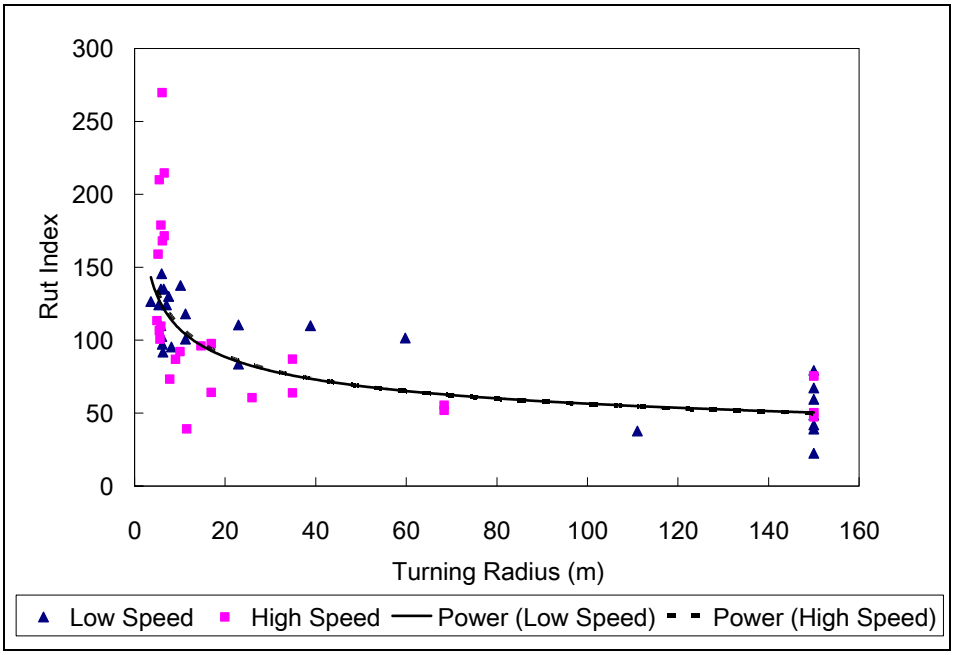

Fig. 3-17 Relationship between HMMWV turning radius and outside rut index influenced by vehicle speeds.

Part 4 Prediction of Rut Depth during Military Vehicle Turning Maneuvers using a Modified Sinkage Numeric

This chapter is a reformatted version of a paper, by the same name, submitted to the Transactions of ASABE by Kun Liu, Paul Ayers, Heidi Howard, Randy Jones, and Alan Anderson. Paper is accepted.

Abstract

Vehicle-induced ruts can cause severe adverse effects on soil and vegetation and reduce a vehicle's mobility potential. Vehicle turning factors including turning radius, velocity, and dynamic weight effects were integrated into the Vehicle Terrain Interaction (VTI) terrain mechanics model to predict rut formation during vehicle turning operations on yielding soils. In the modified VTI model, the resultant force of a single tire is a dynamic variable correlated with the vehicle's weight, velocity, and turning radius. Field tests using an eight-wheeled light armored vehicle (LAV) were conducted and the results analyzed and implemented in a modified VTI sinkage model for turning. The LAV was operated at varying velocities during spiral-pattern turn testing to obtain continuously decreasing radii rutting results. The results of the LAV field tests were analyzed with predictions from the modified VTI, and the conclusion shows that the modified model can be used to predict the influence of turning on soil rutting. Rut depths for both vehicle tracks were predicted for turning operations.

1. Introduction

Off-road vehicles, such as tractors and tanks, are widely used in agriculture, forestry, mining and military operations. The operation of the traction elements of off-road vehicles can form depressions or grooves, known as ruts, in the terrain. Soil ruts affect vehicle performance and the state of the terrain. Rut formation can reduce vehicle traction and the mobility of a vehicle by increasing the rolling resistance. In

some instances, off-road vehicles may become immobilized by deep ruts. From an environmental perspective, ruts also have a long-term negative effect on the landscape. Erosion within ruts is often higher than in the surrounding area due to an increase in compaction, a decrease in rainfall infiltration and an increase in concentrated velocity, thereby increasing surface runoff (Soane et al., 1981; Gatto, 2001). In addition, soil compaction from ruts can impede plant development by damaging the root crown and system.

Historically, research has focused on the interaction between a vehicle and the terrain during straight non-turning activities. However, it has been found that turning has a significant effect on rut formation. Rut depth (RD) is an important index indicating the severity of rut formation. Rut depth is the distance measured between the bottom of the vehicle track and the adjacent undisturbed soil surface. Sinkage is the vertical displacement of the axis of the vehicle. In the following literatures, both rut depth and sinkage will be used. Although rut depth and sinkage are measured from two different perspectives and are not equivalent, the measured difference is small and they can be considered equivalent in values, assuming low soil elasticity and no soil rebound after loading (Affleck, 2005). Braunack and Williams (1993) found that rut depth (RD) increased as the number of passes and turns increased. They studied the influence of turning maneuvers by testing two tracked vehicles, an M113 armored personnel carrier and a Leopard tank, at different soil strengths and moisture conditions. Ayers (1994) used an M113 armored personnel carrier to evaluate rut formation under three turning radii: straight, smooth turn and

sharp turn. He found that a decreased turning radius (TR) could increase soil disturbance and both track rut width and depth. He also noted that the height of the soil pile on the side of the turn increased with sharper turns (decreased turning radii). Affleck et al. (2004) revealed that soil disturbance was significantly increased during turns versus during straight line movement. Affleck evaluated the eight-wheeled all-wheel-drive armored combat Stryker vehicle for environmental impacts during spiral and multi-pass tests. Liu et al. (2007) found that turning significantly increased the rut formation of a Light Armored Vehicle (LAV). In this study both the rut depth and rut width increased with the decrease of turning radius. Observation of the effect of velocity established a correlation between increased vehicle speed and rut depth.

In order to study the interaction between a vehicle and the terrain, a real-time vehicle dynamics simulator (Vehicle Dynamics and Mobility Server (VDMS)), is being developed by the U.S. Army Tank-Automotive Research Development and Engineering Center (TARDEC). This simulator will use the terrain mechanics model, Vehicle Terrain Interface (VTI), being developed at the U.S. Army Engineering Research and Development Center (ERDC). The VTI model, the latest vehicle and terrain interaction model, has been successfully applied in practice (Richmond et al., 2004; Jones et al., 2007; Reid et al., 2007). The following is the portion of the VTI methodology which predicts sinkage for wheeled vehicles in coarse-grained soils:

$$N_s = \frac{G(bd)^{3/2}}{W} \cdot \frac{\delta}{h} \tag{1}$$

$$\Pi_z = N_s \cdot \frac{1}{1 + b/d} \tag{2}$$

$$(\frac{Z}{d})_p = \frac{14}{\Pi_z} \tag{3}$$

$$(\frac{Z}{d})_u = \frac{22}{\Pi_z^{9/8}} \tag{4}$$

where:

N_s = the coarse-grained soil numeric for wheels

Π_z = the coarse-grained sinkage numeric for wheels

$(Z/d)_p$ = the sinkage coefficient for powered wheels

$(Z/d)_u$ = the sinkage coefficient for unpowered wheels

Z = the sinkage for one wheel

G = the cone index gradient

b = the tire section width

d = the nominal wheel diameter

h = the tire section height

δ = the tire deflection

W = the weight beneath a single tire (tire ground reaction force).

Note sinkage and rut depth are used interchangeably for model applications by Willoughby (1988), Affleck (2004), Jones (2007), and Sullivan and Anderson (2000).

2. Objective

This project proposes a modification of the VTI sinkage model to include turning factors for wheeled vehicles. The modified model will be based on field measurements of rut depths of an eight-wheeled LAV (Fig. 4-1) at Fort Lewis, Washington.

3. Model Modification Include Turning

The VTI sinkage model was selected for evaluation and modification to include the influence of soil rutting caused by vehicle turning. The VTI does calculate soil sinkage based on soil strength (Cone Index) using the normal wheel loading, *W* and is the current state of the art for real-time terrain mechanics. However, one significant enhancement to the VTI from this study is the introduction of the effects of lateral dynamic turning loads based on the vehicle characteristics. The mechanism for rut formation is complicated and even more so when vehicles turn in deformable terrains. Soil compaction results from vertical wheel loads, causing stresses on the soil. Soil displacement can be produced from vertical forces when soil bearing capacity is reached. When a vehicle turns, the normal wheel loads change due to the dynamic shift of the vehicle's weight. This weight shift adds forces to the outside tire and reduces the loads on the inside tire.

Lateral and longitudinal forces of the wheel loads can displace soil and form ruts. Longitudinal forces generated from the powertrain for traction are needed to overcome the mechanical and terrain rolling resistance and to propel the vehicle.

These same traction forces also develop wheel slip and displace soil. The rolling resistance of a vehicle is usually significantly higher as a vehicle turns. Turning vehicles add a lateral force to the soil that displaces the soil from the wheel track and towards the outside of the turn. This lateral force is due to the vehicle's centripetal force that is generated during a vehicle turn and is a function of the vehicle velocity and turning radius. In addition, non-steered wheels drag or slide across the soil during turns, producing lateral forces and soil displacement identified as scrape. Fig. 4-2 shows the directions of tire and terrain forces.

Thus, the force between the terrain and the tire that forms ruts while a vehicle is turning is a complicated resultant force vector, $\vec{F}$, shown in Equation 5.

$$\vec{F} = \overrightarrow{w_s} + \overrightarrow{w_d} + \overrightarrow{F_c} + \overrightarrow{F_t} + \overrightarrow{F_s} \tag{5}$$

where:

w_s = the static weight beneath a single tire

w_d = the dynamic weight beneath a single tire (added or subtracted)

F_c = the lateral centripetal force

F_t = the longitudinal traction force

F_s = the sliding force.

4. Field Tests for a Turning Vehicle

Vehicle-terrain impact tests were performed using an LAV at Fort Lewis Military Installation on June 11, 2002. The LAV is an eight-wheeled vehicle which was equipped with Michelin X tires during this study. Table 4-1 shows parameters of the

LAV used in this research. The LAV is capable of varying tire pressure during operations, but the tire pressure was kept at 483 kPa (70 psi) during these tests and operated in rear-four-wheel-drive mode.

The soil texture was characterized as a sandy loam with 67% sand, 29% silt and 4% clay. The average moisture content by dry weight was 37.1%. The field cone index gradient was 2.17 MPa/cm (800 psi/in). The average drop cone was 10.8 cm. Vegetation coverage was 85% with the predominant species classified as colonial bent grass.

The LAV was operated in spiral patterns (constantly decreasing right turning radius) at two speeds. Five high-speed (approximately 8 m/s) and five low-speed (approximately 4 m/s) spirals were conducted. A Trimble AgGPS 132, twelve-channel differential global positioning system (DGPS) receiver with Omnistar Satellite differential correction was mounted on the LAV. Differential GPS data for the vehicle were collected at 1 Hz intervals during testing (Fig. 4-3). Turning radius and velocity were determined from the GPS data. Rut-depth measurements were manually taken every four to seven meters in both the inside and the outside tracks along each of the spiral tracks, resulting in a total of 338 impact points. The rut depth was determined by the maximum measurement taken near the center of the track.

No obvious ruts (> 1 cm) were observed for the LAV operating at low speed. For this study, the rut depths at low speeds were determined as near zero. Fig. 4-4 shows the field measurements of the rut depths for both the inside and the outside

tracks at high speed. Rut depth is not constant and is influenced by the turning maneuver. For high vehicle speeds the rut depth increases as the turning radius decreases. That means when an LAV begins to turn, the rut depth increases due to the additional turning forces imposed on the soil from the tire shoulder. As expected, the outside tracks produced deeper rut depths than the inside tracks. To compress the data range, any turning radius greater than 150 meters was classified as 150 meters and going straight.

The data analysis revealed that the rut formation from the LAV turning is heavily affected by the applied lateral shear stress. The applied lateral shear stress is calculated as the vehicle's centripetal force divided by the average contact area of the tires. Substantial soil ruts formed only when the applied lateral shear stress was higher than an apparently critical value (around 100 kPa) (Fig. 4-5). This critical shear stress was close to the maximum soil shear strength of 84.4 kPa (determined at 103.5 kPa [15 psi] normal stress) measured by a torsional sheargraph. Or the ratio of the applied lateral stress and soil shear strength can be used the express this phenomenon. A ratio greater than 1 (the dash line in Fig. 4-5) is needed to form ruts. The maximum lateral shear stress for low speed is 97.9 kPa, less than the critical value 100 kPa, resulting in no obvious ruts observed. It must be noted that the soil shear strength was measured under a soil surface normal stress of 103.5 kPa (15 psi) and not under the normal stress of approximately 483 kPa (70 psi) produced by the tire pressure of the LAV. Even with this difference in soil shear strength measurements, the outside track produces deeper ruts than the inside track.

Since lateral forces, traction forces, and sliding forces are correlated with turning radius and vehicle velocity, these forces can be represented by a lateral turning force parameter (F_c). This lateral turning force parameter is an important factor when producing ruts during turning. The dynamic weight, w_d (determined by the weight shift produced by the centripetal force), is added to the outside wheel and subtracted from the inside wheel. Thus, the sand numeric can be modified as:

$$N_s = \frac{G(bd)^{3/2}}{b_0(w_s + b_1 k w_d + b_2 F_c)} \cdot \frac{\delta}{h} \tag{6}$$

$$F_c = \frac{mV^2}{TR} \tag{7}$$

$$w_d = \frac{2F_c Z_{cg}}{TW} \tag{8}$$

where:

b_0, b_1, and b_2 = parameters estimating the importance of turning force value

k = an indicator of wheel location (1 for outside wheel, -1 for inside wheel)

m = the mass of the vehicle supported by a single wheel

V = the vehicle velocity

TR = the vehicle turning radius

Z_{cg} = the vertical distance to the vehicle gravity center

TW = the tread width.

Equal distribution of the vehicle weights and centripetal forces is estimated to each of the eight wheels.

5. Model regression

A VTI model modified to incorporate the turning force value was utilized to predict the soil ruts formed during turning. The dependent variable was not sinkage but rut depth, which was measured in the tests and was of interest more from the perspective of soil, though sinkage and rut depth are similar in values. For this model, Equation 12 was used to determine multi-pass soil rutting from four tire passes. Using the nonlinear regression function of JMP 6.0, the parameters (b_0, b_1, and b_2) in Equation 6 were regressed (Fig. 4-6).

$$\Pi_z = N_s \cdot \frac{1}{1+b/d} = \frac{G(bd)^{3/2}}{b_0(w_s + b_1 k w_d + b_2 F_c)} \cdot \frac{\delta}{h} \cdot \frac{1}{1+b/d} \tag{9}$$

$$(\frac{Z}{d})_p = \frac{14}{\Pi_z} = \frac{14}{\frac{G(bd)^{3/2}}{b_0(w_s + b_1 k w_d + b_2 F_c)} \cdot \frac{\delta}{h} \cdot \frac{1}{1+b/d}} \tag{10}$$

$$(\frac{Z}{d})_u = \frac{22}{\Pi_z^{9/8}} = \frac{22}{(\frac{G(bd)^{3/2}}{b_0(w_s + b_1 k w_d + b_2 F_c)} \cdot \frac{\delta}{h} \cdot \frac{1}{1+b/d})^{9/8}} \tag{11}$$

$$Z = \sqrt{Z_p^2 + Z_p^2 + Z_u^2 + Z_u^2} \tag{12}$$

Compared to a Sum of Square Error (SSE) of 4495 when a constant normal tire weight was used to predict the rut depth, the smaller SSE of 595 was determined when the turning force values were included to predict rut depth, resulting in an 86.7% improved SSE. An R square of 0.43 was found using the modified VTI equations. The average difference between measured values and predicted values using the modified VTI model was 0.90 cm. This low R square is more the result of tremendous variation observed in the field data than the lack of ability of the model to reflect observed field trends. Though its R square is low, the model with a dynamic

weight and lateral force correlated with turning radius still can reflect the observed trend for the LAV that rut depth increases with the decrease of turning radius. The result of the modified model is better than that of the original model, which predicts rut depth as a constant during turning. The values of b_1 and b_2 are very large, indicating the weight shift and the lateral force have a significant effect on rut formation for the LAV during turning. In these soil and vehicle conditions, rut formation is primarily caused by the lateral force and other dynamic turning factors.

Another model development technique was employed by splitting the data randomly into two sets. The first set was used to develop another modified VTI prediction model. The regressed results for the unknown parameters of this model are quite similar to the results using full data (Fig. 4-7). For this set, the average difference between measured values and predicted values using the second modified VTI model is 0.69 cm, with an R square of 0.45. The second data set was used to evaluate the model. For the second data set, the average difference between measured values and predicted values using the modified VTI model is 0.86 cm, which is lightly higher than the average difference in the first data set.

Fig. 4-8 shows the comparison of predicted rut depths in the outside track between the original VTI model and the modified model using a resultant force and four constant velocities, 2 m/s, 4 m/s, 6 m/s, and 8 m/s. The predicted rut depth using the original VTI model is always 6 cm no matter the vehicle is turning or going straight, as this model is only concerned with soil strength and vehicle static parameters. The predicted rut depth using the modified model always increases with

decreasing turning radius and increasing velocity, while the predicted rut depth using the original VTI model remains constant. It can also be noticed that as the turning radius increases to a straight path, the modified VTI model does not converge with the original VTI model. The original VTI model was first developed for soft and wet soils. However, the soil for our test was relatively much higher, resulting in variations in prediction. The modified VTI model was regressed from field data. In these soil and vehicle conditions, the modified VTI model provides an improved rut depth prediction.

Fig. 4-9 reveals the modified VTI model's prediction for rut depth in the inside and outside tracks at a vehicle velocity of 6 m/s. Note that a deeper rut is predicted in the outside track, as is shown in Figure 4-4.

6. Conclusion

Field tests for an eight-wheeled LAV were conducted to investigate the relationship between rut depth, turning radius and velocity. Based on the vehicle terrain interaction (VTI) model, turning factors-including weight shift, turning radius and velocity are integrated into the model to predict rut formation during turning. The regression results show that by using turning factors, the modified VTI model was able to predict rut-depth characteristics during the turning maneuver (R^2 of 0.43). Analysis revealed that at constant velocities rut depth will always increase with the decrease of the turning radius for the LAV. The model correctly predicted deeper ruts in the outside vehicle track than in the inside track.

Acknowledgement

We are grateful to the Environmental Security Technology Certification Program (ESTCP) project SI-0815 for providing support for this study.

References

[1] Affleck, R.T., S. Shoop, K. Simmons, and P. Ayers. 2004. Disturbance from off-road vehicle during spring thaw. 12th ASCE conference, Edmonton, Canada.

[2] Ayers, P.D. 1994. Environmental damage from tracked vehicle operation. J. Terramechanics 31(3):173–183.

[3] Braunack, M.V., and B.G. Williams. 1993. The effect of initial soil water content and vegetative cover on surface disturbance by tracked vehicles. J. Terramechanics 30(4): 299-311.

[4] Gatto, L.W. 2001. Overwinter changes to vehicle ruts and natural rills and effects on soil erosion potential. 10th International Soil Conservation Organization Meeting, Purdue University.

[5] Jones, A.R., G.B. McKinley, P.W. Richmond, and D.C. Creighton. 2007. A vehicle terrain interface. Proceedings of the Joint North America, Asia-Pacific ISTVS Conference and Annual Meeting of Japanese Society for Terramechanics, Fairbanks, Alaska.

[6] Liu, K., P. Ayers., H. Howard, and A. Anderson. 2007. Influence of Turning Radius on Military Vehicle Induced Rut Formation. Proceedings of the Joint North America, Asia-Pacific ISTVS Conference and Annual Meeting of Japanese Society

for Terramechanics, Fairbanks, Alaska.

[7] Reid, A.A., S. Shoop, R. Jones, and P. Nunez. 2007. High-fidelity ground platform and terrain mechanics modeling for military applications involving vehicle dynamics and mobility analysis. Proceedings of the Joint North America, Asia-Pacific ISTVS Conference and Annual Meeting of Japanese Society for Terramechanics, Fairbanks, Alaska.

[8] Richmond, P.W., R.A. Jones, D.C. Creighton, and R.B. Ahlvin. 2004. Estimating off-road ground contact forces for a real time motion simulator. JSAE International, JSAE Paper Number: 20042771.

[9] Soane, B.D., P.S. Blackwell, J.W. Dickson, and J.D. Painter. 1981. Compaction by agricultural vehicles: a review. Compaction under tyres and other running gear. Soil Tillage Res. 14.

[10] Sullivan, P.M and A.B. Anderson. 2000. A methodology for estimating Army Training and Testing Area Carrying Capacity (ATTACC) vehicle severity factors and local condition factors. US Army Engineer Research and Development Center, Report Number: A393973.

[11] Willoughby, W.E. and G.W. Turnage. 1988. Review of a procedure for predicting rut depth. Unpublished memo.

Appendix

Fig. 4-1 Light Armored Vehicle (LAV).

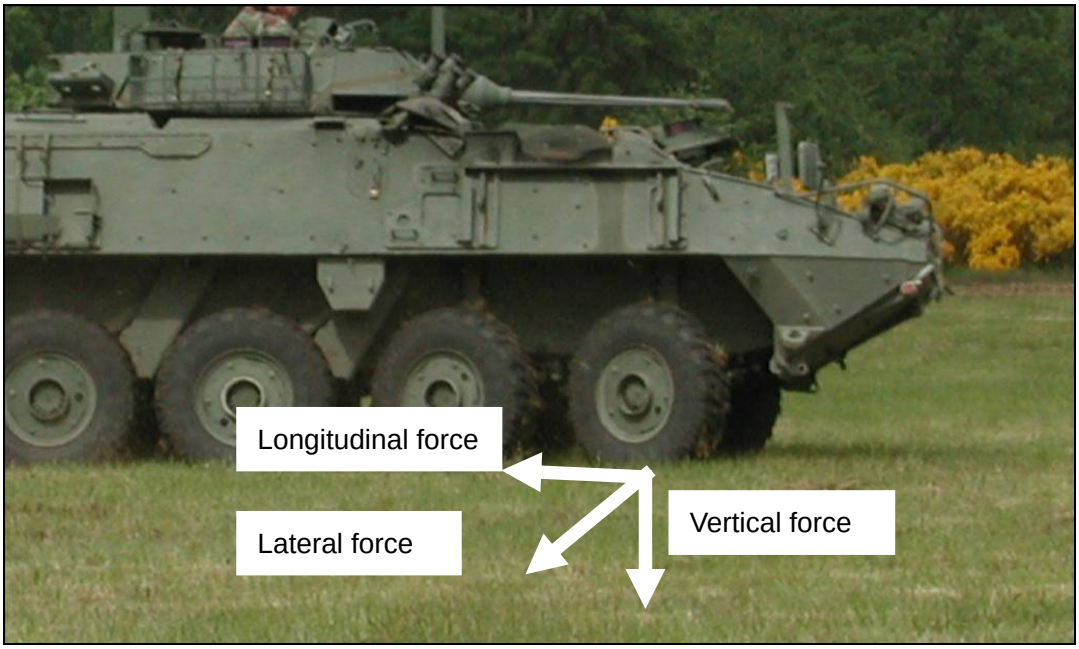

Fig. 4-2 Directions of forces.

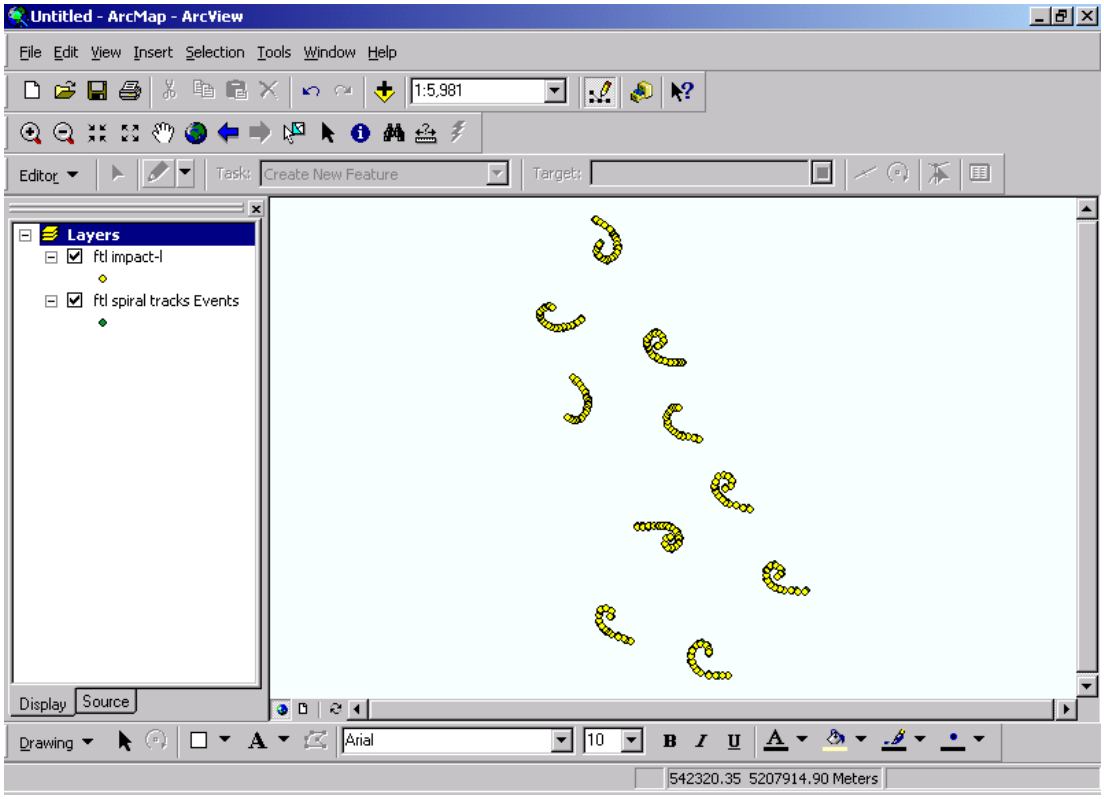

Fig. 4-3 GPS locations for soil rut measurements along the LAV spirals.

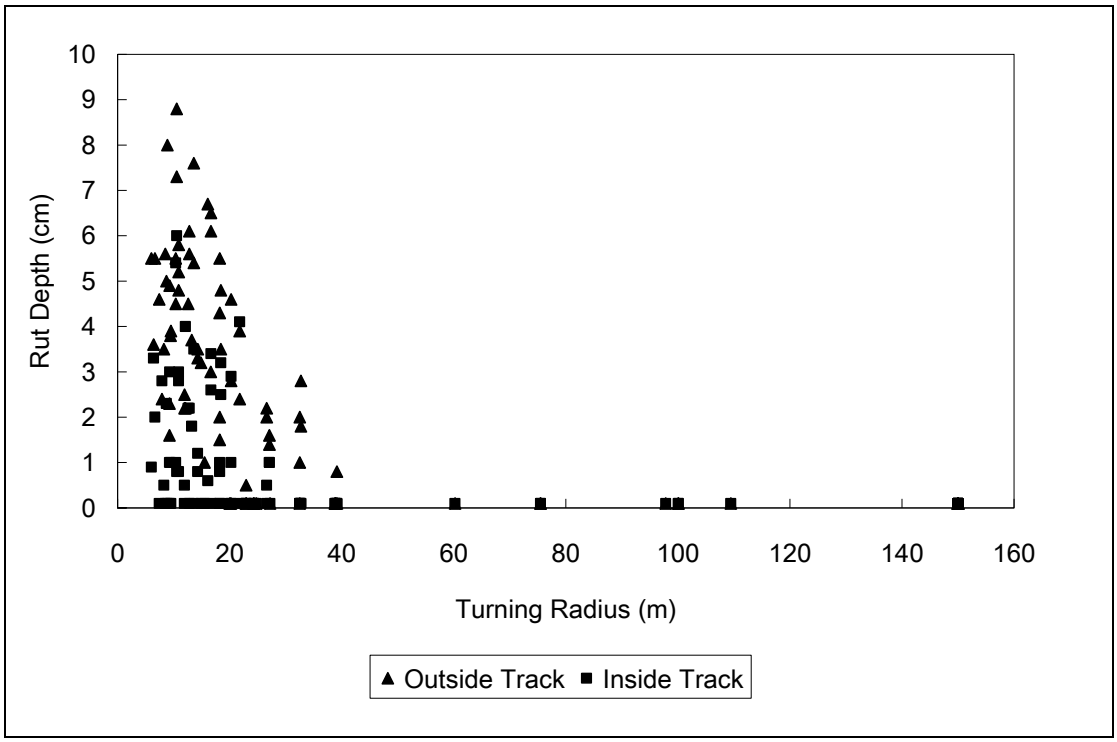

Fig. 4-4 Field measurements of rut depth.

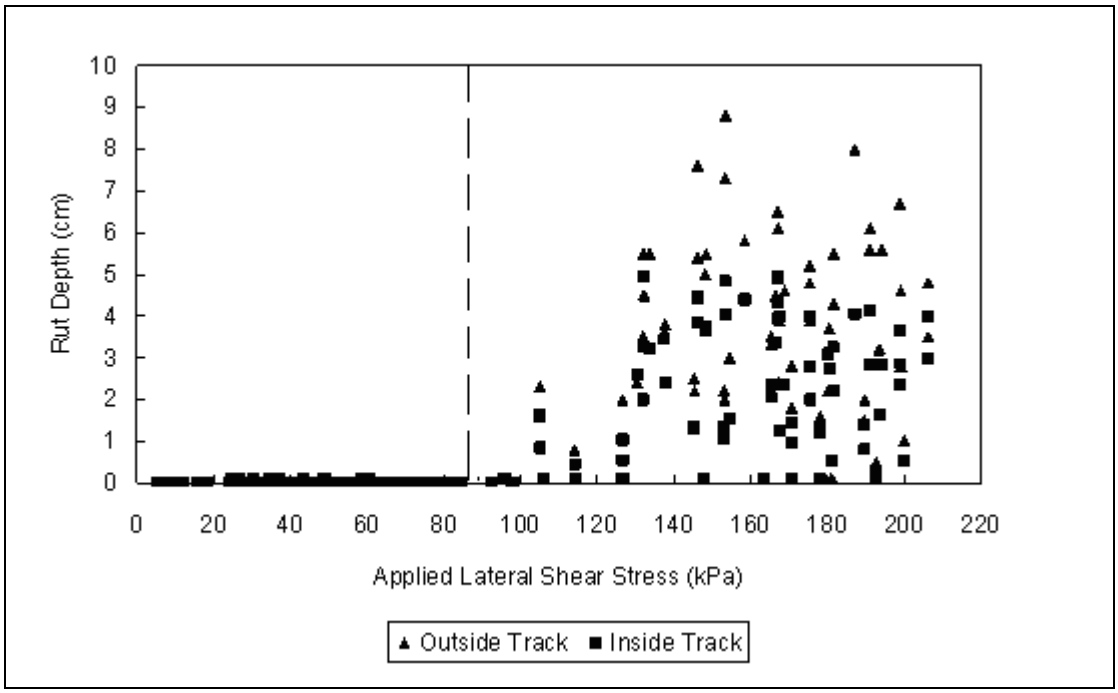

Fig. 4-5 Lateral shear stress and rut depth for the LAV.

Solution

SSE	DFE	MSE	RMSE
595.32860082	335	1.7771003	1.3330793

Parameter	Estimate	ApproxStdErr
b0	0.0000131785	0.02396028
b1	26396.896605	47992917.5
b2	76548.129112	139180601

Solved By: Analytic NR

Fig. 4-6 Nonlinear regression results.

Solution

SSE	DFE	MSE	RMSE
313.20954217	166	1.8868045	1.37361

Parameter	Estimate	ApproxStdErr
b0	0.0000127676	0.03635859
b1	27903.204874	79460416
b2	76548.173804	217996996

Solved By: Analytic NR

Fig. 4-7 Nonlinear regression results using half data.

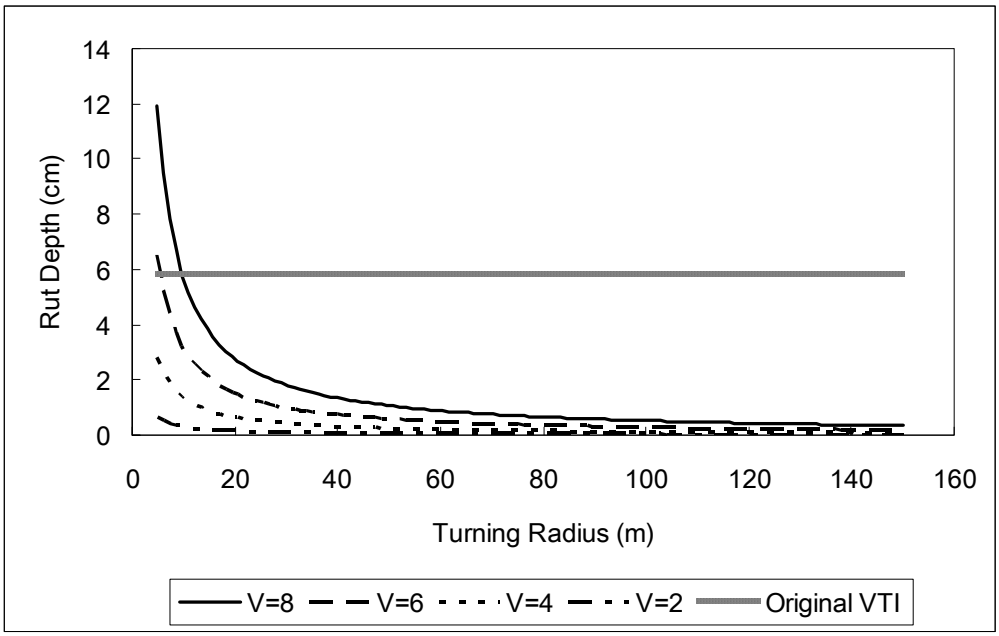

Fig. 4-8 Predicted outside rut depth using constant velocities.

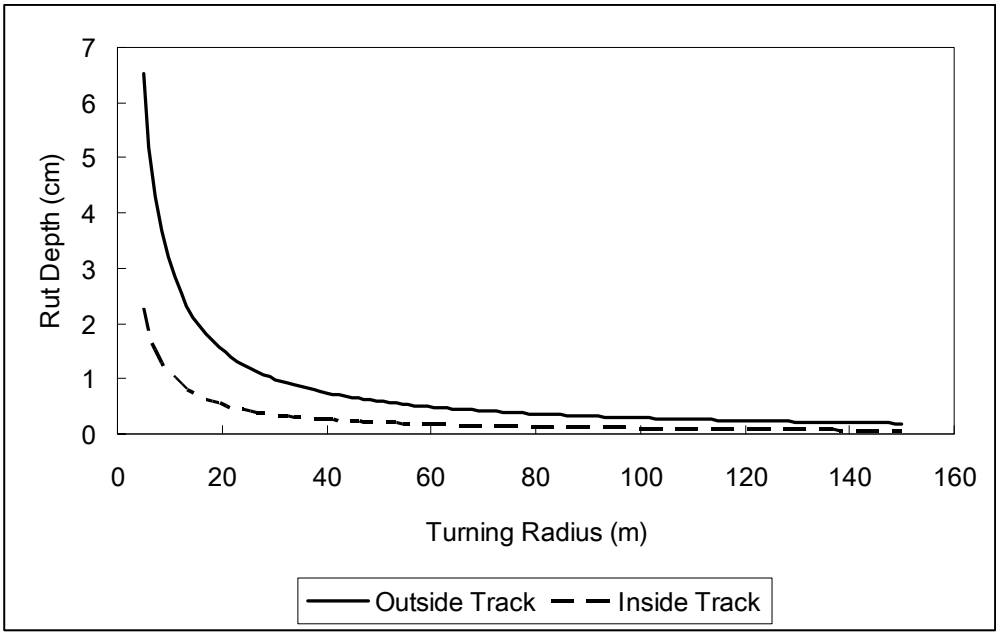

Fig. 4-9 Predicted rut depth at 6 m/s.

Table 4-1 LAV Parameters.

Total Weight	Length	Tread Width	CG Height	Tire Diameter	Tire width	Section Height	Tire Deflection
13930 Kg	6.98 m	2.30 m	1.56 m	111.8 cm	27.9 cm	24.1 cm	6.4 cm

Part 5 Lateral Slide Sinkage Tests for a Tire and a Track Shoe

This chapter is a reformatted version of a paper, by the same name, submitted to Journal of Terramechanics by Kun Liu, Paul Ayers，Heidi Howard，and Alan Anderson. Paper is accepted.

Abstract

Previous field studies have shown the influence of turning vehicles on rut formation or sinkage. In order to further investigate the relationships, lab tests were conduced on a 14.5-20.3 6-PR trailer tire and an Armored Personnel Carrier (APC) track shoe in sand. Lateral forces and lateral displacements were applied to the tire and track shoe under constant normal forces. The tire was pulled laterally and the track shoe was pulled back and forth to represent actual movement during vehicle turning. Results show that the lateral force and lateral displacement generated by turning maneuver affect sinkage severely for wheeled and tracked vehicles. The final sinkage caused by the lateral force for the tire is 3 to 5 times to the static sinkage. For the track shoe, the final sinkage caused by the lateral displacement is about 3 times to the static sinkage.

1. Introduction

Wheeled and tracked vehicles are widely used in agriculture, mining, forestry and the military and need to operate on various terrains. Both the vehicle and terrain parameters can affect sinkage, which has negative influences on vehicle's mobility and soil protection. Factors affecting the sinkage of wheeled and tracked off-road vehicles are very complex. The factors may include soil type, soil strength, water content, vehicle's velocity, mass, and turning radius. Better understanding of the relationships of these factors is needed.

1.1 Slip sinkage

Sinkage by off-road vehicles usually causes two main soil impacts: compaction and displacement. Soil compaction results from normal forces on soil. Soil displacement results from normal forces when its bearing capacity is reached. Soil displacement also occurs when the soil is pushed horizontally. Longitudinal forces in the direction of travel producing slip can displace soil and cause sinkage, referred to as slip sinkage. Lateral forces, perpendicular to the direction of travel and generated when a vehicle is turning, can displace the soil out of the vehicle track and towards the outside of the turn. In a shearing test, slip sinkage is defined in this way: the additional sinkage due to the horizontal shear loading or shear displacement is called slip sinkage (Wong, 2001).

Schwanghart (1968) investigated the relationships between lateral forces, tire loads and slip angles for pneumatic tires in loose soil. Lateral forces on the steered front wheels operating on a sandy clay soil were measured together with wheel sinkage and the negative wheel slip in a soil tank. A function to calculate the lateral force was developed based on wheel load, slip and sinkage. It was found that with the increasing wheel load, sinkage, and slip angle, an increasing size of soil mass was pushed along laterally in front of the wheel, consequently the lateral force also increased.

Durham (1976) tested the powered wheels in the turned mode operating on yielding soil. A 15.2-22.9 (units in cm) 4-PR trailer tire, free of tread, was used for the test. The tire was given different turning angles but the movement direction was

rigidly fixed. Normal wheel loads were from 1000 Newton to 4000 Newton. Tests were conducted at wheel turn angles of 0, 5, 10, 15 and 20 degree. Results showed that the measured lateral forces were varied from 20% to 80% of the normal loads for different turn angles and mobility numbers. The wheel sinkage ranged from 1 cm to 6 cm. It was found that for a given sand mobility number, sinkage increased with the increase of wheel turn angle.

Muro and Hoshika (1995) investigated the tractive performance of a two-axle, two-roller vehicle with rear-wheel drive or brake and the compaction of a decomposed granite soil. It was found that the sinkage of the front roller and the rear roller increased with the increase of the absolute value of the slip of the rear roller, which had positive slip and negative slip. Moreover, the absolute value of the driven or braking force of the rear roller also increased.

Kawase et al. (2006) measured the sinkage and slip of agricultural tires using an indoor traction measurement system under controlled soil conditions. It was observed that these measurements were highly reproducible under all experimental conditions. A larger amount of sand was raked out from under the tire when the slip increased. The results showed a high linear correlation between slip and sinkage: sinkage increased with the increase of slip.

Godwin and Patel (2008) developed a model taking into account tire inflation pressures to predict sinkage and lateral forces for a free rolling wheel. The results showed that due to the deflection of the low inflation pressure tire under high slip angles, the slip angles increased about 5 degree and the lateral forces reduced 5.5%.

Ray et al. (2008) presented a method for estimating the net traction and resistive wheel torques for a differential-steered robot. They found that as lateral forces on steered wheels increased, available longitudinal traction at a given slip ratio became less, and the vehicle had to operate at a higher slip ratio to maintain the same net longitudinal traction. Consequently, a higher slip ratio could form deeper ruts.

To explain the mechanism of slip sinkage in theory is still difficult. Based on experimental evidence, slip sinkage is mainly due to the shear stress on the tire-terrain interface, which causes the transport of terrain material from under it to behind it (Wong, 2001).

Johnson and Burt (1990) introduced a modified Cerruti equation to predict the radial normal stress in an elastic half-space due to a single horizontal point load on the surface. The Cerruti equation was modified to account for an increase in the modulus of elasticity with depth, as the following:

$$\sigma_r = \frac{\nu H \sin^{\nu-2}\phi \cos\theta}{2\pi R^2} \tag{1}$$

where σ_r is the radial stress, ν is the Froelich's concentration factor, H is the shear point load, ϕ is the angle between the shear load vector and the position vector from the point load to the desired load, θ is the angle between the shear load vector and the normal plane that contains the position factor from the shear load to the desired point, R is the radial distance from point load to a desired point. This Cerruti equation can help explain the slip sinkage phenomenon theoretically. There is a sub-surface stress in the vertical direction resulting from the horizontal surface

forces.

AESCO (2006) developed a commercial tire-soil interaction model for industry, dealing with elastic tires in soft soils. They explained that the slip sinkage effect was caused by a digging of the wheel at high wheel slips. The sinkage was calculated from the volume of the soil per time unit which is transported by the tread. In this model, the slip sinkage could lead to a significantly higher rolling resistance.

1.2 Turning vehicles

When a vehicle is turning, both the longitudinal and lateral shear loading and displacement generate sinkage. In this case, the total sinkage of a vehicle consists of two parts: one caused by the static normal force, and the other caused by the shear loading or displacement.

Ayers (1994) measured rut formation for tracked vehicles in turning maneuvers. He divided the turning radius of a M113 armored personnel carrier into three ranges: Straight, Smooth turn and Sharp turn. It was found that the decreased turning radius (sharp turn) could increase soil disturbance and track ruts, and the width and depth of track and height of soil piled increased during the sharp turn.

Braunack and Williams (1993) found that rut depth increased after turning maneuvers in different soil strength and moisture conditions. They found that rut depth increased as the number of passes and turns increased, but especially after turning maneuvers, by testing a M113 armored personnel carrier and a Leopard tank at different soil strength and moisture conditions.

Shoop et al. (2005) conducted vehicle maneuver analysis to predict vehicle impacts on training lands. Terrain disturbance from a Stryker was measured during the winter and spring to evaluate the seasonal impacts. The Stryker was operated in multi-pass ovals and spirals. It was considered that turning was an important factor to determine seasonal impacts on training lands. Shoop et al. (2008) investigated the relationship between tire lateral forces and terrain disturbance during turning maneuvers using an instrumented vehicle. It was found that disturbed width and impact severity increased with the decrease of turning radius. It was also found that the calculated lateral force using GPS data was close to the measured lateral force measured by a tire-mounted load cell, and lateral forces increased with steering angle.

Liu et al. (2007) investigated the influence of turning on wheeled military vehicles induced rut formation. These vehicles were operated in spiral patterns to get continuous turning radii at different speeds. It was found that rut depth, rut width and rut index increased with the decrease of turning radius. Deeper ruts were observed at shaper turns.

Jones et al. (2007) introduced the Vehicle Terrain Interface (VTI) model used in a real-time vehicle dynamics simulator. The VTI model used terrain mechanic methods to predict the interactions between vehicles and terrain. A part of this model was to predict the sinkage for a powered steer wheel at different tire steering angles, where sinkage increased with increase of slip angle, as the following:

$$\frac{Z}{d} = \frac{5}{(Nc_{\alpha} / i_{\alpha}^{1/5})^{5/3}} \tag{2}$$

where Z is the sinkage, d is the wheel diameter, α is the steering angle, Nc_α is the wheel numeric for sinkage at the steering angle α, and i_α is the slip at the steering angle α.

Liu et al. (2009a) conducted tests on military vehicles with different operations. Field tests were conducted both on tracked and wheeled vehicles. Results showed that turning was able to affect rut depth severely. Turning vehicles were shown to form deeper and wider ruts both for wheeled and tracked vehicles. Longitudinal slip sinkage and lateral slip sinkage could be the main reason for these deeper and wider ruts. The longitudinal slip sinkage always occurs no matter when a vehicle is going straight or turning. However, the lateral slip sinkage only occurs when a vehicle is turning. To differentiate the longitudinal slip sinkage and the lateral slip sinkage, the lateral slip sinkage is termed slide sinkage in this paper.

Researchers have invested the phenomenon of slip sinkage for many years. However, most studies on this phenomenon only deal with the longitudinal direction. Some studies on turned tires have been conducted, but their turned tires are not in real turning situations. In these studies the turned tires are pulled in the longitudinal direction. The actual movement of the vehicles during turning is that a turning tire is pulled laterally, and a turning track shoe is pulled back and forth in the lateral direction. The affect of the lateral force and lateral displacement on sinkage when a vehicle is turning needs further investigation. In this paper, the procedure and results of lab tests on lateral slide sinkage for a tire and a track shoe will be introduced.

2. Objectives

The purpose of this study was to investigate the relationships between lateral forces, lateral displacements, and sinkage for a pneumatic tire and a track shoe, in a controlled environment.

3. Experimental approach

3.1 Testing system

The testing device was modified from an Intercomp force test stand (Fig. 5-1). A soil bin was placed on the loading platform, where a hydraulic cylinder was used to manually apply and maintain a constant normal force Fz. In this test, the tire and track shoe were fixed by the testing device, but the soil bin was free to move horizontally. Roller bearings between the soil bin and the platform were used to reduce the horizontal friction force. A relationship between the normal force and the resulting horizontal friction force was determined. A linear actuator was used to apply the lateral force Fx and displacement x. The lateral force was measured by a load cell. Finally, the lateral force on the tire was determined from the lateral force applied by the linear actuator subtracting the friction force on the rollers. The lateral displacement and the normal displacement of the soil bin were measured by two potentiometers. A relationship between the normal force and tire deflection was also determined. The sinkage of the tire (z) is determined from the normal displacement of the soil bin subtracting the tire deflection. The sinkage of the track shoe (z) is

equal to the normal displacement of the soil bin. For the track shoe, an assumption of negligible deflection due to normal forces is made. Fig. 5-2 shows the testing system.

3.2 Tire and track shoe

A Load Star 14.5-20.3 (units in cm) 6-PR trailer tire produced by Load Star was used in this test (Fig. 5-3). This tire is tubeless with a diameter of 52 cm, a width of 18 cm and a maximum load 4050 Newton at 500 kPa. The tire inflation pressure during the test was 140 kPa. This tire is similar to the tire used by Durham (1976).

A track shoe from the Armored Personal Carrier (APC) was used (Fig. 5-4). The track shoe has an 18 cm length and a 10 cm width. The track shoe consists of two parts, an upper steel part and a bottom rubber pad. The pad is 16 cm long, 8 cm wide and 4 cm high.

3.3 Soil preparation

The track shoe and tire were tested using commercial fine sand in an air dry moisture condition with a density of 1.7 g/cm^3. The sand size distribution is 33% in 63-125 μm, 60% in 125-250 μm, and 7% in 250-500 μm. The cone penetration resistance average was 117 kPa for the upper 15 cm sand (ASABE, 1999). The drop cone average was 8.8 cm. The cohesion of the sand was near 0 and the friction angle was 17^o measured using a Cohron torsional sheargraph. Before every single test, the sand was tilled by a rake, and then compacted under a uniform pressure of 6.9 kPa.

3.4 Test procedure

According to field track analysis, it is apparent that a tire always slides away in one direction, toward the outside of the turning circle, for turning wheeled vehicles (Fig. 5-5). The lateral force (centripetal force) must produce some lateral strain when the tire contacts the soil. As a result, the sinkage of the tire increases deeper and deeper under the resultant of the normal force and the lateral force generated by the turning maneuver.

For tracked vehicles, as observed by Li et al. (2007), a turning track shoe slides back toward the inside of the turning circle first, and then slides toward the outside of the turning circle (Fig. 5-6). This procedure happens from the moment the track shoe begins to contact the ground to the moment the track shoe leaves the ground. The track shoe changes the movement direction when it reaches the mid point of the track. In this case, the movement of the track shoe scrapes the soil back and forth under a varying normal force, as each bogie rolls over the track shoe, consequently increasing its sinkage.

The object of this paper was to isolate and analyze these relationships under controlled environments. The lab tests on the track shoe and the tire were conducted under the normal force at four levels: 440 Newton, 890 Newton, 1330 Newton and 1780 Newton. For the tire, a maximum 7.6 cm lateral displacement was used to investigate the relationship between lateral force and sinkage. The speed of the linear actuator producing the lateral displacement was 10 cm/min.

For the track shoe, the lateral displacements were as 1.3 cm in one direction and

2.5 cm in the opposite direction, and 3.8 cm in one direction and 7.6 cm in the opposite direction, to represent the motion of the track shoe during a turn. This allows the investigation on the relationship of lateral displacement and sinkage. The speed of the linear actuator was also 10 cm/min. Both for the tire and the track shoe, every test was repeated three times under each normal force.

4. Results and discussion

4.1 Static sinkage for the tire and track shoe

In the following parts, all the values used will be averages of three tests under each normal force. The loading procedure for the tire and track shoe can be divided into two phases. In the first phase, only the normal force was loaded on the soil bin. Under this normal force, the tire or track shoe started to sink and ruts were formed. Sinkage started when the tire/track print touched the sand surface, measured by the upway movement of soil bin. This kind of sinkage is considered as static sinkage. Fig. 5-7 shows that the static sinkage increases with the increase of the normal force both for the tire and the track shoe.

The static sinkage of the track shoe is less than the static sinkage of the tire under the same normal force, as the contact pressure under the track shoe is less than the contact pressure under the tire. During the test, the contact pressure for the tire kept constant at a pressure which was a little higher than the tire inflation pressure of 140 kPa because of the tire wall. If the tire coefficient was 1.2 (Jakobsen and Dexter, 1989), the contact pressure should be 170 kPa. The tire coefficient was developed

for tires on paved roads, but we used it for sands and the result should be slightly different. For the track shoe, the contact pressure was determined by the normal force/contact area. The highest contact pressure of 100 kPa occurred when the normal force was 1780 Newton.

4.2 Lateral force and lateral displacement for the tire

In the second phase, a lateral displacement was applied to push the soil bin horizontally while the normal force kept constant at 440 Newton, 890 Newton, 1330 Newton and 1780 Newton. The lateral displacement can produce a resulting lateral force in the tire. Fig. 5-8 shows the relationship between lateral force and lateral displacement for the tire. It can be seen that lateral force increases with the increase of lateral displacement. Under the 440 Newton normal force, the lateral force is 291 Newton when the lateral displacement reaches 7 cm. Under the 1780 Newton normal force, the lateral force is 757 Newton at the lateral displacement of 7 cm. To reach the same lateral force, the tire under lower normal forces needs to have greater lateral displacements than the tire under higher normal forces.

4.3 Slide sinkage and lateral displacement for the tire

Fig. 5-9 shows that slide sinkage increases with the increase of lateral displacement. Though the total lateral displacement for the tire is around a half of the tire width, the final sinkage increases by 3 to 5 times the static sinkage formed only by the normal forces because of the increase of slide sinkage. Durham (1976)

reported that the total sinkage varied from 2.5 to 15 cm for a 4-PR trailer tire under 1000 to 4000 Newton normal load with different steering angles.

4.4 Lateral force and slide sinkage for the tire

Slide sinkage started when the lateral displacement was applied. Slide sinkage is the additional sinkage due to the lateral force and displacement. Fig. 5-10 shows the relationship between lateral force and slide sinkage for the tire. It appears that under the same lateral force, lower normal forces have deeper slide sinkage. One possible reason is that lateral force results from the resistance of the soil (Lateral passive earth pressure) for the tire. Low normal forces need large lateral displacements to reach a depth to produce the same lateral force, while high normal forces only need small lateral displacements. Thus the larger lateral displacements are producing higher sinkage. It can be seen that slide sinkage is always increasing with the increase of lateral forces, but its rate tends to decrease with the increase of lateral forces.

Compared to the static sinkage of 1.9 cm under the 1780 Newton normal force, its final sinkage is 5.7 cm after the lateral force is applied, three times the static sinkage. For tire under 440 Newton normal force, its final sinkage is 3.2 cm, five times as the static sinkage.

4.5 Lateral displacement and slide sinkage for the track shoe

Like the loading procedure of the tire, the normal force was applied first to the

track shoe, and then the lateral displacement was applied. The track shoe test was conducted with two cumulative lateral displacements 3.8 cm and 11.4 cm. When the track shoe has a lateral displacement of 1.3 cm back and 2.5 cm forth, its cumulative lateral displacement is 3.8 cm. When the lateral displacement is 3.8 cm back and 7.6 cm forth, the cumulative lateral displacement is 11.4 cm.

Figs. 5-11 and 5-12 show that when a lateral displacement is applied, the slide sinkage of the track shoe is always increasing. At a given lateral displacement, higher normal force can produce deeper slide sinkage, because the track shoe does not have a big cross-sectional area like the tire and the lateral passive earth pressure is not that affective to the track shoe. Under the 440 Newton normal force, its sinkage increases from the static sinkage of 0.3 cm to 0.8 cm at the cumulative lateral displacement of 3.8 cm, and to 1 cm at the cumulative lateral displacement of 11.4 cm, because of the lateral displacement. Under the 1780 Newton normal force, its sinkage increases from the static sinkage of 0.6 cm to 1.1 cm at the cumulative lateral displacement of 3.8 cm, and to 1.7 cm at the cumulative lateral displacement of 11.4 cm. The sudden decrease of slide sinkage with the increased lateral displacement is caused by the shifting of the soil bin when the system fails. The movement brought variability to the sensor measuring the small values of slide sinkage, but the trends are apparent. The lateral displacement causes the final sinkage of the track shoe to increase by almost 3 times to the static sinkage. The slide sinkage is 2 times as deep as the static sinkage.

4.6 Lateral displacement and lateral force for the track shoe

Figs. 5-13 and 5-14 show the lateral forces resulted from lateral movements of the track shoe during the procedure when the lateral displacement is applied in two directions. It can be seen that the track shoe under a higher normal load also generate a higher lateral force. When the track shoe changes its movement direction, the resulted lateral force does not change the direction immediately but gradually over a certain displacement. This could be caused by the deformation of the track shoe attachment system and the rheology of the sand.

4.7 Relationships between sinkage and turning radius

The lateral force on the tire for a turning vehicle should be a function of turning radius, velocity, and mass. The mass is related to the normal force. From the lateral force and the mass, the turning radius of the vehicle can be calculated at a given velocity of 3 m/s, or 10.8 km/h, which is a reasonable speed when a vehicle is turning. In Durham's test (1976), the speed of the tire was approximately 1.5 m/s. Fig. 5-15 shows the relationship between total sinkage and turning radius for the tire. Static sinkage corresponds to that the vehicle is going straight (turning radius>150 m). The treadlines are from regressions using power equations based on calculated turning radius. It can be seen that a turning wheel will sink more under the same lateral force, verifying the results found in previous field studies involving full-size wheeled vehicles (Liu et al., 2009a and Liu et al., 2009b).

The track shoe has two series of lateral displacements. The lateral displacement

was as 1.3 cm in one direction and 2.5 cm in the opposite direction, and 3.8 cm in one direction and 7.6 cm in the opposite direction. Using the model proposed by Li et al. (2007), turning radii of 28 m and 10 m can be calculated for a full-size APC corresponding to the two lateral displacement sets of the linear actuator, respectively. This supports the field studies that for full-size tracked vehicles sharper turns will produce deeper ruts (Liu et al., 2009a and Liu et al., 2009b). Compared to field tests, lower total sinkage was found in the laboratory test due to the normal force limitations of the testing device and slip sinkage was not reproduced. When a full-size vehicle is moving in field test, beside the slide sinkage caused by the lateral movements, there will also be slip sinkage.

Li et al. (2007) indicated that the terrain impact of tracked vehicles were more dependent on turning radius than velocity. Fig. 5-16 shows the relationship between total sinkage and turning radius for the track shoe. Static sinkage corresponds to that the vehicle is going straight (turning radius>150 m). The treadlines are also from regressions using power equations based on calculated turning radius. Similar regression trendlines are used to represent field data results. It can be seen that a track shoe representing a turning vehicle can produce more sinkage under the higher lateral displacement.

5. Conclusions

In this paper, lab tests were conduced to investigate the sinkage of a trailer tire and an APC track shoe, due to lateral forces (or lateral displacements) under given

different levels of normal forces. It can be seen that both for the tire and the track shoe, the sinkage increases with the increase of normal forces. This verifies the sinkage phenomenon of a static vehicle on the soil ground. It is more interesting to see that the slide sinkage due to the lateral force or lateral displacement is much deeper than the sinkage due to the static normal force. The final sinkage caused by the lateral force for the tire is 3 to 5 times the static sinkage. For the track shoe, the final sinkage caused by the lateral displacement is about 3 times the static sinkage. These results show that the lateral force and lateral displacement generated by turning maneuvers affect the sinkage severely for both wheeled and tracked vehicles.

Acknowledgement

We are grateful to the Environmental Security Technology Certification Program (ESTCP) project SI-0815 for providing support for this study.

Reference

[1] AESCO. AS^{2}TM User's guide, Version 1.03. 2006.

[2] ASAE EP542. Procedures for Using and Reporting Data Obtained with the Soil Cone Penetrometer. 1999.

[3] Ayers PD. Environmental damage from tracked vehicle operation. J Terramechanics 1994; 31(3): 173-183.

[4] Braunack MV, Williams BG. The effect of initial soil water content and vegetative cover on surface disturbance by tracked vehicles. J Terramechanics 1993; 30(4): 299-311.

[5] Durham GN. Powered wheels in the turned mode operating on yielding soils. U.S. Army Engineer Waterways Experiment Station, Technical report: M-76-9; 1976.

[6] Godwin RJ, Patel NM. Force prediction model for high stiffness pneumatic tyres. In: 2008 ASABE Annual International Meeting. Providence, Rhode Island; 2008.

[7] Jakobsen BF, Dexter AR. Prediction of soil compaction under pneumatic tyres. J Terramechanics 1989; 26(2): 107-119.

[8] Johnson CE, Burt EC. A method of predicting soil stress state under tires. Transactions of ASAE 1990; 33(3): 713-717.

[9] Jones A, McKinley G, Richmond P, Creighton D. A vehicle terrain interface. In: ISTVS conference. Fairbanks, Alaska; 2007.

[10] Kawase Y, Nakashima H, Oida A. An indoor traction measurement system for agricultural tires. J Terramechanics 2006; 43(3): 317-327.

[11] Liu K, Ayers P, Howard H, Anderson A. Influence of turning radius on military vehicle induced rut formation. In: ISTVS conference. Fairbanks, Alaska; 2007.

[12] Liu K, Ayers P, Howard H, Anderson A. Influence of turning radius on wheeled military vehicle induced rut formation. J Terramechanics 2009b; 46(2): 49-55.

[13] Liu K, Ayers P, Howard H, Anderson A. Influences of soil and vehicle parameters on soil rut formation. J Terramechanics 2009a; accepted.

[14] Muro T, Hoshika Y. Tractive performance and compaction effect of a road roller running on a weak sandy soil. J Terramechanics 1995; 32(5): 245-261.

[15] Ray LR, Brande DC, Lever JH. Estimation of net traction for differential-steered wheeled robots. J Terramechanics 2009; 46(3): 75-87.

[16] Schwanghart H. Lateral forces on steered tyres in loose soil. J Terramechanics 1968; 5(1): 9-29.

[17] Shoop S, Affleck R, Collins C, Larsen G, Barna L, Sullivan P. Maneuver analysis methodology to predict vehicle impacts on training lands. J Terramechanics 2005; 42(3): 281-303.

[18] Shoop S, Coutermarsh B, Ayers P, Anderson A, Affleck R. Tire force and terrain disturbance measurement during turning maneuvers. Transactions of ASABE 2008; 51(6): 1869-1878.

[19] Wong JY. Theory of ground vehicles. New York, Wiley - Interscience; 2001.

Appendix

Fig. 5-1 Intercomp force test stand.

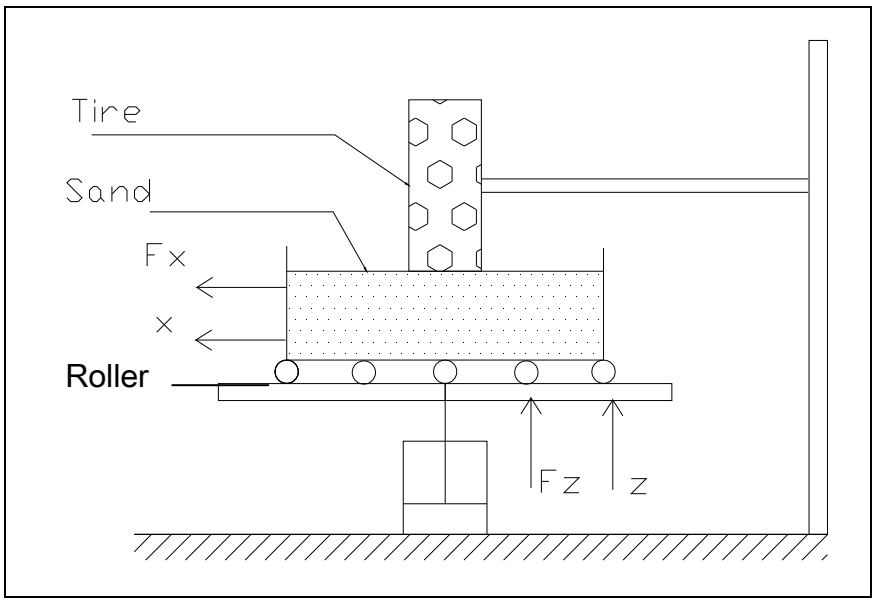

Fig. 5-2 Lateral sinkage test setup.

Fig. 5-3 Trailer tire.

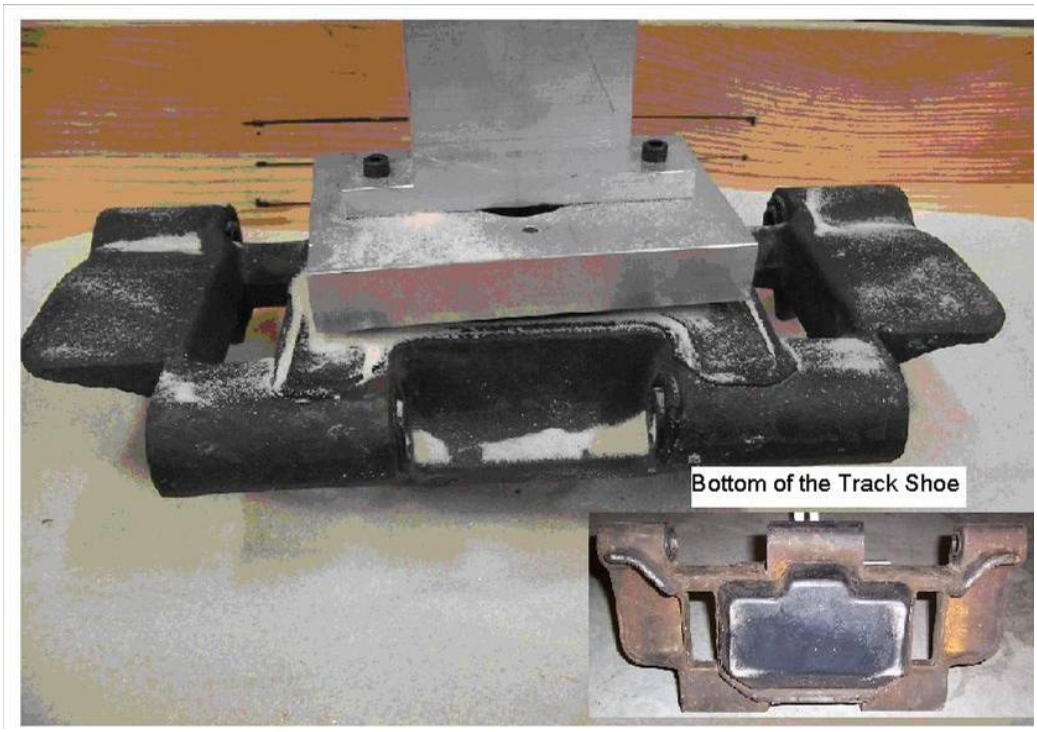

Fig. 5-4 Track shoe.

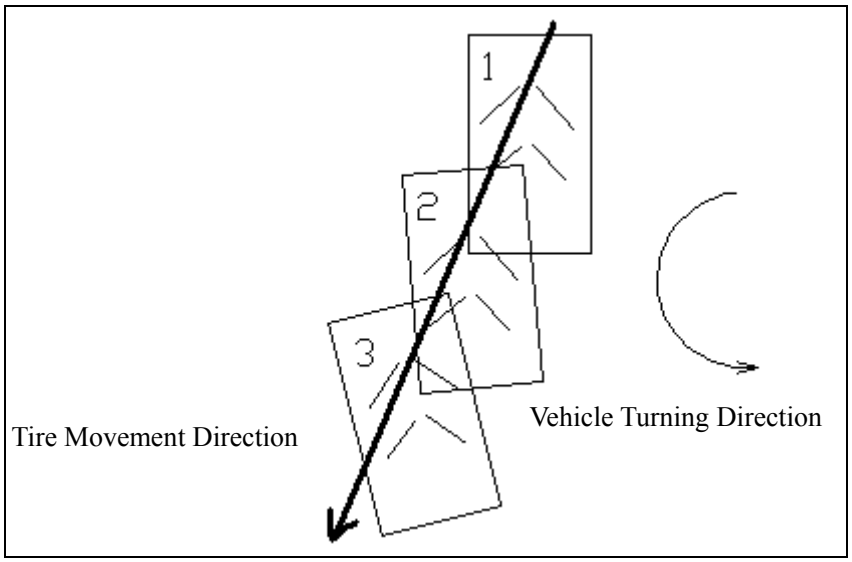

Fig. 5-5 A turning tire.

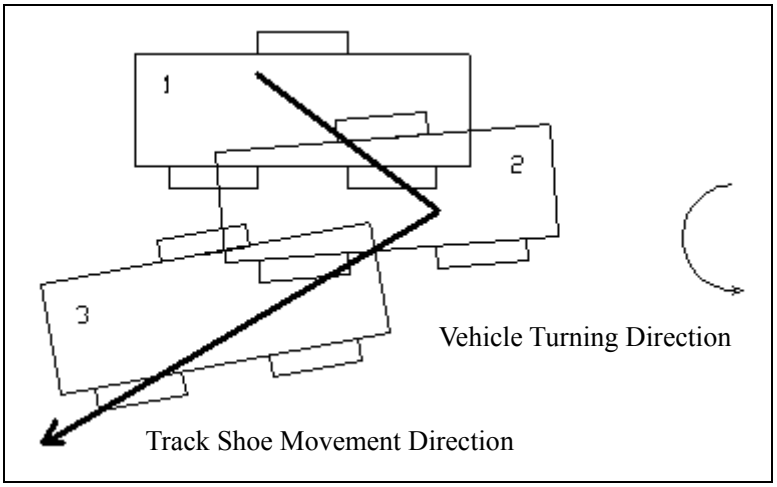

Fig. 5-6 A turning track shoe.

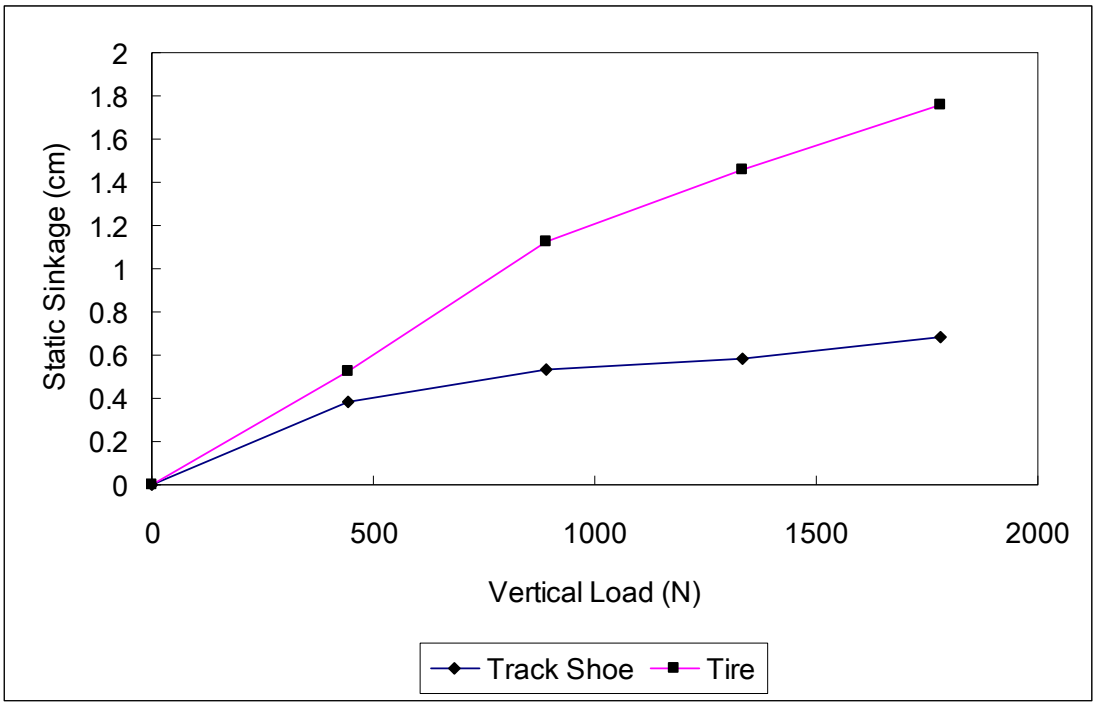

Fig. 5-7 Static sinkage for the tire and track shoe.

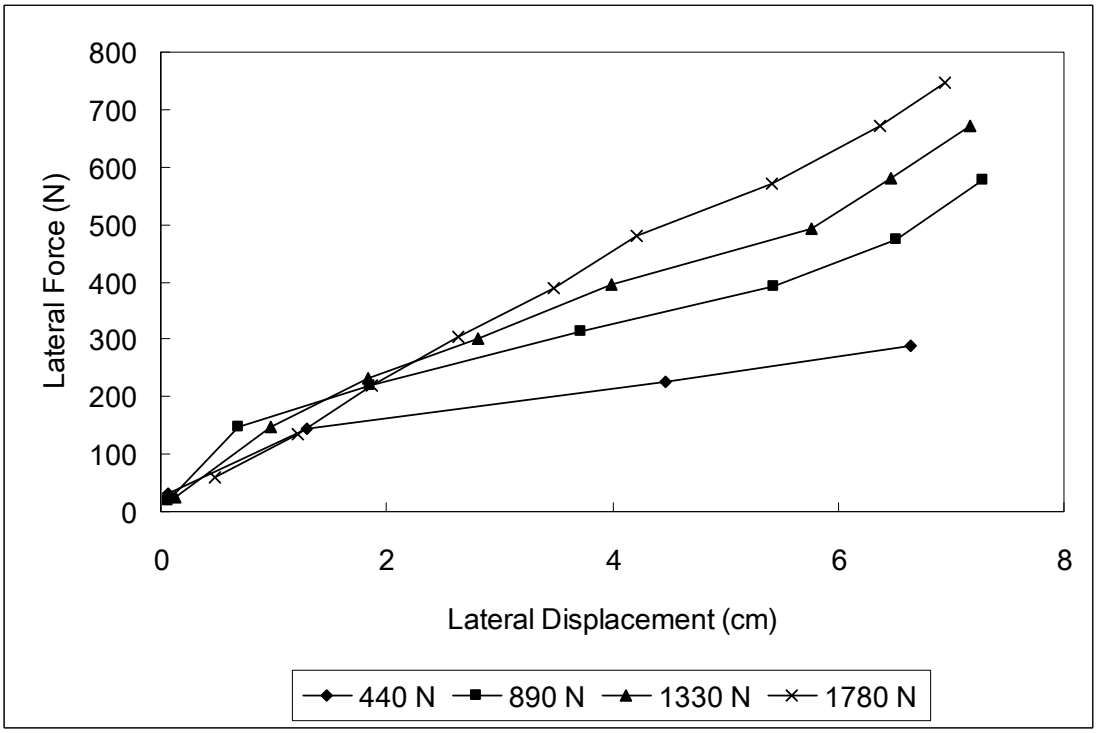

Fig. 5-8 Lateral displacement and lateral force for the tire.

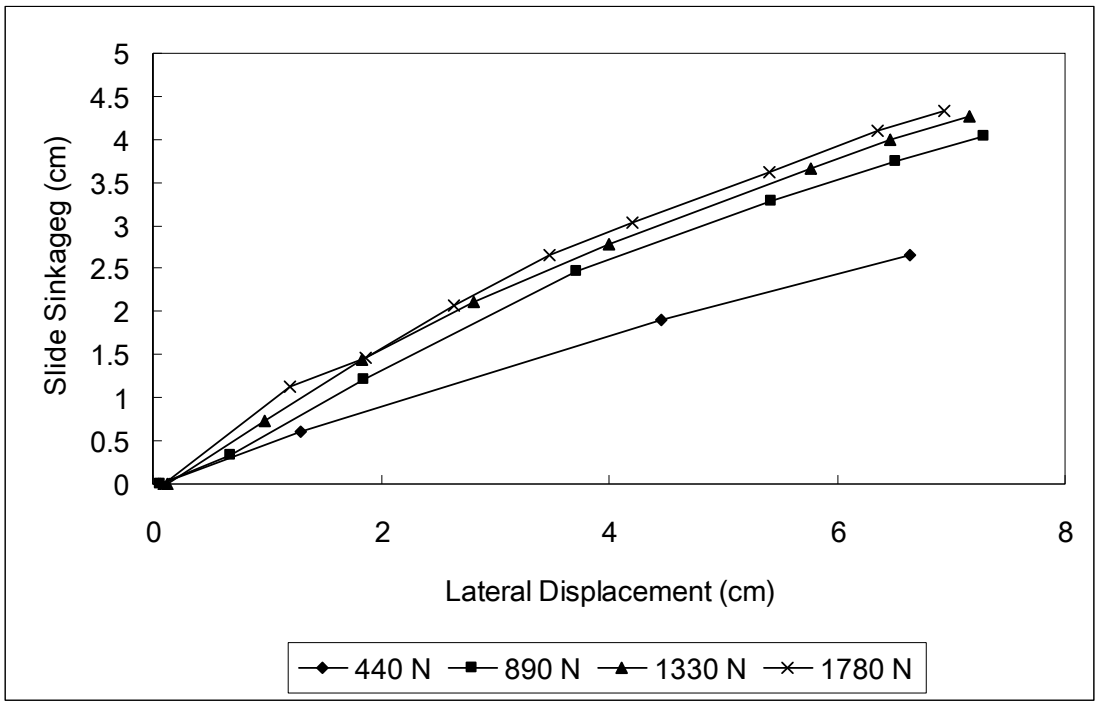

Fig. 5-9 Slide sinkage and lateral displacement for the tire.

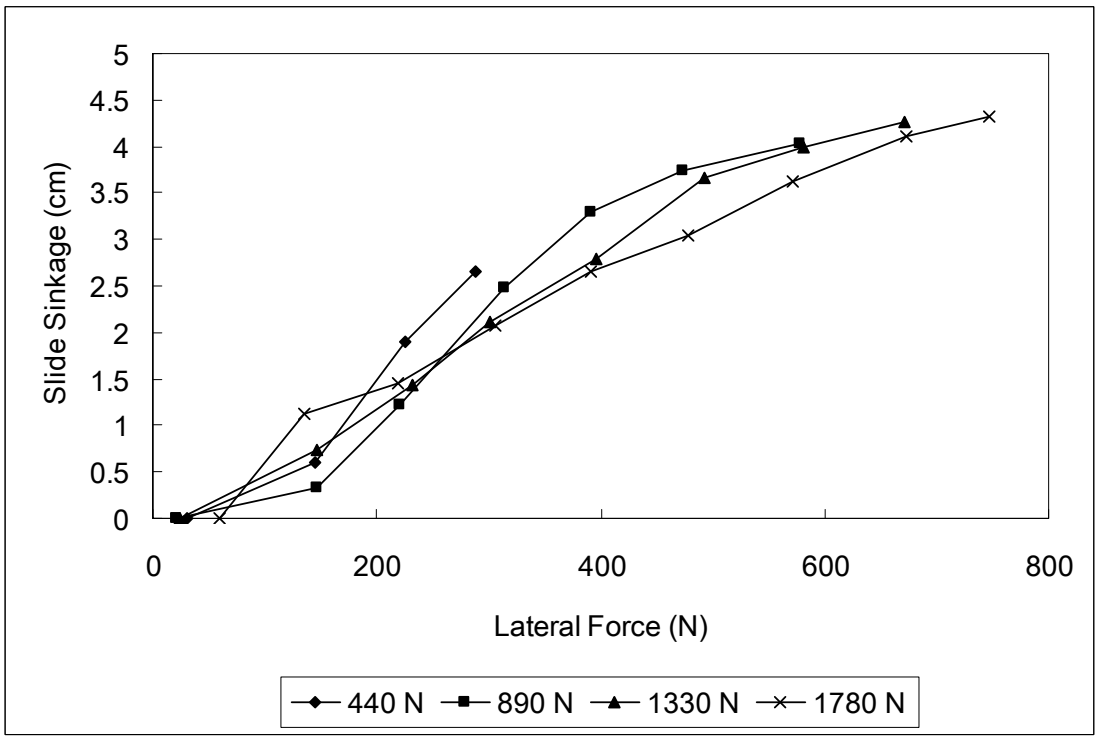

Fig. 5-10 Lateral force and slide sinkage for the tire.

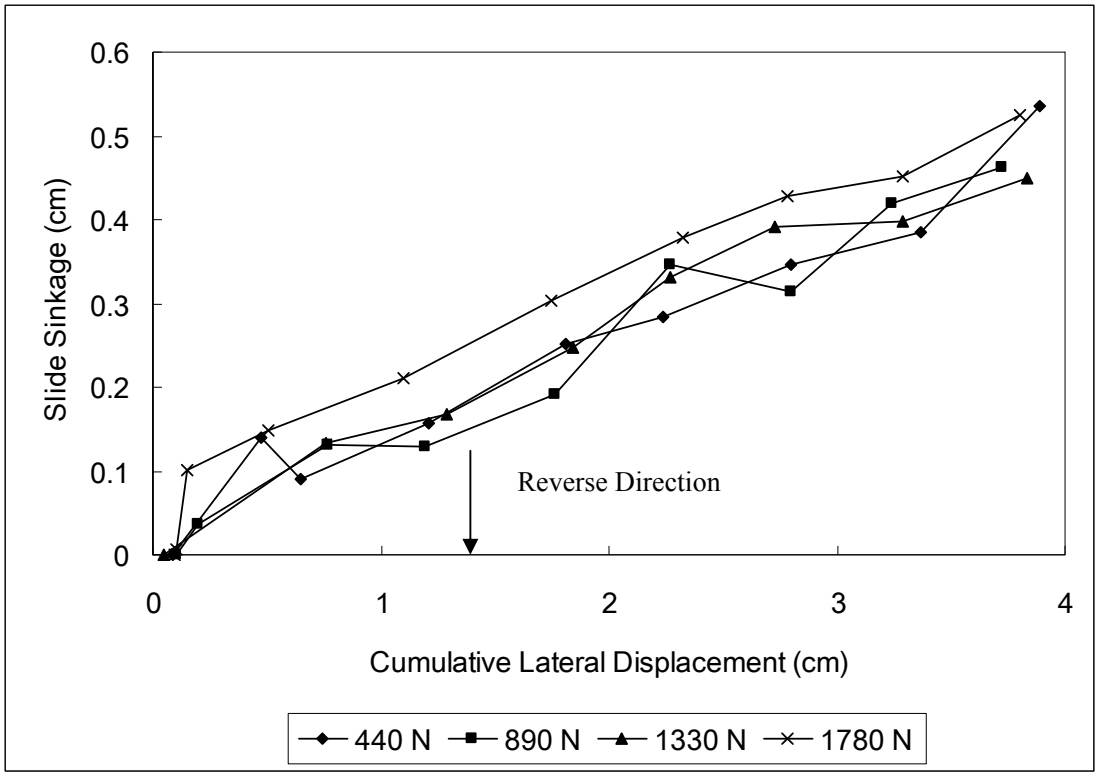

Fig. 5-11 Slide sinkage at a maximum 3.8 cm cumulative lateral displacement.

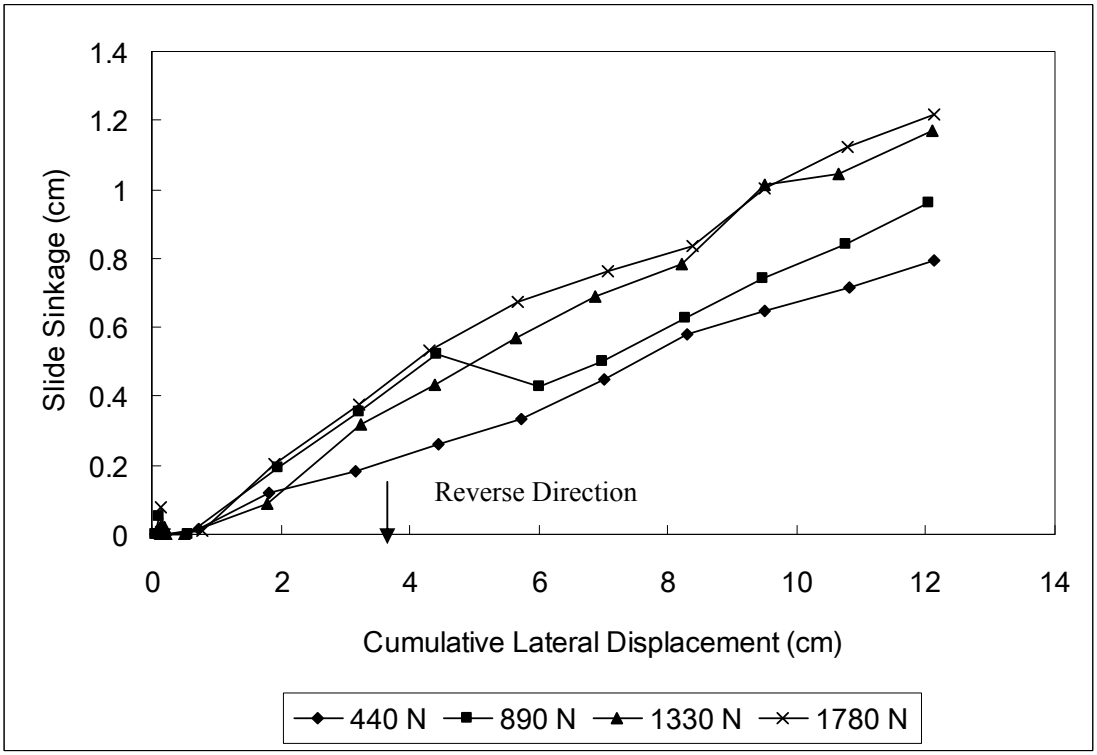

Fig. 5-12 Slide sinkage at a maximum 11.4 cm cumulative lateral displacement

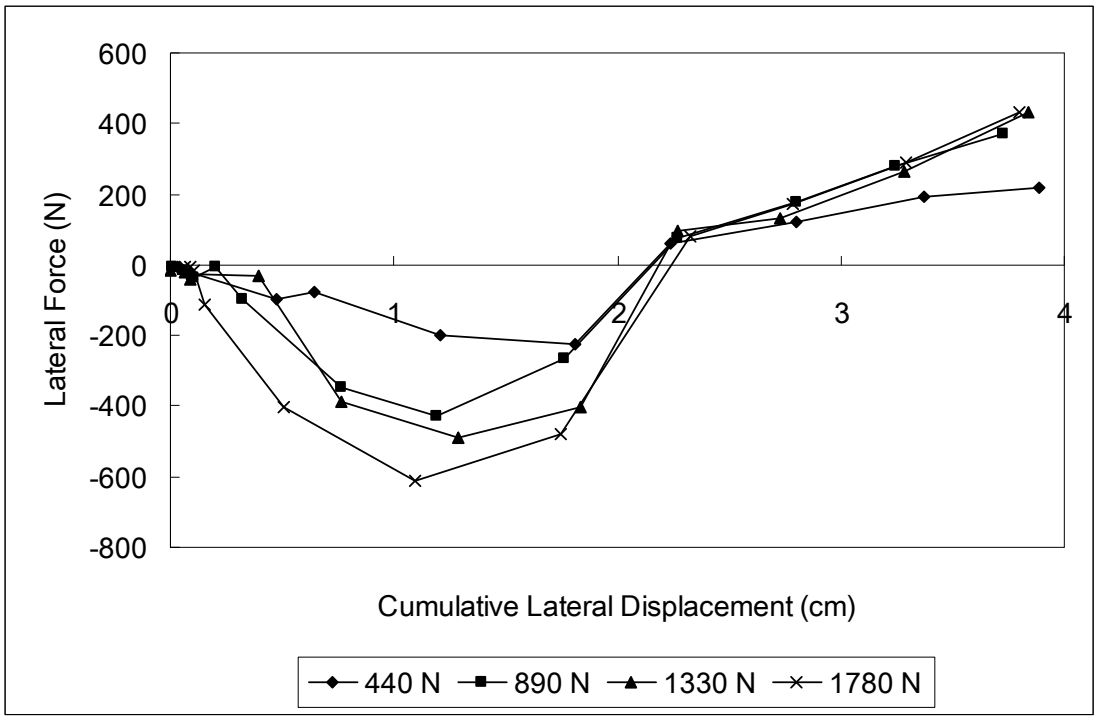

Fig. 5-13 Lateral force at a maximum 3.8 cm cumulative lateral displacement.

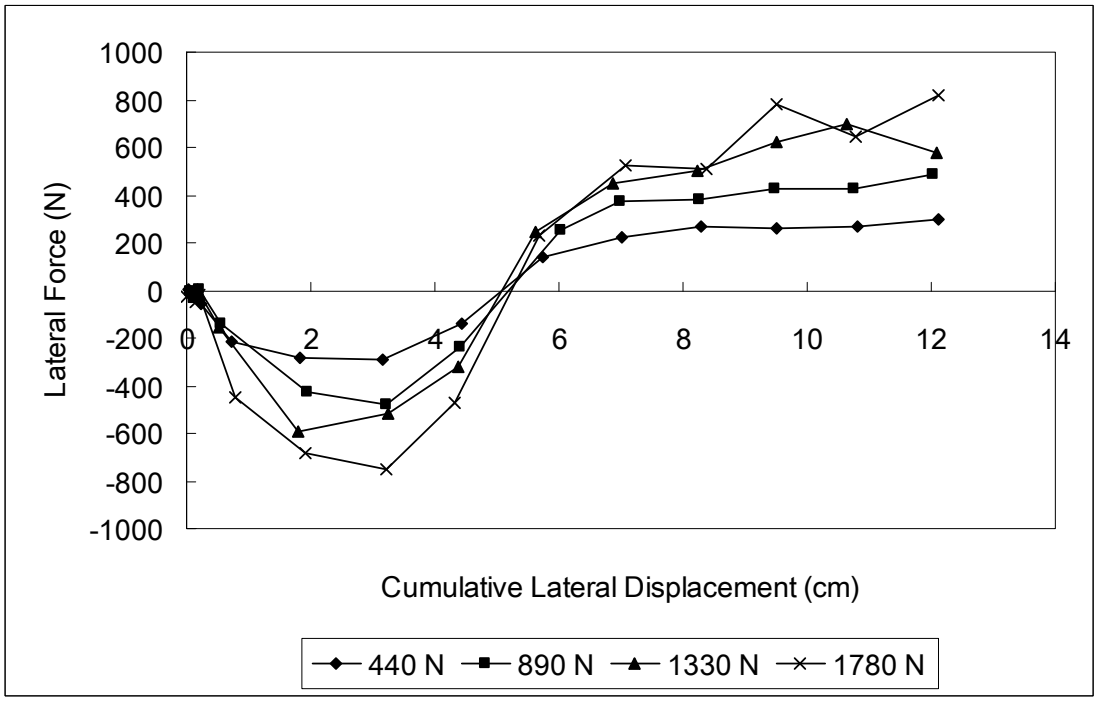

Fig. 5-14 Lateral force at a maximum 11.4 cm cumulative lateral displacement.

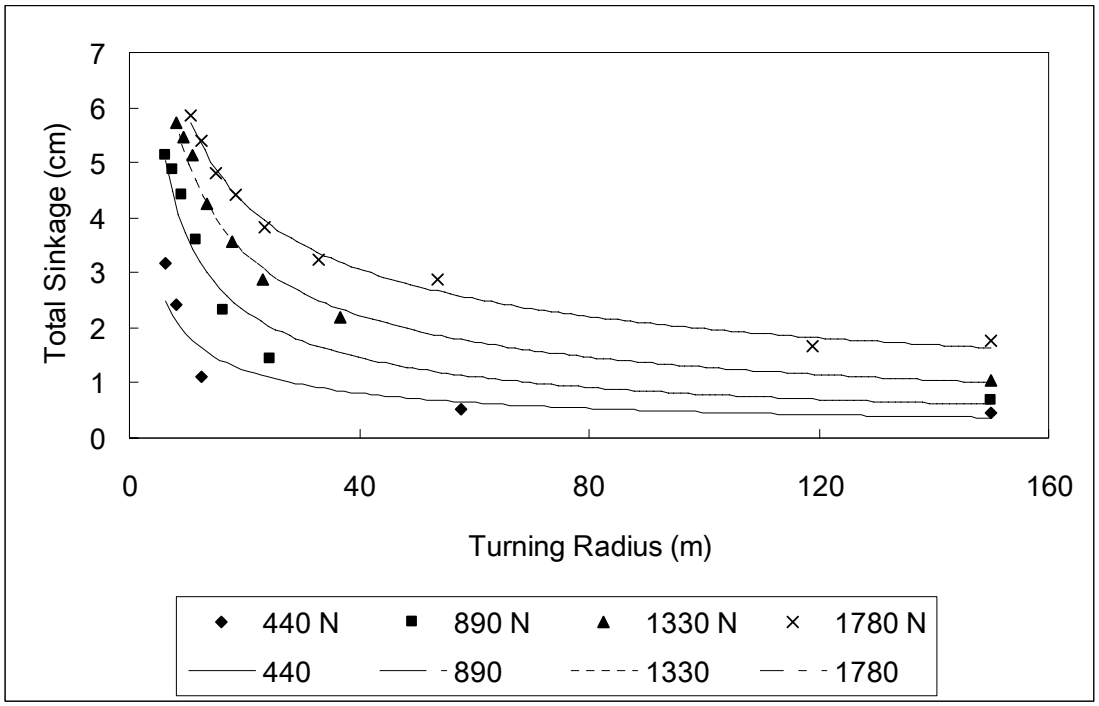

Fig. 5-15 Total sinkage and turning radius for the tire.

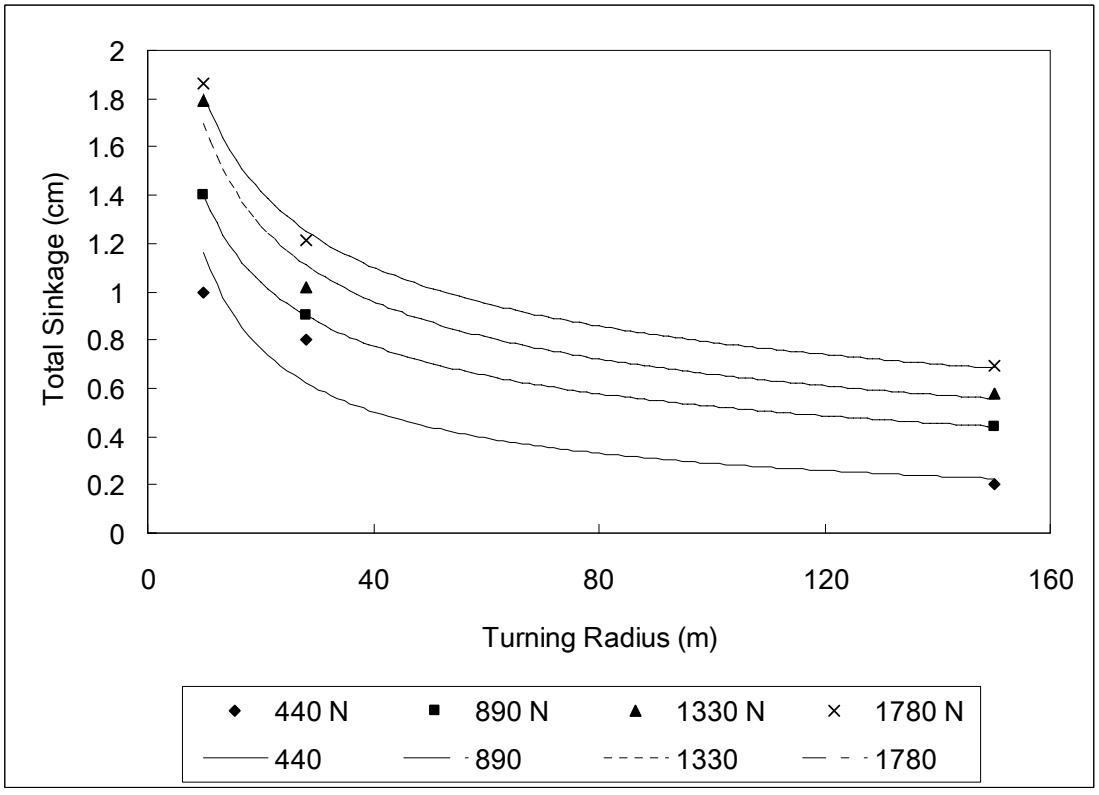

Fig. 5-16 Total sinkage and turning radius for the track shoe.

Part 6 Multi-pass Rutting Study for Turning Wheeled and Tracked Vehicles

This chapter is a reformatted version of a paper, by the same name, submitted to the Transactions of ASABE by Kun Liu, Paul Ayers, Heidi Howard, Alan Anderson and James Kane. Paper is under review.

Abstract

In this paper, the effects of vehicle multiple passes and turning maneuvers are investigated on rutting for wheeled and tracked vehicles. Field tests were conducted at Fort Riley in August, 2008, on a combat tank M1A1, an Armored Personnel Carrier (APC), a Heavy Expanded Mobility Tactical Truck (HEMTT), and a High Mobility Multi-purpose Wheeled Vehicle (HMMWV). These vehicles were operated in spiral patterns to evaluate a variety of turning radii. Each vehicle was driven in its same rut up to 8 passes along each spiral. A Vehicle Tracking System (VTS) was mounted onto each vehicle to utilize the Global Positioning System (GPS) to determine vehicle dynamics (velocity and turning radius). Compared to a single pass, results show that soil deformation and compaction increase with the increase of the number of passes. Rut depths increase from 65% to 548% of the initial rut depths under the effects of the combination of the multi-pass and turning maneuvers after multiple passes. The multi-pass coefficient (a=2) is proper to predict multi-pass rut depth for turning vehicles in loose soils. It is also verified that turning maneuvers can affect rut depth significantly, either positively or negatively.

1. Introduction

Vehicle multi-pass behavior is an important phenomenon in vehicle and soil dynamics. Compared to a single pass, soil deformation and compaction are expected to increase when multiple passes occur. This phenomenon has been investigated while vehicles are traveling straight, but the influence of multi-pass turns has not been

investigated thoroughly.

1.1 Effects of multiple passes on rut formation

Holm (1969) investigated the behavior of a pneumatic tire in multi-pass operation over the same path. Drawbar pull, rolling resistance, tire deflection, slip and sinkage were measured to evaluate the multi-pass behavior in soft soils. The tests were conducted in a soil bin using three different tires with smooth and deep threads. The wheel load varied from 600 kPa to 1200 kPa. It was found that soil density increased with consecutive passes and the greatest sinkage occurred on first pass.

Abele et al. (1984) investigated the long-term effects of off-road vehicles on terrain at two sites in northern Alaska. An air cushion vehicle, two light tracked vehicles, and three wheeled vehicles were used to observe their effects on surface depression, thaw depth, vegetation damage, and traffic signature visibility. It was found that multiple passes produced increased soil and vegetation damage. The traffic signatures for the multiple passes remained longer and still could be seen after 10 years.

Abebe et al. (1989) conducted an experimental study of soil compaction caused by multiple loadings from a rigid wheel. It was found that the number of passes and the load as independent variables significantly affected the compaction capacity of soil, based on the analysis of soil volume and compaction index. The bulk of the compaction process occurred during the first three passes of a loaded wheel. Under a 600 Newton vertical load, the specific soil volume under the wheel was compacted

to 30% of its initial volume after twelve passes.

Ansorge and Godwin (2008) conducted research on the effect of the passage of multi-axle harvesting machines on soil compaction in controlled conditions. They found that the rear tire had a significant influence on soil density when following a leading tire. They also found that the soil surface created by first pass had a higher strength layer which was able to withstand the load of the subsequent passes and protect the soil below from further compaction.

1.2 Multi-pass models

Jakobsen and Dexter (1989) presented a computer program for prediction of the influence of traffic on agricultural soil compaction. In this program, soil compression and wheel sinkage depended on a number of factors including the number of passes. It was found that the contact pressure increased during the multi-pass test because the ground contact area decreased with the increase of wheel passes, resulting in further increases in soil density and strength. Harnisch et al. (2007) also found that multi-pass traffic could produce highly compacted soils because of the smaller area of the tire–ground contact.

Affleck (2005), Jones et al. (2007), and Reid et al. (2007) introduced the terrain mechanics methods used to predict the physical interactions of vehicles and terrain surfaces in a real-time vehicle dynamics simulator being developed by the US Army. The sinkage for multiple wheel and track passes z_n was calculated using an empirical equation:

$$z_n = n^{1/a} \cdot z$$

(1)

where n is the number of passes, z is the sinkage for first pass, and α is the soil multi-pass coefficient. This model was originally developed for a single tire by the Waterway Experiment Station (WES). In this model, the coefficient is 2 (Jones et al., 2007). Affleck (2005) applied this model to calculate the sinkage of multiple passes for wheeled and tracked vehicles. In order to calculate the rut depth for any pass, Saarilahti (2002) developed a general multi-pass equation:

$$z_n = \left({z_{n-1}}^{a_n} + {z_1}^{a_n} \right)^{1/a_n} \tag{2}$$

where z_n is the rut depth after n^{th} pass, z_{n-1} is the rut depth after $n-1^{th}$ pass, z_1 is the estimated rut depth of n^{th} pass without no prior soil disturbance, first wheel pass rut depth, and α_n is the multi-pass coefficient for the n^{th} wheel pass. Saarilahti (2002) also reported the range of multi-pass coefficients in different soil and load conditions. For loose soil and low load, the value is from 2 to 3. For medium bearing soil and medium load, it is 3 to 4. For bearing soil and heavy load, it is from 4 to 5.

1.3 Effects of turning maneuvers on rut formation

Beside the multi-pass phenomenon, vehicle operation is an important factor affecting rut formation as well. The rut formation of a turning vehicle is different from a vehicle moving in a straight path, in the sense that usually, a turning vehicle forms deeper ruts. Turning vehicles also add a lateral force to the soil, displacing the

soil out of the vehicle track and towards the outside of the turn.

Braunack and Williams (1993) estimated the effect of initial soil water content and vegetative cover on soil surface disturbance caused by tracked vehicles. In their field tests, multiple passes and turning were two independent treatments, which were randomly allocated to plots within each block. It was found that rut depth increased as the number of passes and turns increased, but especially after turning maneuvers, by testing a M113 armored personnel carrier and a Leopard tank at different soil strength and moisture conditions.

Ayers (1994) investigated soil surface disturbance from tracked vehicle operation. Soil surface disturbance measurements were conducted using an M113 armored personnel carrier, which was operated in spiral patterns. It was found that the decreased turning radius (sharp turn) would increase soil disturbance, track ruts, and the width and depth of tracks. The height of soil pile also increased as a result of sharp turns.

Affleck (2005) measured rut depth for two wheeled and two tracked vehicles during spring thaw seasons. These vehicles were operated in turning, multi-pass maneuvers，and in combinations of both. Vehicles performed turning maneuvers by traversing from a small radius to larger radii. The multi-pass tests were composed of lanes with one, three, eight, and thirteen passes. The results generally showed that for these four vehicles soil displacement increased in volume as the number of passes increased. Rut depth also had a significant increase. Particularly for the Stryker, an 8 wheeled vehicle, the effect of the combination of turning and multi-pass maneuvers

on rutting was considerable. It was found that soil displacement severely increased with the increase of the number of passes on straight paths and was significantly higher on sharper turns.

Liu et al. (2009a) investigated the influence of vehicle and soil parameters on rut formation of off-road military vehicles in field tests, conducted at Fort Riley. Measured soil parameters included soil texture and moisture. Vehicle parameters included vehicle type, turning radius and velocity. It was found that turning maneuvers had statistically significant effects on rut formation of military off-road vehicles. All three indicators describing the degree of rut formation, rut width, rut depth and rut index, increased significantly when the vehicles changed operation from straight paths to turns, except a Heavy Expanded Mobility Tactical Truck (HEMTT). For the HEMTT, sharp turns formed shallower ruts because of the separation of wheels at sharp turns. Liu et al. (2009b) investigated the influence of turning radius on wheeled military vehicle induced rut formation. Turning radius was classified into three ranges: sharp turns, intermediate turns and straight. It was found that rut depth, rut width and rut index increased with the decrease of turning radius, especially when turning radius was less than 20 m.

In summary, from these published studies both the multi-pass phenomenon and turning factor have influences on rut formation. However, when a vehicle is negotiating a multi-pass turn, the increased rut formation needs to be better quantified, as past research is limited.

2. Objectives

The objective of this study was to investigate the influences of the combination of vehicle multiple passes and turning maneuvers on rut depth of wheeled and tracked vehicles at Fort Riley, Kansas.

3. Vehicle and soil description

Four vehicles were used for this study: a combat tank M1A1 (Fig. 6-1), an Armored Personnel Carrier (APC) (Fig. 6-2), an 8-wheeled Heavy Expanded Mobility Tactical Truck (HEMTT) (Fig. 6-3), and a 4-wheeled High Mobility Multi-purpose Wheeled Vehicle (HMMWV) (Fig. 6-4). These vehicles can be classified as two tracked vehicles and two wheeled vehicles. Table 6-1 shows the parameters of these vehicles.

The field tests were conducted at Fort Riley on August 12, 2008. The soil type was Wymore silty clay loam with an average volumetric water content of 25.5%. The averaged cone index was 606 kPa for the upper 15 cm soil. The average drop cone was 7.8 cm. Using a Cohnon torsional sheargraph, the average friction angle was measured as 23^{o} and average cohesion was 17 kPa, while using a Torvane the average cohesion was measured as 14 kPa. Cohesion, friction angle, cone index and water content were measured at the center of the 14 spirals. Drop cone was taken at each impact point.

4. Experimental procedures

A Vehicle Tracking System (VTS) was mounted onto each vehicle to utilize the Global Positioning System (GPS) in tracking the vehicle. The VTS consisted of a Trimble AgGPS 132, 12-channel receiver with Omnistar Satellite differential correction. The differential GPS data for the vehicle was collected every second.

The vehicles were operated in spiral patterns to produce a constantly decreasing turning radius. Every vehicle was driven in its same rut up to 8 passes along each spiral. Rut depth measurements were manually taken every 4 to 7 meters along each spiral track, and GPS positions were taken at each measurement point using the same VTS that was used to collect the vehicle tracking data. Vehicle velocity and turning radius were derived from the GPS tracking data (Li et al., 2007a). Turning radius was calculated using a three-point method (Haugen, 2003). To compress the data range, any turning radius greater than 150 meters was classified as 150 meters. Using the distance between two GPS points and the time interval, vehicle velocity was determined. Rut depth measurements were joined to the vehicle turning radius using the ArcMap of the ESRI's ArcGIS Geographical Information System (GIS). The measurements of rut depth were divided into three turning radius (TR) classes (Sharp turns: TR <30 m; Intermediate turns: TR =30-80 m; and Straight: TR >80 m). Table 6-2 shows the spiral information. Except the M1A1 tank, all the vehicles repeated the multi-pass operation up to 8 passes in the same rut.

5. Results and discussions

5.1 M1A1 combat tank

All the vehicles have two rut measurements, one for the inside track and the other for the outside track. Previous studies show that the placement of tracks (outside and inside) can affect rut formation (Ayers, 1994; Liu et al., 2009b). In this paper, the difference between outside tracks and inside tracks are not considered and the rut depth data analyzed are average from the two tracks. Fig. 6-5 shows the averaged rut depth of the M1A1 tank in three turning radius classes. It can be seen that the M1A1 tank on turns can produce deeper ruts than on straight paths. It is found that the turning track shoe of the M1A1 tank slid back toward the inside of the turning circle first, and then slid forth toward the outside of the turning circle during the test. In this case, the lateral movement of the track shoe scraped the soil back and forth under normal forces, consequently increasing rut depth. The increase of rut depth caused by this phenomenon is less dependent on the M1A1 tank's velocity (Li et al., 2007a). Even at a low velocity, turning maneuvers still can produce deeper ruts for this tracked vehicle.

Fig. 6-6 shows the fitted trend lines to predict rut depth based on field measurements for the M1A1 tank. Figs. 6-5 and 6-6 show that rut depth increases with the increase of the number of passes. Figs. 6-5 and 6-6 also show that rut depth increases with the decrease of turning radius. A turning M1A1 tank can produce deeper ruts.

5.2 Armored Personnel Carrier (APC)

Fig. 6-7 shows the averaged rut depth of the APC in two turning radius classes. There is no data in the class of intermediate turns. As the vehicle operator transitioned too quickly into the turns, it was difficult to maintain the intermediate turns with the vehicle steering mechanism. It can be seen that turning maneuvers produce deeper ruts for the APC. Sharp turns form deeper ruts than straight paths. For the APC, rut depth also increases with the increase the number of passes.

5.3 Heavy Expanded Mobility Tactical Truck (HEMTT)

Fig. 6-8 shows the averaged rut depth of the HEMTT in two classes of turning radius. There is no data in the class of intermediate turns due to the quick transition from straight to sharp turn. For this vehicle straight traffic produced deeper ruts than turning in some phases. The turning situation for the 8-wheeled HEMTT is different from tracked vehicles. When the HEMTT is going straight, all the four wheels on each side are running in the same rut, which is already a multi-pass rut. However, when the vehicle is turning, the track of the four wheels separates and every wheel will form a new rut, which is a single-pass rut and may be shallower, depending on vehicle turning factors (Li et al., 2007b). Similar to the tracked vehicles, the multi-pass phenomenon can produce deeper ruts for wheeled vehicles. Rut depth increases with the increase of the number of passes (Affleck, 2005). With the vehicle going straight, its rut is deep because of the multi-pass effect. When turning sharply, its rut is also deep because of the turning effect, which increases the lateral

forces on the tire.

5.4 High Mobility Multi-purpose Wheeled Vehicle (HMMWV)

Fig. 6-9 shows the averaged rut depth of the HMMWV in three classes of turning radius. It can be seen that the multi-pass phenomenon can produce deeper ruts. Rut depth increases with the increase of the number of passes. Intermediate turns and sharp turns form deeper ruts than going straight. Fig. 6-9 also shows the effect of turning on rut depth for the HMMWV. It can be seen that intermediate turns, which are expected to form shallower ruts, actually form deeper ruts than sharp turns. This is partially because rut depth varied with turning conditions and the two wheels at first had the same track then separated. In addition, it was difficult to keep the HMMWV at a constant velocity during the test. When the HMMWV was turning sharply, the driver had to reduce the velocity for safety reasons. For the HMMWV, it is the centripetal force generated by turning which causes this light wheeled vehicle to produce a lateral displacement, resulting in deeper ruts. If the turning velocity reduces, the centripetal force subsequently reduces too, consequently forming shallower ruts. During the field tests, the HMMWV was operated at two velocities, averaged high at 2.7 m/s and averaged low at 1.9 m/s. Fig. 6-10 shows the measured data at high and low velocities. It is can be seen that rut depth increases with the decrease of turning radius and the increase of the number of passes. It is also found that high velocity can form slightly deeper ruts than low velocity for the HMMWV, though the difference is minimal.

5.5 Comparison of field measured increase of rut depth

Table 6-3 shows the increase of rut depth after multi-pass traffic to the initial rut depth (first pass) calculated using field measured data. Table 6-3 also shows the regressed multi-pass coefficient α and R square for every vehicle using a power equation fit. It can be seen that for vehicles in this test the averaged increase based on field data are close to the predicted values using the WES model (α=2), except the HMWWV. The α value for the HMMWV is lower than the other vehicles and the increases for the HMMWV are higher, which means that the multi-pass phenomenon has more considerable effects on the HMMWV than the other vehicles. During the field test it was seen that after first pass and second pass, the rut depth of the HMMWV began to increase very sharply. When the HMMWV conducted its first pass, the vehicle was actually supported by the vegetation, which acted like a cushion to reduce the soil compaction and displacement. The roots of the vegetation also hold the soil together and resisted moving. With continued passes, the vegetation was broken and the vehicle contacted soil directly, resulting in a sharp increase in rut depth.

After 8 passes, the HMMWV rut depth increases by the highest value of 548% of its initial rut depth, while the APC rut depth increases by the lowest value of 166%. For the M1A1, its final rut depth increases by 87% after 4 passes. The combination of the multi-pass phenomenon and turning maneuver increases rut depth significantly for all these four vehicles. In general, the multi-pass coefficient (α=2) discussed by

Jones et al. (2007) is accurate to predict multi-pass rut formation in common conditions. Although in these field conditions for tracked vehicles the regressed multi-pass coefficients using field data are actually a little higher and for wheeled vehicles they are a little lower. The regressed values are also in the range for loose soils documented in Saarilahti's report (2002).

In order to investigate the turning effects, Table 6-4 shows the increase of rut depth on turns to the rut depth on straight paths calculated using field data. For the M1A1 tank, rut depth on intermediate turns increases by 28% of the value of straight paths, and rut depth on sharp turns increases by 36% of the value of straight paths. For the APC, rut depth on sharp turns increases by 39% of the value of straight paths. For the HEMTT, rut depth on sharp turns increases only by 6%. For the HMMWV, it has wider data variability than the other vehicles as velocity is also a treatment here. Despite the wider variability, it still can be seen that turning maneuvers have a significant effect on rut depth. Rut depth on intermediate turns increases by 65% of the value of straight paths, and rut depth on sharp turns increases by 25%. Note that turning factors may form shallower ruts with negative increase in some phases for wheeled vehicles, because both the track separation when turning and the resistance to rutting provided the vegetative support. The values of increase in this paper are similar to the data from former Fort Riley tests (Liu et al., 2009a).

6. Conclusions

To investigate the effects of the combination of multiple passes and turning

maneuvers, field tests on four vehicles were conducted at Fort Riley during the summer in 2008. Vehicles were operated in spiral patterns and repeated passing in same spiral ruts.

It is found that rut depth increases with the increase of the number of passes. This is verified by the tests on all vehicles. Rut depth increases obviously with the decrease of turning radius for every vehicle except the HEMTT. For the HEMTT, the track separates out and every single wheel forms a new rut at sharp turns, which may be shallower. Multiple passes and turning maneuvers have the most considerable effects on the HMMWV. The HMMWV rut depth increases by the highest value of 548% of its initial rut depth under the effects of the combination of the multi-pass and turning maneuvers after 8 passes. Intermediate turns contribute a highest increase of 65% of rut depth compared to straight paths for the HMMWV. For the M1A1, APC and HEMTT, the regressed multi-pass coefficients are close to 2. For the HMMWV, its regressed multi-pass coefficient is 1.2, lower than the other three vehicles because of the effect of vegetation. The multi-pass coefficient (α=2) is proper to predict multi-pass rut depth for turning vehicles in loose soils. In summary, the combination of the multi-pass phenomenon and turning maneuvers can cause increased damage on soil and vegetation for most tracked and wheeled vehicles.

Acknowledgement

The authors thank Phil Woodford and Chris Otto of Fort Riley Military Installation for helping with coordination efforts and field assistance and expertise. The authors also thank the U.S. Army Corps of Engineers, Construction Engineering

Research Laboratory for project support. The authors are also grateful to the Environmental Security Technology Certification Program (ESTCP) project SI-0815 for providing support for this study.

References

[1] Abebe, A. T., T. Tanaka, and M. Yamazaki. 1989. Soil compaction by multiple passes of a rigid wheel relevant for optimization of traffic. *J Terramechanics* 26(2): 139-148.

[2] Abele, G., J. Brown, and M. C. Brewer. 1984. Long-term effects of off-road vehicle traffic on tundra terrain. *J Terramechanics* 21(3): 283-294.

[3] Affleck, R. T. 2005. Disturbance measurements from off-road vehicles on seasonal terrain. Technical Report: TR-05-12, U.S. Army Cold Regions Research and Engineering Laboratory.

[4] Ansorge, D. and R. J. Godwin. 2008. The effect of tyres and a rubber track at high axle loads on soil compaction—Part 2: Multi-axle machine studies. *Biosystems Engineering* 99: 338 – 347.

[5] Ayers, P. D. 1994. Environmental damage from tracked vehicle operation. *J Terramechanics* 31(3): 173-183.

[6] Braunack, M. V. and B. G. Williams. 1993. The effect of initial soil water content and vegetative cover on surface disturbance by tracked vehicles. *J Terramechanics* 30(4): 299-311.

[7] Harnisch, C., B. Lach, and R. Jakobs. 2007. ORSIS – News and further

developments. *J Terramechanics* 44(1): 35-42.

[8] Haugen, L. B., P. D. Ayers, and A. B. Anderson. 2003. Vehicle movement patterns and vegetative impacts during military training exercises. *J Terramechanics* 40(2): 83-95.

[9] Holm, I. C. 1969. Multi-pass behaviour of pneumatic tires. *J Terramechanics* 6(3): 47-71.

[10] Jakobsen, B. F. and A. R. Dexter. 1989. Prediction of soil compaction under pneumatic tyres. *J Terramechanics* 26(2): 107-119.

[11] Jones, A., G. McKinley, P. Richmond, and D. Creighton. 2007. A vehicle terrain interface. *In: ISTVS conference*. Fairbanks, Alaska.

[12] Li, Q., P. D. Ayers, and A. B. Anderson. 2007a. Modeling of terrain impact caused by tracked vehicles. *J Terramechanics* 44(6): 395-410.

[13] Li, Q., P. D. Ayers, and A. B. Anderson. 2007b. Prediction of impacts of wheeled vehicles on terrain *J Terramechanics* 44(2): 205-215

[14] Liu, K., P. Ayers, H. Howard, and A. Anderson. 2009b. Influence of turning radius on wheeled military vehicle induced rut formation. *J Terramechanics* 46(2): 49-55.

[15] Liu, K., P. Ayers, H. Howard, and A. Anderson. 2009a. Influences of soil and vehicle parameters on soil rut formation. *J Terramechanics*. In press.

[16] Reid, A. A., S. Shoop, R. Jones, and P. Nunez. 2007. High-fidelity ground platform and terrain mechanics modeling for military applications involving vehicle dynamics and mobility analysis. *In: ISTVS conference*. Fairbanks, Alaska.

[17] Saarilahti, M. 2002. Soil interaction model. *Quality of Life and Management of Living Resources Contract, No. QLK5-1999-00991*. Department of Forest Resource Management, University of Helsinki.

Appendix

Fig. 6-1 Combat tank M1A1.

Fig. 6-2 Armored Personnel Carrier.

Fig. 6-3 Heavy Expanded Mobility Tactical Truck.

Fig. 6-4 High Mobility Multipurpose Wheeled Vehicle.

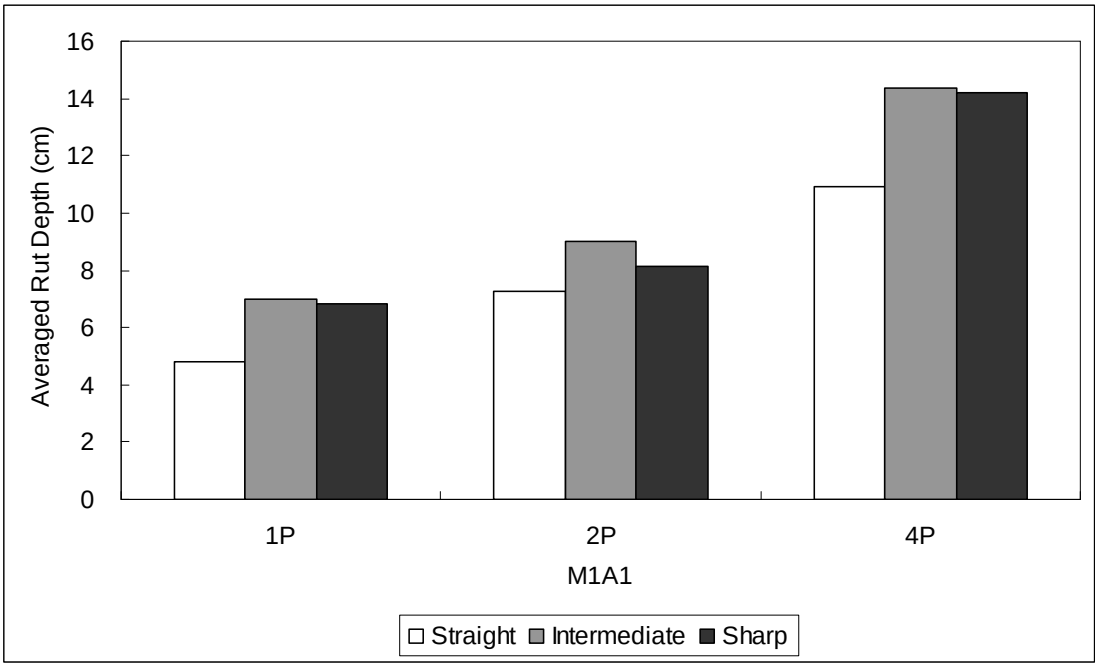

Fig. 6-5 Rut depth comparison of the M1A1 tank.

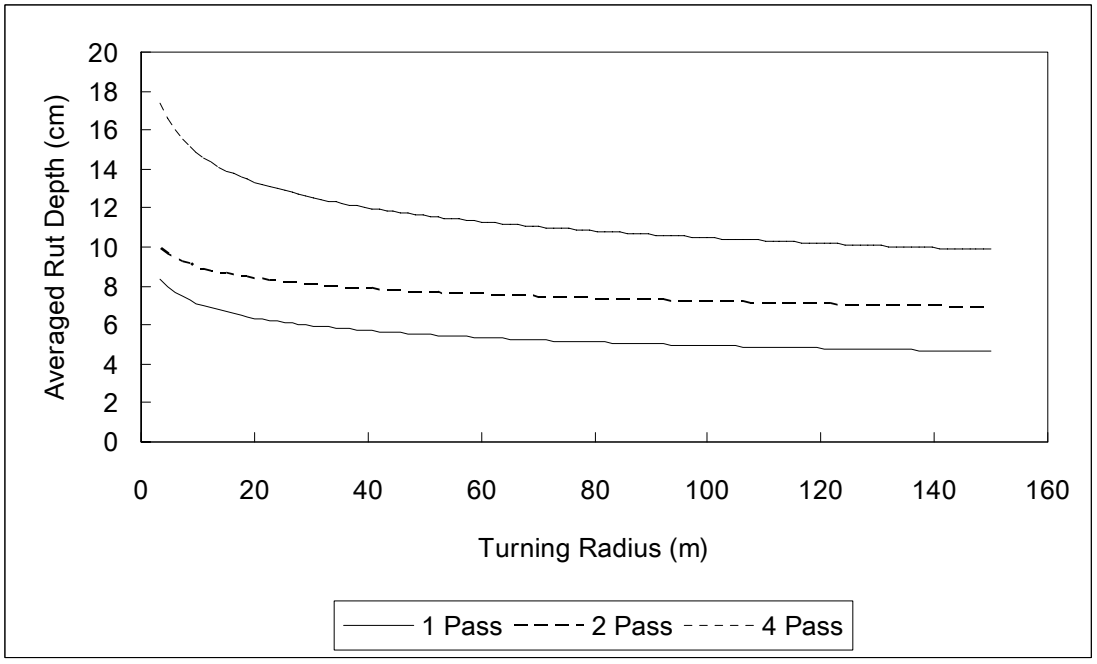

Fig. 6-6 Rut depth and turning radius of the M1A1 tank.

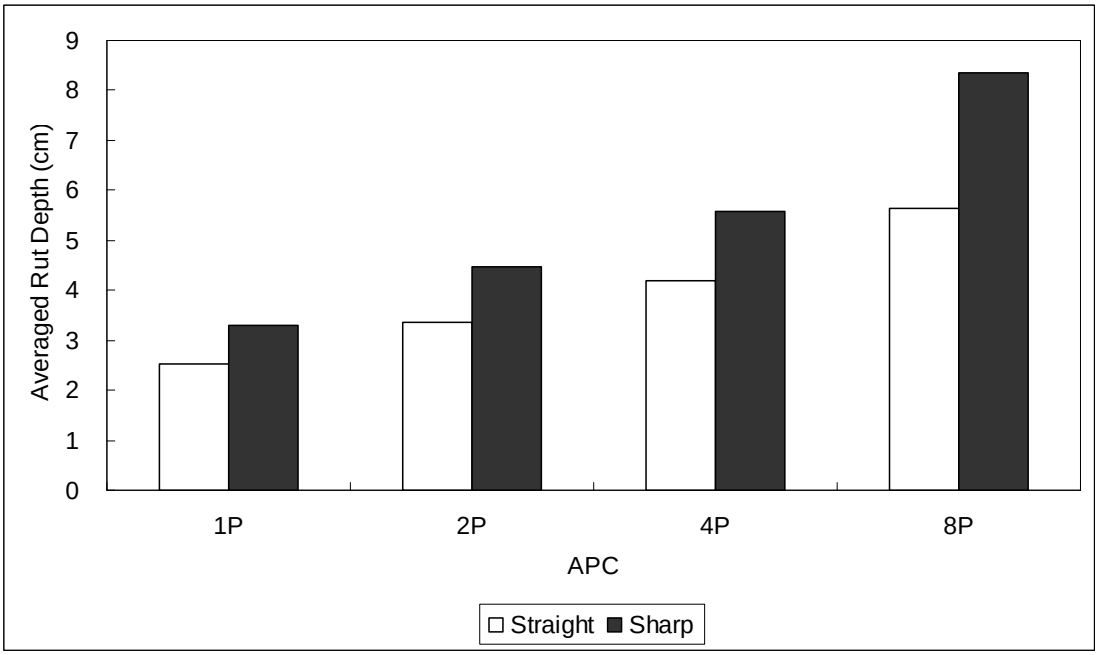

Fig. 6-7 Rut depth comparison of the APC.

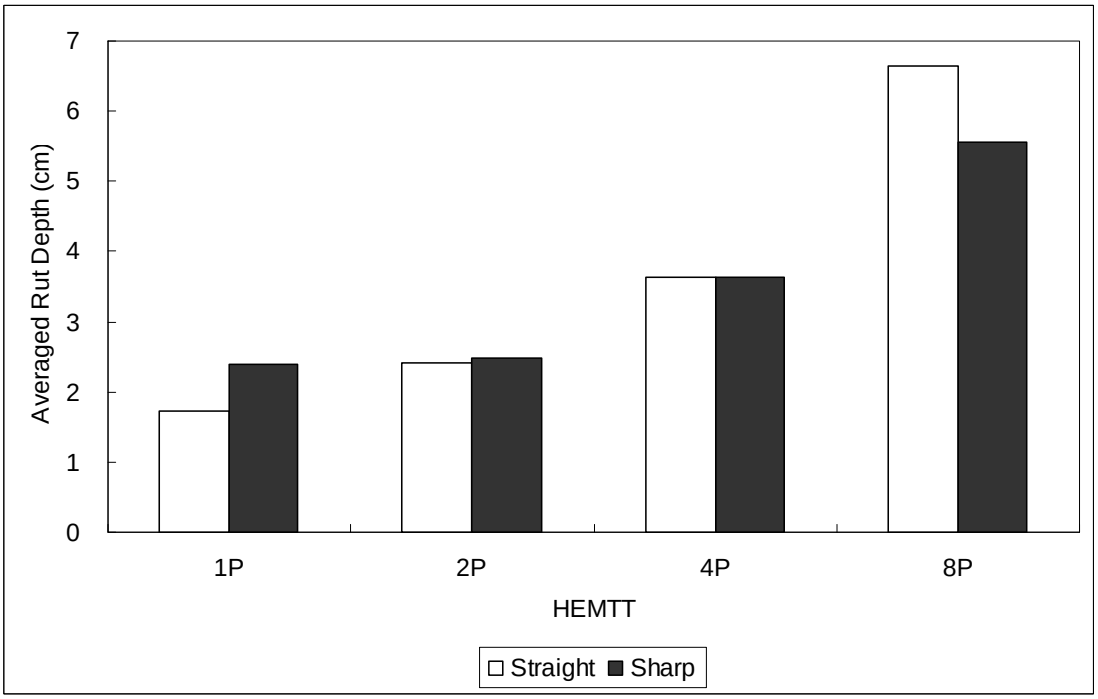

Fig. 6-8 Rut depth comparison of the HEMTT.

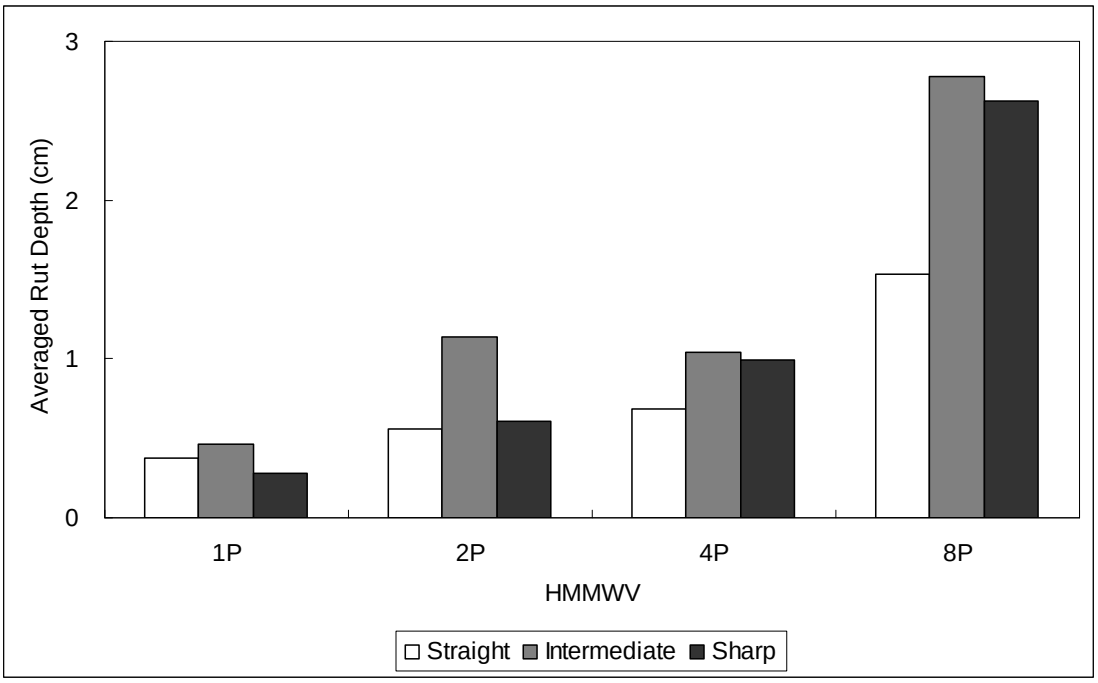

Fig. 6-9 Rut depth comparison of the HMMWV.

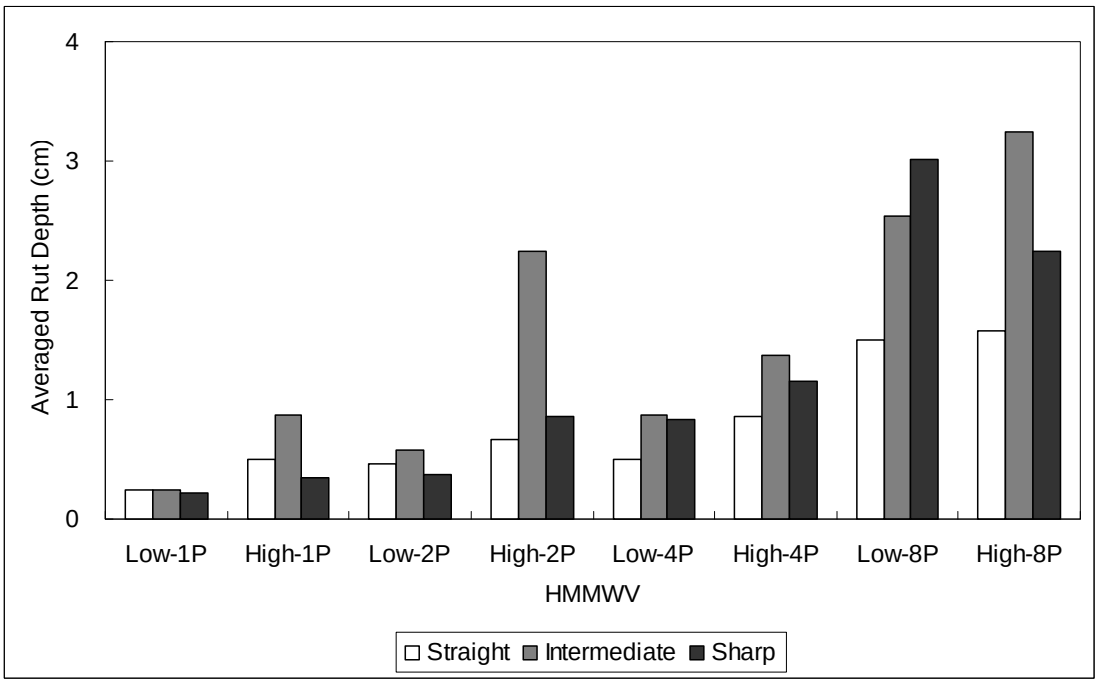

Fig. 6-10 Rut depths at different velocities for the HMMWV.

Table 6-1 Vehicle parameters.

	Vehicle Type	Vehicle Weight (kg)	Track/Tire Width (cm)
M1A1	Track	57153	63.0
APC	Track	11709	38.0
HEMTT	Wheel	24948	31.0
HMMWV	Wheel	3493	29.5

Table 6-2 Spiral ID and correlated information.

Spiral ID	Vehicle Type	Number of Impact Points	Number of Passes	Average Velocity (m/s)
1	M1A1	16	4	4.8
2	M1A1	16	4	3.0
3	M1A1	16	4	3.5
4	M1A1	16	4	4.4
5	APC	14	8	4.0
6	APC	14	8	3.3
7	APC	14	8	3.4
8	HEMTT	12	8	2.9
9	HEMTT	12	8	4.1
10	HEMTT	12	8	2.9
11	HMMWV	12	8	1.9
12	HMMWV	12	8	3.0
13	HMMWV	12	8	2.0
14	HMMWV	12	8	2.5

Table 6-3 Multi-pass rut depth increase

		% Increase from First Pass				α	R^2
		1 Pass	2 Pass	4 Pass	8 Pass		
M1A1	Straight	0	27	99		2.0	0.97
	Intermediate	0	31	94		2.1	0.99
	Sharp	0	10	67		2.7	0.88
	Average	0	23	87		2.2	0.96
APC	Straight	0	49	85	173	2.1	0.99
	Sharp	0	34	74	160	2.2	0.99
	Average	0	42	79	166	2.2	0.99
HEMTT	Straight	0	39	109	282	1.6	0.98
	Sharp	0	4	52	133	2.4	0.91
	Average	0	21	80	208	1.9	0.96
HMMWV	Straight	0	49	82	310	1.6	0.93
	Intermediate	0	149	127	506	1.1	0.68
	Sharp	0	116	251	827	1.0	0.99
	Average	0	105	153	548	1.2	0.95
α=2 (Jones et al., 2007)		0	41	100	183	2.0	

Table 6-4 Turning rut depth increase

		% Increase from Straight Paths		
		Straight	Intermediate	Sharp
M1A1	1 Pass	0	28	51
	2 Pass	0	31	30
	4 Pass	0	25	26
	Average	0	28	36
APC	1 Pass	0		46
	2 Pass	0		32
	4 Pass	0		38
	8 Pass	0		39
	Average	0		39
HEMTT	1 Pass	0		38
	2 Pass	0		2
	4 Pass	0		0
	8 Pass	0		-16
	Average	0		6
HMMWV	1 Pass	0	22	-24
	2 Pass	0	103	9
	4 Pass	0	53	46
	8 Pass	0	81	71
	Average	0	65	25

Part 7 Conclusions

In this dissertation, a comprehensive study was conducted to investigate the influences of turning maneuvers of military off-road vehicles on rut formation, which can bring negative effects on vehicle mobility and environment. Rut depth, rut width and rut index were used as the main indicators to quantify rut formation. Vehicle turning radius (TR) and velocity were indicators of turning maneuvers. Field tests were conducted at Yuma Proving Grounds, Fort Riley and Fort Lewis. Vehicles include a combat tank M1A1, an M113 Armored Personnel Carrier (APC), a Heavy Expanded Mobility Tactical Truck (HEMTT), a Light Armored Vehicle (LAV) and a High Mobility Multi-purpose Wheeled Vehicle (HMMWV). A Vehicle Tracking System (VTS) was mounted onto each vehicle to utilize the Global Positioning System (GPS). The vehicles were operated in spiral patterns to get constantly decreasing turning radius, including multi-pass operations. Lab tests on a tire and a track shoe were conducted to investigate the effects of lateral forces generated by turning on rut formation.

In the first paper, Influence of Soil and Vehicle Parameters on Soil Rut Formation, field data were analyzed using the Statistics Analysis System (SAS) 9.1 to make statistical conclusions relative to vehicle and soil parameters. The treatments were vehicle parameters, including vehicle type, weight, velocity and turning radius, and soil parameters, including soil texture and moisture. Results show that vehicle parameters (vehicle type, weight, velocity and turning radius) and soil parameters (soil texture and moisture) are statistically significant to affect rut formation. The M1A1 tank will cause the most serious environmental damage, the widest and deepest

rut and highest rut index. When the soil is dry, vehicles do not easily produce ruts, but vehicles can produce deep ruts on wet soil. Soil texture does not have significant effects on rut depth. However, vehicles can form wider ruts on clay soil. At high speed vehicles can form deeper ruts, but speed does not have effects on rut width. Turning maneuvers have significant effects on rut formation. For the M1A1 tank, APC and HMMWV, turning maneuvers can increase rut depth, rut width and rut index. For the HEMTT, turning maneuvers can increase rut width and rut index, but its rut depth decreases when it is turning, from a multi-pass rut to four single-pass ruts. The M1A1 tank has deeper inside ruts, while the APC has wider outside ruts.

In the second paper, Influence of Turning Radius on Wheeled Military Vehicle Induced Rut Formation, it shows that the heavy LAV produces deeper ruts than the light HMMWV. Turning maneuvers also produce deeper ruts. Rut depth increases with the decrease of turning radius. Rut width increases with the decrease of turning radius for both vehicles. Rut index also increases with the decrease of turning radius. The outside rut depth is deeper than the inside rut depth for the same vehicle when the vehicle turns, while, the outside rut width and the inside rut width are almost the same. The outside rut index is higher than the inside rut index for the LAV, but for the HMMWV they are the same.

In the third paper, Prediction of Rut Depth during Military Vehicle Turning Maneuvers using a Modified Sinkage Numeric, the vehicle terrain interaction (VTI) model was chosen to modify to predict rut depth during turning maneuvers for an eight-wheeled LAV. Turning factors-including weight shift, turning radius and

velocity are integrated into the model. The regression results show that by using turning factors, the modified VTI model was able to predict rut-depth characteristics during the turning maneuver (R^2 of 0.43). This R square value is much better than the original model. Analysis revealed that at constant velocities, rut depth will always increase with the decrease of the turning radius for the LAV. The model correctly predicted deeper ruts in the outside vehicle track than in the inside track.

In the fourth paper, Lateral Slide Sinkage Tests for a Tire and a Track Shoe, lab tests were conduced to investigate the sinkage of a trailer tire and an APC track shoe, due to lateral forces (or lateral displacements) under given different levels of normal forces. It can be seen that both for the tire and the track shoe, the sinkage increases with the increase of normal forces. This verifies the sinkage phenomenon of a static vehicle on the soil ground. It is more interesting to see that the slide sinkage due to the lateral force or lateral displacement is much deeper than the sinkage due to the static normal force. This confirms the model modifications determined in the third paper. The final sinkage caused by the lateral force for the tire is 3 to 5 times the static sinkage. For the track shoe, the final sinkage caused by the lateral displacement is about 3 times the static sinkage. These results show that the lateral force and lateral displacement generated by turning maneuvers affect the sinkage severely for both wheeled and tracked vehicles.

In the last paper, Multi-pass Rutting Study for Turning Wheeled and Tracked Vehicles, the effects of the combination of multiple passes and turning maneuvers were investigated. Vehicles were operated in spiral patterns and repeated passing in

same spiral ruts. It is found that rut depth increases with the increase of the number of passes. This is verified by the tests on all vehicles. Rut depth increases obviously with the decrease of turning radius for every vehicle except the HEMTT. For the HEMTT, the track separates out and every single wheel forms a new rut at sharp turns, which may be shallower. Compact to the LAV, the HEMMT was turning at a lower velocity with less lateral forces. Multiple passes and turning maneuvers have the most considerable effects on the HMMWV. The HMMWV rut depth increases by the highest value of 548% of its initial rut depth under the effects of the combination of the multi-pass and turning maneuvers after 8 passes. Intermediate turns contribute a highest increase of 65% of rut depth compared to straight paths for the HMMWV. For the M1A1, APC and HEMTT, the regressed multi-pass coefficients are close to 2. For the HMMWV, its regressed multi-pass coefficient is 1.2, lower than the other three vehicles because of the effect of vegetation. The multi-pass coefficient (α=2) is proper to predict multi-pass rut depth for turning vehicles in loose soils. In summary, the combination of the multi-pass phenomenon and turning maneuvers can cause increased damage on soil and vegetation for most tracked and wheeled vehicles.

This comprehensive study with wide ranges of vehicles, soil conditions, and operating maneuvers was conduced on rut formation. This study provides better understanding in rut formation by military vehicles during turning.

Vita

Kun Liu was born in Yichun, Heilongjiang, China, on January 21, 1982. He attended his grade school, middle school and high school in this beautiful small city. He attended Northeast Agricultural University in Harbin, China, and received his B.S. in Agricultural Engineering in 2003 and an M.S. in Agricultural Engineering in 2006, under the direction of Dr. Enchen Jiang. Then he was enrolled in the University of Tennessee to pursue his PhD in Biosystems Engineering, under the direction of Dr. Paul Ayers. Kun Liu received his PhD in December, 2009.